2010-07-13

Charged, Rotating Black Holes in Higher Dimensions

Christopher Bruce Verhaaren
Brigham Young University - Provo

Charged, Rotating Black Holes in Higher Dimensions

Chris Verhaaren

A thesis submitted to the faculty of
Brigham Young University
in partial fulfillment of the requirements for the degree of

Master of Science

Eric Hirschmann, Chair
David Neilsen
Ross L. Spencer

Department of Physics and Astronomy

Brigham Young University

August 2010

ABSTRACT

Charged, Rotating Black Holes in Higher Dimensions

Chris Verhaaren

Department of Physics and Astronomy

Master of Science

We present a method for solving the Einstein-Maxwell equations in a five dimensional, asymptotically flat, black hole spacetime with three commuting Killing vector fields. In particular, we show that by reducing the dimension of the Einstein-Maxwell equations in a Kaluza-Klein like manner we can determine the components of the metric and vector potential which lie in the direction of the Killing vector fields. These components are determined by nine scalar fields each of which satisfy a partial differential equation in two variables. These equations take the form of an elliptic operator set equal to a nonlinear source. We find evidence that particular combinations of these fields satisfy Dirichlet boundary conditions, and are well suited to numerical solution using Green functions. Using this method we generate numerical solutions to the 4+1 Einstein-Maxwell equations corresponding to charged generalizations of the Myers-Perry solution. We also discover symmetry relations among the scalar equations which constrain their functional forms and posit the existence of two rigidity-theorem-like relations for electrovac spacetimes and sketch how their use generalizes our method to $N + 1$ dimensions.

ACKNOWLEDGMENTS

Contents

List of Figures

Chapter 1

Introduction

Ever since their discovery, black holes have motivated scientists to better understand theories of gravity. While physical study of their properties remains elusive, their theoretical existence alone has encouraged deeper questions and predictions about the nature of space, time, and the universe. Similar questions have led to theories which attempt to unify the forces of nature. Since these theories of quantum gravity must reduce to our current theories in appropriate limits, and because black holes make up a large part of the interface between classical and quantum effects, the black holes predicted by these theories are of particular interest.

As a first step we must understand the characteristics of black holes as predicted by general relativity (GR), our current model of gravity. Unsurprisingly, the majority of investigations into black holes assume a universe with three spatial directions and one time direction. Such a 3+1 dimensional spacetime is a natural choice in light of current observations. However, many unified theories require a universe with a dimensionality beyond the 4 observed, so a catalogue of higher dimensional GR black holes might be useful for comparison.

A first, perhaps naïve, guess might be that such higher dimensional black holes somehow

"naturally" generalize from 3+1 black holes. This idea motivates a brief study of four dimensional black holes. We begin with an indispensable trait as far as cataloging is concerned, namely uniqueness. It has been shown (see [1] for example) that under modest conditions (such as asymptotic flatness and stationarity) 3+1 black holes are completely determined by their mass, angular momentum, and electromagnetic charge.

The Kerr-Newman [2] (KN) solution to the 3+1 Einstein-Maxwell equations is the most general black hole since it incorporates mass, angular momentum, and electric charge. The previously discovered solutions (named for their discoverers): (1) Schwarzschild [3] which incorporates mass only, (2) Reissner-Nordström [4, 5] which has mass and charge, and (3) Kerr [6] which has mass and angular momentum, can all be thought of as limiting cases of the KN solution.

Clearly, properties of the KN solution must hold in some form for all 3+1 black holes. In particular, it has been shown that these black hole spacetimes include a null surface which is a topological two-sphere (S^2) [7]. This surface, called the event horizon, is a one way boundary that separates the so-called interior of the black hole from events outside the horizon.

There is also a connection between the symmetries of a 3+1 black hole spacetime and its temporal evolution. For instance, a black hole is spherically symmetric if and only if it is static [8]. If a black hole is stationary (in a steady state) it must be axisymmetric [7]. There are many more properties of black holes which we have not discussed. While these other aspects of black hole mechanics are important, they fall outside the scope of this work. We therefore direct the interested reader to one of the many texts on GR, such as Wald [9].

As we make the transition to higher dimensional GR we find that some aspects of 3+1 GR generalize intuitively to $N+1$ dimensions while others do not generalize at all. However, it is useful to explain some of the appeal of extra dimensional theories. The work of Kaluza [10] and Klein [11] was one of the first serious forays into extra dimensional GR. They

discovered that if an extra dimension has a $U(1)$ symmetry, the 4+1 Einstein equations can be separated into the 3+1 Einstein equations and the 3+1 Maxwell equations. The fly in the ointment is that besides these two sets of equations, which have a clear physical interpretation, their formalism also generates a scalar field referred to as the dilaton which has no agreed upon physical meaning. This extra scalar field notwithstanding, it is remarkable that by introducing an extra dimension the theories of gravity and electromagnetism are unified. A very heuristic explanation of why so many unification theories require many extra dimensions is that, similar to Kaluza-Klein (KK) theory, including more dimensions gives the theory enough freedom to incorporate more forces.

So, with extra dimensions we might unify the forces. Unification with gravity immediately leads to black holes in higher dimensions. Alternatively, since all observational evidence supports a 3+1 dimensional universe it may be the case that there are no extra dimensions. We might then ask why spacetime has this 3+1 dimensional structure. The first higher dimensional black hole solutions were found while addressing this question. Tangherlini [12] generalized both the Schwarzschild and Reissner-Nordström black holes to $N+1$ dimensions to see if 3+1 black holes were in some way special. These black holes have been shown to be static and unique just as the 3+1 case [13]. The topology of their event horizon is that of an $(N-1)$-sphere (S^{N-1}) which is a natural generalization of their four dimensional counterparts.

The generalization of Kerr black holes to higher dimensions proved to be more complicated. The major challenge comes from the multiple independent angular momenta in higher dimensional spacetimes[1]. In fact, $\lfloor \frac{N}{2} \rfloor$ independent angular momenta must be taken into account for the $N+1$ dimensional rotating black hole.[2] The Myers-Perry (MP) solution [14]

---

[1]In technical terms, the independent planes of rotation for a body in an N dimensional space correspond to the Casimir invariants associated to the group of rigid rotations in $\mathbb{R}^N$, namely $SO(N)$.

[2]$\lfloor \frac{N}{2} \rfloor$ refers to the integer part of $\frac{N}{2}$.

models higher dimensional black holes with all possible angular momenta.

The MP black hole's event horizon topology in five dimensions is S^3 like the Tangerlini solutions. However, uniqueness does not immediately follow as it does for static black holes. Emparan and Reall [15] discovered a a black ring (a black hole with a topologically toroidal[3] event horizon) solution in 4+1 spacetime. Such a black ring can have the same mass and angular momenta as a MP black hole, but does not share other important properties. Clearly, more parameters are needed to uniquely define a rotating black object in higher dimensions. In fact, as the dimension of the spacetime increases, more exotic horizon topologies become possible, see Fig. 6 of [16]. However, hope for some type of uniqueness remains. It has been shown [17,18] that when certain aspects of black holes (including horizon topology) are carefully defined, rotating black holes can be uniquely characterized.

It is also worth noting the implications of stationarity on higher dimensional spacetimes. Recall that in the 3+1 case stationarity implied the existence of axisymmetry. Now, in higher dimensions there are more than one possible axisymmetries that can exist in a spacetime, as exemplified by the MP solution. However, in higher dimensions stationarity only implies one axisymmetry [19].

While increasingly exotic black objects become possible in higher dimensions, an $N + 1$ generalization of the KN solution is noticeably absent. Since 1986, when the MP solution was published, a charged MP solution of the Einstein-Maxwell equations has withstood general solution. Even so, some analytical and numerical work has been produced. On the numerical side, Kunz *et al.* [20, 21] have provided numerical solutions for the special cases of only one angular momentum and equal angular momenta in 4+1, 6+1, and 8+1 dimensional spacetimes. Of course, in order to find these solutions the authors also made significant analytical deductions about the nature of the black hole solutions they were seeking. Similar and further analysis was made by Aliev and Frolov [22]. Their work has

---

[3]Specifically, the horizon's topological structure is $S^1 \times S^2$.

been mainly perturbative, including an analytic solution in the limit of small rotation [23].

The intent of this work is to find a general numerical solution of the 4+1 Einstein-Maxwell equations corresponding to an electrically charged MP black hole. These equations are generated from the Einstein-Maxwell action in five dimensions

$$S = \int \left(\frac{Rc^4}{16\pi G} - \frac{1}{4} F^{ab} F_{ab} \right) \sqrt{-g} \; d^5 x, \tag{1.1}$$

where G is Newton's gravitational constant, c is the speed of light in vacuum, R is the scalar curvature, and F_{ab} the Maxwell field tensor. By varying this action with respect to the metric and the electromagnetic vector potential one can derive the Einstein and Maxwell equations:

$$G_{ab} = \frac{8\pi G}{c^4} \, T_{ab} \tag{1.2}$$

$$\nabla_b F^{ab} = 0 \tag{1.3}$$

where G_{ab} and T_{ab} are respectively the Einstein and Stress-Energy tensors.

In order to make this problem tractable, we use dimensional reduction with respect to the assumed symmetries of the spacetime. This technique was first made precise by Geroch [24] and since the symmetries we assume are all $U(1)$, certain similarities with KK theory will become apparent.

Since the 4+1 MP solution is asymptotically flat and has an event horizon with S^3 topology, we assume these conditions as we begin our analysis. These assumptions are natural both as a charged generalization of the MP solution and as a higher dimensional generalization of the KN solution. As a parallel assumption to asymptotic flatness, we will assume the standard condition that the vector potential vanishes at spatial infinity.

We will also assume that the black hole spacetime is stationary and allows two independent planes of rotation. These three symmetries will allow us to reduce the Einstein-Maxwell equations from five dimensions to two dimensions. Similar to KK theory, this will generate three Maxwell-like fields on the remaining two dimensional manifold and nine unknown

scalar functions. Six of these functions result from the reduction of the geometry and three from the reduction of the Maxwell field. We will show that these Maxwell-like fields are made trivial by enforcing local flatness. Additionally, the scalar functions can be chosen to have a form well adapted to numerical analysis. Specifically, we will show that each can be defined by one of a family of elliptic differential operators set equal to a nonlinear source. In addition, they will satisfy Dirichlet boundary conditions at spatial infinity and the event horizon.

These properties allow us to construct a Green function for this family of operators. With these functions in hand we will generate a numerical solution for the scalar fields. When these fields have been specified, it becomes a relatively simple matter to solve the two dimensional GR problem.

As we analyze our decomposed equation set we will show how the equivalence of the two axisymmetries lead to relationships between the unknown scalar functions. These relationships constrain the form of these functions. In addition we postulate the existence of two rigidity-like theorems for electrovac spacetimes.

Unless otherwise specified we will choose units such that $c = G = 1$. Our assumed metric has signature $+3$ and we take the sign convention found in Wald [9] for components of the Einstein-Maxwell equations.

Chapter 2

Geometry and Symmetries

The power of the formalism we introduce in this thesis depends on our ability to reduce the dimension of the 4+1 Einstein-Maxwell equations by "dividing out" the symmetries of a spacetime. As explained in Chapter 1, we assume that the solution we wish to solve for has three independent symmetries.

These symmetries correspond to commuting Killing vector fields on the spacetime manifold. Specifically, we assume a stationary spacetime with two independent axisymmetries. This corresponds to the existence of a timelike Killing vector field together with two spacelike Killing vector fields with closed orbits. Each of these Killing vector fields can be thought of as generating a $U(1)$ symmetry group. As a result, following KK, we expect three Maxwell-like fields to be generated as we divide out these symmetries. We also obtain a set of scalar fields generalizing the single dilaton of KK.

The method and mathematical consistency of this process is due to Geroch [24]. He has shown that the quotient space resulting from such an operation is a submanifold orthogonal to the Killing vector field related to the symmetry of the initial space. This allows us to completely separate portions of the Einstein-Maxwell equations into linearly independent components that lie along each Killing vector in the submanifold.

In this chapter we employ this method to reduce the dimensionality of our problem from five to two. Specifically, we find the relation between the five and two dimensional metrics and then build up the geometric components of the Einstein equations from that relation.

2.1 Metric Properties

We begin with a differentiable manifold $\mathcal{M}$ with metric g_{ab} that admits one timelike Killing vector field t^a and two independent spacelike Killing vector fields ϕ^a and ψ^a whose orbits are closed[1]. We denote their norms by:

$$t^a t_a = -c^2, \quad \phi^a \phi_a = b^2, \quad \psi^a \psi_a = a^2. \tag{2.1}$$

It is convenient to choose coordinates on the manifold adapted to these vector fields; namely,

$$t^a = (\partial_t)^a, \quad \phi^a = (\partial_\phi)^a, \quad \psi^a = (\partial_\psi)^a. \tag{2.2}$$

This choice of coordinates ensures that every quantity defined on $\mathcal{M}$ is a function of the remaining two coordinates only. Next, for convenience we define a scaled Killing vector V^a by

$$V^a \equiv \frac{\psi^a}{a^2}, \tag{2.3}$$

and define

$$^{(4)}g_{ab} \equiv g_{ab} - a^2 V_a V_b, \tag{2.4}$$

which is the metric on the four dimensional submanifold of $\mathcal{M}$ orthogonal to V^a. This orthogonality is easily verified:

$$^{(4)}g_{ab}V^a = g_{ab}V^a - a^2 V_a V_b V^a$$
$$= V_b - \frac{a^2}{a^2}V_b = 0. \tag{2.5}$$

---

[1] That is to say the orbits of the spacelike Killing vector fields are topological circles.

We can now use this four metric to project ϕ^a into the four manifold. We do this to create linear combinations of the Killing vectors which are guaranteed to be orthogonal both to each other and the remaining submanifold. We begin by defining the vector

$$^{(4)}\phi^a \equiv {}^{(4)}g^a{}_b\phi^b = \phi^a - a^2 V^a V_b \phi^b$$

$$= \phi^a - \psi^a V_\phi, \tag{2.6}$$

where we have defined $V_\phi \equiv \phi^b V_b$. We then define the norm

$$^{(4)}\phi^{a(4)}\phi_a = b^2 - a^2 V_\phi^2 \equiv p^2. \tag{2.7}$$

As before, we scale this vector by p^2 and define

$$U^a \equiv \frac{^{(4)}\phi^a}{p^2}, \tag{2.8}$$

which can be used to define the metric on the three manifold orthogonal to both V^a and U^a:

$$^{(3)}g_{ab} \equiv g_{ab} - a^2 V_a V_b - p^2 U_a U_b. \tag{2.9}$$

Now, since

$$V^a U_a = V^a \left(\phi_a - \psi_a V_\phi \right) \frac{1}{p^2}$$

$$= \left(V_\phi - V_\phi \right) \frac{1}{p^2} = 0 \tag{2.10}$$

it can easily be shown that $^{(3)}g_{ab}$ is orthogonal to V^a and U^a (similar to (2.5)) as desired.

It is important to notice that our order of projecting out Killing vectors has preferred one direction over the other in the subsequent derivations. Its possible to keep both Killing vector fields on an equal footing (see Appendix C), but we will proceed as we have begun. We choose to do this because certain functions that appear naturally in our present formalism become awkward in the symmetric case. However, we will use some of the insights gained from the symmetric formalism in later chapters.

Returning to our construction, we use the three metric (2.9) to project t^a into the three manifold. Explicitly,

$$^{(3)}t^a \equiv {}^{(3)}g_{ab}t^b = t^a - \psi^a t^b V_b - {}^{(4)}\phi^a t^b U_b$$

$$= t^a - \psi^a \left(V_t - U_t V_\phi \right) - \phi^a U_t, \tag{2.11}$$

where we have defined $V_t \equiv t^a V_a$ and $U_t \equiv t^a U_a$. We then find the norm

$$^{(3)}t^{a\,(3)}t_a = - \left(c^2 + a^2 V_t^2 + p^2 U_t^2 \right) \equiv -Q^2, \tag{2.12}$$

and as before we scale (2.11) by the norm to define

$$T^a \equiv \frac{{}^{(3)}t^a}{Q^2}. \tag{2.13}$$

We note

$$T^a V_a = \frac{1}{a^2 Q^2} \left(V_t - V_t \right) = 0, \tag{2.14}$$

$$T^a U_a = \frac{1}{p^2 Q^2} \left(U_t - U_t \right) = 0, \tag{2.15}$$

which shows that we can define the two dimensional metric σ_{ab} on a submanifold of $\mathcal{M}$ which is orthogonal to all three Killing vectors by

$$\sigma_{ab} \equiv g_{ab} - a^2 V_a V_b - p^2 U_a U_b + Q^2 T_a T_b. \tag{2.16}$$

We will call this submanifold $\mathcal{N}$. Notice that we have constructed the vectors V^a, U^a, and T^a to be orthogonal to each other and to $\mathcal{N}$. We use this property to treat V^a, U^a, T^a, and σ_{ab} as linearly independent "directions" in $\mathcal{M}$.

As with the Kaluza-Klein case, we expect these dimensional reductions to generate Maxwell-like fields with the scaled, orthogonal Killing vectors acting as vector potentials. These fields will appear naturally in our formulation of the Einstein-Maxwell equations. We define these fields as:

$$W_{ab} = \partial_a T_b - \partial_b T_a, \quad Y_{ab} = \partial_a U_b - \partial_b U_a, \quad Z_{ab} = \partial_a V_b - \partial_b V_a. \tag{2.17}$$

We then separate these fields into pieces lying along each Killing vector and the field in $\mathcal{N}$. This is done by making the definition ${}^{(2)}W_{ab} = \sigma_a{}^c \sigma_b{}^d W_{cd}$ and similarly for the other fields. We find

$$
\begin{aligned}
W_{ab} &= g_a{}^c g_b{}^d W_{cd} \\
&= \left(\sigma_a{}^c + a^2 V_a V^c + p^2 U_a U^c - Q^2 T_a T^c\right)\left(\sigma_b{}^d + a^2 V_b V^d + p^2 U_b U^d - Q^2 T_b T^d\right) W_{cd} \\
&= {}^{(2)}W_{ab}.
\end{aligned}
\tag{2.18}
$$

Similarly, we have

$$
Y_{ab} = {}^{(2)}Y_{ab} + T_a \partial_b U_t - T_b \partial_a U_t
\tag{2.19}
$$

$$
Z_{ab} = {}^{(2)}Z_{ab} - U_a \partial_b V_\phi + U_b \partial_a V_\phi + T_a \left(\partial_b V_t - U_t \partial_b V_\phi\right) - T_b \left(\partial_a V_t - U_t \partial_a V_\phi\right).
\tag{2.20}
$$

We now write the line element for the metric in terms of the 2 metric and the components and norms of the Killing vectors. Our coordinates are chosen to be $x^a = (t, x^1, x^2, \phi, \psi)$ with t, ϕ, and ψ adapted to our Killing vectors as indicated previously. This choice constrains our metric coefficients to be functions of the remaining coordinates x^1 and x^2, which we have left completely general. Then we can write the full line element from (2.16) as

$$
\begin{aligned}
ds^2 ={}& -\left(Q^2 - a^2 V_t^2 - p^2 U_t^2\right) dt^2 + 2\left(a^2 V_1 V_t + p^2 U_1 U_t + Q^2 T_1\right) dt dx^1 \\
&+ 2\left(a^2 V_2 V_t + p^2 U_2 U_t + Q^2 T_2\right) dt dx^2 + 2\left(a^2 V_t V_\phi + p^2 U_t\right) dt d\phi \\
&+ 2a^2 V_t dt d\psi + \left(\sigma_{11} + a^2 V_1^2 + p^2 U_1^2 - Q^2 T_1^2\right) dx^1 dx^1 \\
&+ 2\left(\sigma_{12} + a^2 V_1 V_2 + p^2 U_1 U_2 - Q^2 T_1 T_2\right) dx^1 dx^2 + 2\left(a^2 V_1 V_\phi + p^2 U_1\right) dx^1 d\phi \\
&+ 2a^2 V_1 dx^1 d\psi + \left(\sigma_{22} + a^2 V_\theta^2 + p^2 U_2^2 - Q^2 T_2^2\right) dx^2 dx^2 + 2\left(a^2 V_2 V_\phi + p^2 U_2\right) dx^2 d\phi \\
&+ 2a^2 V_2 dx^2 d\psi + \left(p^2 + a^2 V_\phi^2\right) d\phi^2 + 2a^2 V_\phi d\phi d\psi + a^2 d\psi^2,
\end{aligned}
\tag{2.21}
$$

where U_1 denotes the x^1 component of U_a, etc.

2.2 Asymptotic Flatness

Now, (2.21) is not particularly enlightening or useful. In order to better understand and hopefully simplify this metric we enforce asymptotic flatness. This assumption constrains the behavior of the unknown metric coefficients at spatial infinity. This will also motivate our choice of the coordinates x^1 and x^2.

For example, asymptotic flatness requires that at spatial infinity, or infinitely far away from the black hole, the metric must become flat. Equivalently, the metric must become Minkowski space, which in 4+1 dimensions and Cartesian-like coordinates can be written as

$$ds^2 = -dt^2 + dx^2 + dy^2 + dz^2 + dw^2. \tag{2.22}$$

Our Cartesian-like coordinates t, x, y, z, and w can take on any real value. However, these coordinates are not adapted to the assumed symmetries of our spacetime. Recall that the spacelike Killing vectors of $\mathcal{M}$ have closed orbits. This precludes the adapted coordinates taking on all value in the reals. Typically, we choose such coordinates to take values over a finite interval such as $[0, 2\pi]$.

With this property in mind, one might think spherical coordinates in 4+1 dimensions would be a good choice. Minkowski space can be expressed in these coordinates as:

$$ds^2 = -dt^2 + dr^2 + r^2 \left[d\theta^2 + \sin^2 \theta \left(d\phi^2 + \sin^2 \phi \, d\psi^2 \right) \right], \tag{2.23}$$

where $t \in \mathbb{R}$, $r \in [0, \infty)$, both θ and ϕ take values from the interval $[0, \pi]$, and $\psi \in [0, 2\pi]$. This coordinate system is closer to what we would like, but only ψ has a "full" orbital period. If either θ or ϕ were to take on values larger than π we would double count points and our coordinates would not be well defined.

For this reason we choose to use bi-azimuthal coordinates. For flat space the line element in these coordinates is

$$ds^2 = -dt^2 + dr^2 + r^2 \left(d\theta^2 + \sin^2 \theta d\phi^2 + \cos^2 \theta d\psi^2 \right), \tag{2.24}$$

where $t \in \mathbb{R}$, $r \in [0, \infty)$, both ϕ and ψ range over $[0, 2\pi]$, and $\theta \in [0, \frac{\pi}{2}]$. Because both ϕ and ψ parameterize closed orbits, these coordinates seem best adapted to the symmetries of our spacetime. To correspond to this choice, we pick $x^1 = r \in [0, \infty)$ and $x^2 = \theta \in [0, \frac{\pi}{2}]$. Taking advantage of the fact that any two dimensional Riemannian metric is conformally flat, we can write the line element of σ_{ab}

$$^{(2)}ds^2 = e^{2\alpha} \left(dr^2 + r^2 d\theta^2 \right) \tag{2.25}$$

where α is an as yet undetermined function of r and θ.

Now that we have decided what form (2.21) will take at infinity we can find the asymptotic limits of the metric coefficients. Because the Killing vectors do not become null at infinity (that is, their norms do not become zero) we immediately see that V_t, V_r, V_θ, V_ϕ, U_t, U_r, U_θ, T_r, and T_θ must all vanish at spatial infinity. It then follows that at spatial infinity

$$\alpha \to 0 \quad Q^2 \to 1 \quad p^2 \to r^2 \sin^2 \theta \quad a^2 \to r^2 \cos^2 \theta. \tag{2.26}$$

2.3   The Ricci Tensor

Now that all the building blocks have been defined, we can construct the geometric components of the Einstein equations. We begin with the metric connection

$$\begin{aligned}
\Gamma^a_{bc} &= \frac{1}{2} g^{ad} \left(\partial_b g_{cd} + \partial_c g_{bd} - \partial_d g_{bc} \right) \\
&= {}^{(2)}\Gamma^a_{bc} + \frac{1}{2} \sigma^{ad} \Xi_{bcd} + \frac{1}{2} V^a \Omega_{bc} + \frac{1}{2} U^a \Sigma_{bc} - \frac{1}{2} T^a \Pi_{bc}
\end{aligned} \tag{2.27}$$

where we have made the following definitions

$$^{(2)}\Gamma^a_{bc} \equiv \frac{1}{2}\sigma^{ad}\left(\partial_b\sigma_{cd} + \partial_c\sigma_{bd} - \partial_d\sigma_{bc}\right) \tag{2.28}$$

$$\Xi_{bcd} \equiv a^2\left(V_b{}^{(2)}Z_{cd} + V_c{}^{(2)}Z_{bd}\right) - a^2\left(V_bU_c + V_cU_b\right)\partial_dV_\phi$$
$$+ a^2\left(V_bT_c + V_cT_b\right)\left(\partial_dV_t - U_t\partial_dV_\phi\right) + p^2\left(U_b{}^{(2)}Y_{cd} + U_c{}^{(2)}Y_{bd}\right)$$
$$+ p^2\left(U_bT_c + U_cT_b\right)\partial_dU_t - Q^2\left(T_b{}^{(2)}W_{cd} + T_c{}^{(2)}W_{bd}\right)$$
$$- V_bV_c\partial_da^2 - U_bU_c\partial_dp^2 + T_bT_c\partial_dQ^2 \tag{2.29}$$

$$\Omega_{bc} \equiv \partial_b\left(a^2V_c\right) + \partial_c\left(a^2V_b\right) \tag{2.30}$$

$$\Sigma_{bc} \equiv \partial_b\left(p^2U_c\right) + \partial_c\left(p^2U_b\right) + a^2\left(V_b\partial_cV_\phi + V_c\partial_bV_\phi\right) \tag{2.31}$$

$$\Pi_{bc} \equiv \partial_b\left(Q^2T_c\right) + \partial_c\left(Q^2T_b\right) + p^2\left(U_b\partial_cU_t + U_c\partial_bU_t\right)$$
$$+ a^2[V_b\left(\partial_cV_t - U_t\partial_cV_\phi\right) + V_c\left(\partial_bV_t - U_t\partial_bV_\phi\right)]. \tag{2.32}$$

Last, we separate the Ricci tensor as defined by

$$R_{ab} = \partial_c\Gamma^c_{ab} - \partial_b\Gamma^c_{ac} + \Gamma^e_{ab}\Gamma^c_{ec} - \Gamma^e_{ac}\Gamma^c_{eb}. \tag{2.33}$$

We can express the five dimensional Ricci tensor in 2-covariant form by defining Δ_c as the covariant derivative with respect to the 2-metric ,σ_{ab}, on $\mathcal{N}$. In accordance with [24] the operator Δ_c is defined on the 2-manifold and with respect to σ_{ab} by

$$\Delta_cA^a{}_b \equiv \sigma^d{}_c\sigma^a{}_e\sigma^f{}_b\nabla_dA^e{}_f. \tag{2.34}$$

This is equivalent to

$$\Delta_c{}^{(2)}A^a{}_b = \partial_c{}^{(2)}A^a{}_b + {}^{(2)}\Gamma^a_{cd}{}^{(2)}A^d{}_b - {}^{(2)}\Gamma^d_{cb}{}^{(2)}A^a{}_d, \tag{2.35}$$

where we have highlighted the fact that Δ_c must operate on tensors living on $\mathcal{N}$. Recall that because we chose coordinates adapted to our Killing vectors, any scalar function f on $\mathcal{N}$ will satisfy

$$\Delta_cf = \partial_cf. \tag{2.36}$$

The Ricci tensor then takes the form[2]

$$
\begin{aligned}
R_{ab} = \sigma_a{}^c \sigma_b{}^d &\left[{}^{(2)}R_{cd} - \frac{1}{a}\Delta_c\Delta_d a - \frac{1}{p}\Delta_c\Delta_d p - \frac{1}{Q}\Delta_c\Delta_d Q - \frac{a^2}{2p^2}\Delta_c V_\phi \, \Delta_d V_\phi \right. \\
&\quad + \frac{p^2}{2Q^2}\Delta_c U_t \, \Delta_d U_t + \frac{a^2}{2Q^2}\left(\Delta_c V_t - U_t\Delta_c V_\phi\right)\left(\Delta_d V_t - U_t\Delta_d V_\phi\right) \\
&\quad \left. + \frac{a^2}{2}\,{}^{(2)}Z_c{}^e\,{}^{(2)}Z_{ed} + \frac{p^2}{2}\,{}^{(2)}Y_c{}^e\,{}^{(2)}Y_{ed} - \frac{Q^2}{2}\,{}^{(2)}W_c{}^e\,{}^{(2)}W_{ed} \right] \\
+ 2V_{(a}\sigma_{b)}{}^d &\left[\frac{1}{2a^3 pQ}\Delta_c\left(a^3 pQ\,{}^{(2)}Z_d{}^c\right) \right] \\
+ 2U_{(a}\sigma_{b)}{}^d &\left[\frac{1}{2ap^3 Q}\Delta_c\left(ap^3 Q\,{}^{(2)}Y_d{}^c\right) + \frac{a^2}{2p^2}\,{}^{(2)}Z_d{}^c\Delta_c V_\phi \right] \\
+ 2T_{(a}\sigma_{b)}{}^d &\left[\frac{1}{2apQ^3}\Delta_c\left(apQ^3\,{}^{(2)}W_d{}^c\right) + \frac{p^2}{2Q^2}\,{}^{(2)}Y_d{}^c\Delta_c U_t + \frac{a^2}{2Q^2}\,{}^{(2)}Z_d{}^c\left(\Delta_c V_t - U_t\Delta_c V_\phi\right) \right] \\
+ V_a V_b &\left[\frac{-a}{pQ}\Delta^c\left(pQ\Delta_c a\right) + \frac{a^4}{4}\,{}^{(2)}Z^{cd}\,{}^{(2)}Z_{cd} + \frac{a^4}{2p^2}\Delta_c V_\phi \, \Delta^c V_\phi \right. \\
&\quad \left. - \frac{a^4}{2Q^2}\left(\Delta_c V_t - U_t\Delta_c V_\phi\right)\left(\Delta^c V_t - U_t\Delta^c V_\phi\right) \right] \\
+ 2V_{(a}U_{b)} &\left[\frac{-p}{2aQ}\Delta^c\left(\frac{Qa^3}{p}\Delta_c V_\phi\right) + \frac{a^2 p^2}{4}\,{}^{(2)}Z^{cd}\,{}^{(2)}Y_{cd} - \frac{a^2 p^2}{2Q^2}\left(\Delta_c V_t - U_t\Delta_c V_\phi\right)\Delta^c U_t \right] \\
+ 2V_{(a}T_{b)} &\left[\frac{Q}{2ap}\Delta^c\left(\frac{a^3 p}{Q}\left(\Delta_c V_t - U_t\Delta_c V_\phi\right)\right) - \frac{a^2 Q^2}{4}\,{}^{(2)}Z^{cd}\,{}^{(2)}W_{cd} \right] \\
+ U_a U_b &\left[\frac{-p}{aQ}\Delta^c\left(aQ\Delta_c p\right) + \frac{p^4}{4}\,{}^{(2)}Y^{cd}\,{}^{(2)}Y_{cd} - \frac{a^2}{2}\Delta_c V_\phi \, \Delta^c V_\phi - \frac{p^4}{2Q^2}\Delta_c U_t \, \Delta^c U_t \right] \\
+ 2U_{(a}T_{b)} &\left[\frac{Q}{2ap}\Delta^c\left(\frac{ap^3}{Q}\Delta_c U_t\right) - \frac{p^2 Q^2}{4}\,{}^{(2)}Y^{cd}\,{}^{(2)}W_{cd} + \frac{a^2}{2}\left(\Delta_c V_t - U_t\Delta_c V_\phi\right)\Delta^c V_\phi \right] \\
+ T_a T_b &\left[\frac{Q}{ap}\Delta^c\left(ap\Delta_c Q\right) + \frac{Q^4}{4}\,{}^{(2)}W^{cd}\,{}^{(2)}W_{cd} - \frac{p^2}{2}\Delta_c U_t \, \Delta^c U_t \right. \\
&\quad \left. - \frac{a^2}{2}\left(\Delta_c V_t - U_t\Delta_c V_\phi\right)\left(\Delta^c V_t - U_t\Delta^c V_\phi\right) \right]
\end{aligned}
\tag{2.37}
$$

While the above expression looks unwieldy, recall that each combination of vectors or tensors not enclosed in brackets are linearly independent. In the subsequent chapter we similarly separate the stress-energy tensor, leading to a set of scalar equations rather than one tensor equation.

---

[2]The parenthesis around indices denotes symmetrization in the usual way: $T_{(ab)} \equiv \frac{1}{2}\left(T_{ab} + T_{ba}\right)$.

Chapter 3

Electromagnetic Considerations

In the last chapter we expressed the Ricci tensor, which will serve as the geometric part of the Einstein equations, as a set of linearly independent terms. In this chapter we separate the electromagnetic stress-energy tensor in a similar way. We will then be able to equate each linearly independent term through the Einstein equations. These associated terms make explicit the two dimensional tensorial equation, a set of six scalar equations, and the three Maxwell-like equations mentioned in Chapter 1. Similarly, we will separate the 4+1 Maxwell equations into a two dimensional Maxwell equation on the submanifold $\mathcal{N}$ and three additional scalar equations.

3.1   The Stress-Energy Tensor

Since we wish to find solutions to the Einstein-Maxwell equations we must construct the stress-energy tensor T_{ab} for electromagnatism and decompose it as we did the Ricci tensor. Where before we began with the metric g_{ab} as our fundamental quantity, here we begin with the electromagnetic vector potential A_a. From this potential we define the Maxwell field

tensor F_{ab} in the usual way

$$F_{ab} = \partial_a A_b - \partial_b A_a, \tag{3.1}$$

so that the stress-energy tensor for electromagnetism becomes

$$4\pi T_{ab} = F_a{}^d F_{bd} - \frac{1}{4} g_{ab} F_{cd} F^{cd}. \tag{3.2}$$

We also make the following definitions for convenience in subsequent equations:

$$V^a A_a \equiv A_V \quad U^a A_a \equiv A_U \quad T^a A_a \equiv A_T \tag{3.3}$$

and

$$E_a \equiv \Delta_a(Q^2 A_T) + p^2 A_U \Delta_a U_t + a^2 A_V \left(\Delta_a V_t - U_t \Delta_a V_\phi \right) \tag{3.4}$$

$$B_a \equiv \Delta_a(p^2 A_U) + a^2 A_V \Delta_a V_\phi. \tag{3.5}$$

Note that E_a, B_a, and $\Delta_a(a^2 A_V)$ are vectors that live strictly in $\mathcal{N}$. Using the above definitions the stress-energy tensor may be expressed as

$$\begin{aligned}
4\pi T_{ab} = \sigma_a{}^c \sigma_b{}^d & \left[{}^{(2)}F_c{}^e \, {}^{(2)}F_{de} + \frac{1}{a^2} \Delta_c(a^2 A_V) \Delta_d(a^2 A_V) + \frac{1}{p^2} B_c B_d - \frac{1}{Q^2} E_c E_d \right. \\
& \left. - \frac{1}{4} \sigma_{cd} \left\{ {}^{(2)}F^{ef} \, {}^{(2)}F_{ef} + \frac{2}{a^2} \Delta_e(a^2 A_V) \Delta^e(a^2 A_V) + \frac{2}{p^2} B^e B_e - \frac{2}{Q^2} E^e E_e \right\} \right] \\
& + 2 V_{(a} \sigma_{b)}{}^d \left[- {}^{(2)}F_d{}^e \Delta_e(a^2 A_V) \right] + 2 U_{(a} \sigma_{b)}{}^d \left[- {}^{(2)}F_d{}^e B_e \right] + 2 T_{(a} \sigma_{b)}{}^d \left[{}^{(2)}F_d{}^e E_e \right] \\
& + V_a V_b \left[\frac{1}{2} \Delta^e(a^2 A_V) \Delta_e(a^2 A_V) - \frac{a^2}{4} \, {}^{(2)}F^{ef} \, {}^{(2)}F_{ef} - \frac{a^2}{2p^2} B^e B_e + \frac{a^2}{2Q^2} E^e E_e \right] \\
& + 2 V_{(a} U_{b)} \left[\Delta_e(a^2 A_V) B^e \right] + 2 V_{(a} T_{b)} \left[- \Delta_e(a^2 A_V) E^e \right] + 2 U_{(a} T_{b)} \left[- B_e E^e \right] \\
& + U_a U_b \left[\frac{1}{2} B^e B_e - \frac{p^2}{4} \, {}^{(2)}F^{ef} \, {}^{(2)}F_{ef} - \frac{p^2}{2a^2} \Delta^e(a^2 A_V) \Delta_e(a^2 A_V) + \frac{p^2}{2Q^2} E^e E_e \right] \\
& + T_a T_b \left[\frac{1}{2} E^e E_e + \frac{Q^2}{4} \, {}^{(2)}F^{ef} \, {}^{(2)}F_{ef} + \frac{Q^2}{2a^2} \Delta^e(a^2 A_V) \Delta_e(a^2 A_V) + \frac{Q^2}{2p^2} B^e B_e \right].
\end{aligned} \tag{3.6}$$

The last quantity we need for the Einstein equations is the trace of T_{ab}, which we denote $T^a{}_a \equiv T$. This is readily computed from (3.6):

$$4\pi T = \frac{1}{2Q^2} E^e E_e - \frac{1}{4} \, {}^{(2)}F^{ef} \, {}^{(2)}F_{ef} - \frac{1}{2a^2} \Delta^e(a^2 A_V) \Delta_e(a^2 A_V) - \frac{1}{2p^2} B^e B_e. \tag{3.7}$$

3.2 Maxwell's Equations

We next consider Maxwell's equations in source free regions. In terms of F_{ab} these can be written as

$$\nabla_b F^{ab} = 0 \tag{3.8}$$

$$\partial_{[a} F_{bc]} = 0 \tag{3.9}$$

where the square brackets on the indices denote antisymmetrization. Because our definition of the field tensor (3.1) is explicitly antisymmetric (3.9) is trivially satisfied, and only (3.8) remains to be solved.

As before, we decompose these equations along and orthogonal to the directions defined by our assumed Killing vectors. Since we are working with a vector rather than tensor equation the separation is simpler. Explicitly,

$$0 = \nabla_b F^{ab} = \sigma^a{}_c \nabla_b F^{cb} + V^a \left[a^2 V_c \nabla_b F^{cb} \right] + U^a \left[p^2 U_c \nabla_b F^{cb} \right] - T^a \left[Q^2 T_c \nabla_b F^{cb} \right]. \tag{3.10}$$

Again, because each term is linearly independent of the others each term must vanish individually. This leads to the following equations

$$\frac{1}{apQ} \Delta_e \left(apQ \, {}^{(2)}F^{ae} \right) = 0 \tag{3.11}$$

$$\frac{1}{apQ} \Delta_e \left(\frac{pQ}{a} \Delta^e(a^2 A_V) \right) = \frac{1}{2} \, {}^{(2)}F^{ef} \, {}^{(2)}Z_{ef} + \frac{1}{p^2} B^e \Delta_e V_\phi - \frac{1}{Q^2} E^e \left(\Delta_e V_t - U_t \Delta_e V_\phi \right) \tag{3.12}$$

$$\frac{1}{apQ} \Delta_e \left(\frac{aQ}{p} B^e \right) = \frac{1}{2} \, {}^{(2)}F^{ef} \, {}^{(2)}Y_{ef} - \frac{1}{Q^2} E^e \Delta_e U_t \tag{3.13}$$

$$\frac{1}{apQ} \Delta_e \left(\frac{ap}{Q} E^e \right) = \frac{1}{2} \, {}^{(2)}F^{ef} \, {}^{(2)}W_{ef}. \tag{3.14}$$

The first of these equations is readily identified as Maxwell's equations on $\mathcal{N}$ in source free regions. The remaining three equations are all scalar and have similarities in their sources. Each is sourced by one the KK Maxwell fields contracted with the physical Maxwell field. Additionally, (3.12) and (3.13) are sourced by interactions between functions associated with rotations and the components of the projections of the vector potential.

Chapter 4

Simplifying the Einstein Equations

The results of chapters 2 and 3 give us all we need to pose the Einstein-Maxwell equations in our formalism. However, due to the multiplicity of terms in (2.37) and (3.6) we are motivated to simplify these equations as much as possible before we solve them.

In our units, the Einstein equations of general relativity are

$$R_{ab} - \frac{1}{2}g_{ab}R = 8\pi T_{ab}, \tag{4.1}$$

where R is the Ricci scalar defined by $R \equiv R^a{}_a$. By taking the trace of both sides of (4.1) we find

$$R\frac{2-n}{2} = 8\pi T, \tag{4.2}$$

where n is the dimension of spacetime. This allows us to rewrite the Einstein equations in five dimensions as

$$R_{ab} = 8\pi \left(T_{ab} - \frac{1}{3}g_{ab}T \right). \tag{4.3}$$

We then use the linear independence of each Killing vector "direction" to equate terms on each side of (4.3) using (2.37), (3.6), and (3.7).

4.1 E&M in Two Dimensions

First, we note the similarity between the equation for the two dimensional E&M field (3.11) and the equations for the three Maxwell-like fields from the dimensional reduction:

$$\frac{1}{2a^3pQ}\Delta_c\left(^{(2)}Z^{ac}a^3pQ\right) =^{(2)}F^{ac}\Delta_c\left(a^2A_v\right) \tag{4.4}$$

$$\frac{1}{2ap^3Q}\Delta_c\left(^{(2)}Y^{ac}ap^3Q\right) =^{(2)}F^{ac}B_c - \frac{a^2}{2p^2}\,^{(2)}Z^{ac}\Delta_cV_\phi \tag{4.5}$$

$$\frac{1}{2apQ^3}\Delta_c\left(^{(2)}W^{ac}apQ^3\right) = -\,^{(2)}F^{ac}E_c - \frac{p^2}{2Q^2}\,^{(2)}Y^{ac}\Delta_cU_t$$

$$- \frac{a^2}{2Q^2}\,^{(2)}Z^{ac}\left(\Delta_cV_t - U_t\Delta_cV_\phi\right). \tag{4.6}$$

We can simplify all these equations by taking advantage of the properties of E&M in two dimensions.

Consider an arbitrary antisymmetric Maxwell-like field f^{ab} on a two dimensional manifold $\mathcal{N}$ with metric $\sigma_{ab}(x^1,x^2)$ and covariant derivative Δ_c. The defining relation for f^{ab} (similar to (3.8)) is

$$\Delta_af^{ab} = -j^b \tag{4.7}$$

where j^b is a source term. Now, due to the antisymmetry of f^{ab}

$$\Delta_b\Delta_af^{ab} = \Delta_b\left(\partial_af^{ab} + \Gamma^a_{ac}f^{cb} + \Gamma^b_{ac}f^{ac}\right)$$

$$= \partial_b\left(\partial_af^{ab} + \Gamma^a_{ac}f^{cb}\right) + \Gamma^b_{bd}\left(\partial_af^{ad} + \Gamma^a_{ac}f^{cd}\right)$$

$$= \partial_b\left(\Gamma^a_{ac}f^{cb}\right) - \Gamma^a_{ac}\partial_bf^{cb}$$

$$= f^{cb}\partial_b\Gamma^a_{ac}$$

$$= f^{cb}\partial_b\partial_c\ln\sqrt{\sigma} = 0 \tag{4.8}$$

where we have used the fact that the product of antisymmetric and symmetric quantities vanish as well as the identity

$$\Gamma^a_{ac} = \partial_c\ln\sqrt{\sigma} \tag{4.9}$$

where σ is the determinant of the metric. Then, by combining (4.7) and (4.8) we find the following constraint on j^a

$$0 = \Delta_b j^b$$

$$= \partial_b j^b + j^c \partial_c \ln \sqrt{\sigma}$$

$$= \frac{1}{\sqrt{\sigma}} \partial_b \left(j^b \sqrt{\sigma} \right) \tag{4.10}$$

or, in terms of components

$$\partial_1 \left(j^1 \sqrt{\sigma} \right) = -\partial_2 \left(j^2 \sqrt{\sigma} \right). \tag{4.11}$$

Simplification enters at this point by defining a scalar function $P(x^1, x^2)$ such that

$$\partial_2 P = j^1 \sqrt{\sigma} \quad \partial_1 P = -j^2 \sqrt{\sigma}. \tag{4.12}$$

Notice that P has been constructed to satisfy (4.11) identically. This allows us to solve for j^a as follows

$$j^a = \varepsilon^{ab} \partial_b P$$

$$= \varepsilon^{ab} \Delta_b P, \tag{4.13}$$

where ε^{ab} is the Levi-Civita tensor. In terms of the completely antisymmetric symbol $[a\ b]$[1] it is defined by

$$\varepsilon^{ab} = \frac{1}{\sqrt{\sigma}} [a\ b]. \tag{4.14}$$

This definition of j^a leads to a simple solution of f^{ab}. By substituting (4.13) into (4.7) we find

$$\Delta_a f^{ab} = -\varepsilon^{ba} \Delta_a P$$

$$= -\Delta_a \left(\varepsilon^{ba} P \right), \tag{4.15}$$

---

[1]That is to say $[a\ b] = -[b\ a]$.

which leads to

$$\Delta_a \left(f^{ab} - \varepsilon^{ab} P \right) = 0. \tag{4.16}$$

This shows that f^{ab} is exactly P multiplied by ε^{ab} up to a constant multiple of ε^{ab}. By absorbing this constant into the definition of P we find the result

$$f^{ab} = \varepsilon^{ab} P. \tag{4.17}$$

Returning to our four Maxwell-like fields we can define

$$^{(2)}F^{ab} \equiv \hat{f} \varepsilon^{ab} \quad ^{(2)}Z^{ab} \equiv \hat{z} \varepsilon^{ab} \quad ^{(2)}Y^{ab} \equiv \hat{y} \varepsilon^{ab} \quad ^{(2)}W^{ab} \equiv \hat{w} \varepsilon^{ab} \tag{4.18}$$

where $\hat{f}$, $\hat{z}$, $\hat{y}$, and $\hat{w}$ are scalar functions of r and θ. We then rewrite (3.11) as a scalar equation

$$\Delta_c \left(apQ\varepsilon^{ac} \hat{f} \right) = 0$$
$$\varepsilon^{ac} \partial_c \left(apQ\hat{f} \right) = 0$$
$$\partial_c \left(apQ\hat{f} \right) = 0. \tag{4.19}$$

Then for some constant k_1 we have

$$\hat{f} = \frac{k_1}{apQ}. \tag{4.20}$$

Recalling the asymptotic behavior of a, p, and Q from (2.26) we can make the definition

$$apQ = r^2 \sin\theta \cos\theta F(r, \theta), \tag{4.21}$$

where F goes to one at spatial infinity. This definition make explicit that at $\theta = 0$ and $\theta = \frac{\pi}{2}$ $\hat{f}$ diverges, unless $k_1 = 0$. So, we find

$$\hat{f} = 0. \tag{4.22}$$

This result agrees with [22] where the authors show that in a 4+1 spacetime with the Killing vectors of the MP solution the vector potential only has components in the directions of the

Killing vectors. We say that such a vector potential is circular. In fact, such a result must be true since our spacetime satisfies the requirements of theorems which prove electromagnetic potential circularity(see Carter's corollary to theorem 7 in [25]). We have, in effect, explicitly proved this theorem for our special case.

Besides agreeing with previous work, the vanishing of $\hat{f}$ also begins the simplification of our equation set. For instance, (4.4) becomes

$$\Delta_c \left(a^3 p Q \varepsilon^{ac} \hat{z} \right) = 0, \tag{4.23}$$

which leads analogously to

$$\hat{z} = 0. \tag{4.24}$$

Similarly, (4.5) and (4.6) lead to

$$\hat{y} = 0 \quad \hat{w} = 0. \tag{4.25}$$

Our progress toward simplification is marked. Already, the four two dimensional Maxwell fields have been shown to be identically zero. In the next section we show that this allows us to further simplify the metric.

4.2 Gauge Choice

Now that we have shown that the Maxwell fields vanish on the two manifold, we have constrained the r and θ components of the Killing vectors. These constraint equations leave room for a gauge choice in certain metric coefficients. For example, from (2.18) we find

$$^{(2)}W_{ab} = W_{ab} = \partial_a T_b - \partial_b T_a = 0 \tag{4.26}$$

as a constraint on the components of T_a. However, this relation only constrains the r and θ components since each component is independent of t, ϕ, and ψ and T^a is orthogonal to ψ^a

and ϕ^a. We also notice that this constraint does not uniquely define T_r or T_θ. Specifically, any T'_a such that

$$T'_a = T_a + \partial_a \chi \tag{4.27}$$

for any scalar function $\chi(r, \theta)$ still satisfies (4.26). A convenient choice for χ is

$$\partial_a \chi = -T_a \tag{4.28}$$

where we have tacitly restricted the index to r and θ. With this choice we immediately find

$$T'_a = T_a - T_a = 0 \tag{4.29}$$

or more specifically

$$T_r = 0 \quad T_\theta = 0. \tag{4.30}$$

With T_r and T_θ set to zero we move on to the next constraint (2.19). Notice again that only the U_r and U_θ components are constrained. With this in mind we restrict indices to r and θ as before. Under this restriction (2.19) becomes

$$^{(2)}Y_{ab} = \partial_a U_b - \partial_b U_a = 0. \tag{4.31}$$

We then argue exactly as before that

$$U_r = 0 \quad U_\theta = 0. \tag{4.32}$$

The last constraint (2.20) has the analogous effect, namely

$$V_r = 0 \quad V_\theta = 0. \tag{4.33}$$

When we consider the metric as written in (2.21) it is clear that the gauge choice made in this section substantially simplifies the metric. In effect we have chosen a gauge in which the metric has no cross terms between the two-manifold and the subspace spanned by the Killing vectors.

4.3 The Einstein-Maxwell Equations

While further simplification would be welcome, we have reached the point where simplifications are harder to come by. Still, we have solved four equations, and their solution does simplify the remaining equations considerably.

We now write the remaining Einstein equations. First, the two dimensional Einstein equation on $\mathcal{N}$ is

$$
\begin{aligned}
^{(2)}R_{ab} =& \frac{1}{a}\Delta_a\Delta_b a + \frac{1}{p}\Delta_a\Delta_b p + \frac{1}{Q}\Delta_a\Delta_b Q + \frac{a^2}{2p^2}\Delta_a V_\phi\,\Delta_b V_\phi - \frac{p^2}{2Q^2}\Delta_a U_t\,\Delta_b U_t \\
& - \frac{a^2}{2Q^2}\left(\Delta_a V_t - U_t\Delta_a V_\phi\right)\left(\Delta_b V_t - U_t\Delta_b V_\phi\right) + \frac{2}{a^2}\Delta_a\left(a^2 A_V\right)\Delta_b\left(a^2 A_V\right) \\
& + \frac{2}{p^2}B_a B_b - \frac{2}{Q^2}E_a E_b - \frac{2}{3}\sigma_{ab}\left[\frac{1}{a^2}\Delta_c\left(a^2 A_V\right)\Delta_c\left(a^2 A_V\right)\right. \\
& \left. + \frac{1}{p^2}B^c B_c - \frac{1}{Q^2}E^c E_c\right].
\end{aligned}
\tag{4.34}
$$

The immediate forms of the scalar equations are

$$
\begin{aligned}
\frac{a}{pQ}\Delta^c\left(pQ\Delta_c a\right) =& \frac{a^4}{2p^2}\Delta_c V_\phi\,\Delta^c V_\phi - \frac{a^4}{2Q^2}\left(\Delta_c V_t - U_t\Delta_c V_\phi\right)\left(\Delta^c V_t - U_t\Delta^c V_\phi\right) \\
& - \frac{2}{3}\left[2\Delta_c\left(a^2 A_V\right)\Delta^c\left(a^2 A_V\right) - \frac{a^2}{p^2}B^c B_c + \frac{a^2}{Q^2}E^c E_c\right]
\end{aligned}
\tag{4.35}
$$

$$
\begin{aligned}
\frac{p}{aQ}\Delta^c\left(aQ\Delta_c p\right) =& -\frac{a^2}{2}\Delta_c V_\phi\,\Delta^c V_\phi - \frac{p^4}{2Q^2}\Delta_c U_t\,\Delta^c U_t - \frac{2}{3}\left[2B^c B_c\right. \\
& \left. - \frac{p^2}{a^2}\Delta_c\left(a^2 A_V\right)\Delta^c\left(a^2 A_V\right) + \frac{p^2}{Q^2}E^c E_c\right]
\end{aligned}
\tag{4.36}
$$

$$
\begin{aligned}
\frac{Q}{ap}\Delta^c\left(ap\Delta_c Q\right) =& \frac{p^2}{2}\Delta_c U_t\,\Delta^c U_t + \frac{a^2}{2}\left(\Delta_c V_t - U_t\Delta_c V_\phi\right)\left(\Delta^c V_t - U_t\Delta^c V_\phi\right) \\
& + \frac{2}{3}\left[2E^c E_c + \frac{Q^2}{a^2}\Delta_c\left(a^2 A_V\right)\Delta^c\left(a^2 A_V\right) + \frac{Q^2}{p^2}B^c B_c\right]
\end{aligned}
\tag{4.37}
$$

$$
\frac{p}{2aQ}\Delta^c\left(\frac{a^3 Q}{p}\Delta_c V_\phi\right) = -\frac{a^2 p^2}{2Q^2}\left(\Delta^c V_t - U_t\Delta^c V_\phi\right)\Delta_c U_t - B^c\Delta_c\left(a^2 A_V\right)
\tag{4.38}
$$

$$
\frac{Q}{2ap}\Delta^c\left(\frac{a^3 p}{Q}\left[\Delta_c V_t - U_t\Delta_c V_\phi\right]\right) = -E^c\Delta_c\left(a^2 A_V\right)
\tag{4.39}
$$

$$
\frac{Q}{2ap}\Delta^c\left(\frac{ap^3}{Q}\Delta_c U_t\right) = -\frac{a^2}{2}\left(\Delta^c V_t - U_t\Delta^c V_\phi\right)\Delta_c V_\phi - B^c E_c.
\tag{4.40}
$$

While this is the initial form of the equations, certain combinations may be simpler to solve.

Notice for example, that we can combine (4.35), (4.36), and (4.37) into

$$\Delta^c \Delta_c \left(apQ \right) = 0. \tag{4.41}$$

Similarly, we can combine (4.35) and (4.37) into

$$\frac{1}{apQ} \Delta^c \left(p\Delta_c aQ \right) = \frac{a^2}{2p^2} \Delta_c V_\phi \, \Delta^c V_\phi + \frac{p^2}{2Q^2} \Delta_c U_t \, \Delta^c U_t - \frac{2}{3a^2} \Delta_c \left(a^2 A_V \right) \Delta^c \left(a^2 A_V \right)$$
$$+ \frac{4aQ}{3p} B^c B_c + \frac{2}{3Q^2} E^c E_c \tag{4.42}$$

and (4.36) and (4.37) into

$$\frac{1}{apQ} \Delta^c \left(a\Delta_c pQ \right) = \frac{a^2}{2Q^2} \left(\Delta_c V_t - U_t \Delta_c V_\phi \right) \left(\Delta^c V_t - U_t \Delta^c V_\phi \right) - \frac{a^2}{2p^2} \Delta_c V_\phi \, \Delta^c V_\phi$$
$$+ \frac{4}{3a^2} \Delta_c \left(a^2 A_V \right) \Delta^c \left(a^2 A_V \right) - \frac{2}{3p^2} B^c B_c + \frac{2}{3Q^2} E^c E_c. \tag{4.43}$$

The reasoning behind these last two combinations is not as clear as the first. However, we will see in the following chapter that these combinations have definite Dirichlet boundary conditions, which will be essential for our numerical method.

For completeness we restate the remaining Maxwell equations:

$$\frac{1}{apQ} \Delta_e \left(\frac{pQ}{a} \Delta^e (a^2 A_V) \right) = \frac{1}{p^2} B^e \Delta_e V_\phi - \frac{1}{Q^2} E^e \left(\Delta_e V_t - U_t \Delta_e V_\phi \right) \tag{4.44}$$

$$\frac{1}{apQ} \Delta_e \left(\frac{aQ}{p} B^e \right) = -\frac{1}{Q^2} E^e \Delta_e U_t \tag{4.45}$$

$$\frac{1}{apQ} \Delta_e \left(\frac{ap}{Q} E^e \right) = 0. \tag{4.46}$$

While the last two of these look relatively simple, recall from chapter 3 that E^a and B^a are shorthands for longer expressions. In summary, the remaining equations are a two dimensional tensorial equation and nine scalar equations. In the following chapter we will motivate which combinations of these scalar equations are best suited to numerical solution.

Chapter 5

Boundary Conditions

In chapter 4 we wrote the Einstein-Maxwell equations after imposing our simplifying assumptions. Specifically, we found nine equations with second order derivative operators acting on our unknown scalar functions. From the theory of partial differential equations, we know that in order to completely determine these functions we will need to specify boundary conditions at spatial infinity and the event horizon.

Our assumption of asymptotic flatness and the vanishing of the vector potential at infinity determine the behavior of all the scalar functions at spatial infinity. In particular they all approach some constant value. In addition, because we know the asymptotic behavior of every function we can easily find the behavior of their combinations. However, we also need a set of boundary conditions at the event horizon before we can solve the equations. We will motivate a choice of functions which, in addition to approaching a constant value at infinity, will become constants on the event horizon.

5.1   Using the Rigidity Theorem

In Chapter 1 we mentioned that there are a collection of theorems that establish the uniqueness of black holes in four dimensions. One of the components of these theorems has been called the rigidity theorem [7]. This theorem proves the existence of a Killing vector field that at the horizon is (i) tangent to the generators of the event horizon and thus a null vector and (ii) is orthogonal to timelike and spacelike Killing vectors that determine the stationarity and axisymmetry of the spacetime. (Additional discussion of this theorem can be found in Appendix A.)

This theorem has a higher dimensional extension. From the 4+1 rigidity theorem [19] we know there exists a vector field

$$\chi^a = t^a - \Omega_\phi \phi^a - \Omega_\psi \psi^a \tag{5.1}$$

with constants Ω_ϕ and Ω_ψ, which, on the event horizon, satisfies

$$\chi^a \chi_a = 0, \quad \chi^a t_a = 0, \quad \chi^a \phi_a = 0, \quad \chi^a \psi_a = 0. \tag{5.2}$$

More particularly, at the horizon χ^a is tangent to the generators of the event horizon, which implies that it is null.

Since the inner product between χ^a and the Killing vectors vanishes at the horizon, we have the relations

$$\chi^a \psi_a \big|_{r_h} = a^2 \left(V_t - \Omega_\psi - V_\phi \Omega_\phi \right) = 0 \tag{5.3}$$

and

$$\chi^a \phi_a \big|_{r_h} = b^2 \left(U_t - \Omega_\phi \right) + a^2 V_\phi \left(V_t - U_t V_\phi - \Omega_\psi \right) = 0 \tag{5.4}$$

where r_h denotes the coordinate location of the event horizon. We can then substitute (5.3) into (5.4) as

$$p^2 \left(U_t - \Omega_\phi \right) = 0. \tag{5.5}$$

Since p^2 does not vanish at the horizon (or equivalently U^a does not become null) we find

$$U_t\big|_{r_h} = \Omega_\phi, \tag{5.6}$$

where Ω_ϕ can be thought of as the angular velocity of the event horizon in the ϕ direction. Using this relation in (5.4) we also find

$$(V_t - U_t V_\phi)\big|_{r_h} = \Omega_\psi. \tag{5.7}$$

Again, we can interpret Ω_ψ as the angular velocity of the event horizon in the ψ direction. We can then use (5.6) and (5.7) to show

$$\chi^a t_a\big|_{r_h} = -Q^2\big|_{r_h} = 0 \tag{5.8}$$

at the horizon.

It is clear that the results of the rigidity theorem motivate solving for certain combinations of the scalar fields. For instance, from (5.7) we choose to solve for the function

$$W \equiv V_t - U_t V_\phi \tag{5.9}$$

since we know the boundary condition at the horizon, and from asymptotic flatness W must vanish at spatial infinity. In contrast, (5.6) tells us that U_t, which "naturally" comes out of our equation set, is a good function (in the sense of having a known constant value on the horizon) to solve for.

We can also define three more functions with known boundary conditions using (2.26) and (5.8). Recall equations (4.41), (4.42), and (4.43), which we claimed would be useful later. Since we know Q vanishes on the horizon, and we know the asymptotic forms of a, p, and Q we can define the following functions

$$apQ \equiv r^2 \cos\theta \sin\theta F, \quad aQ \equiv r\cos\theta G, \quad pQ \equiv r\sin\theta H \tag{5.10}$$

where F, G, and H all vanish at the event horizon and become 1 at spatial infinity. Thus, from the rigidity theorem we have found the form of five of the nine functions to solve for.

5.2   Rotational Cross Term and E&M

Choosing which combinations of the remaining functions have definite boundary conditions is not as straightforward. As far as we are aware there are no theorems that motivate the following identities. In these cases we rely on known solutions in the 3+1 and 4+1 cases. We will see that both the boundary conditions for the rotational cross term function and the E&M functions will suggest new rigidity-theorem-like vectors.

By considering the MP metric (see section B.2) we find that the combination $\dfrac{V_\phi}{p^2}$ is constant at the horizon with constant value $\Omega_\phi \Omega_\psi$ as defined above. This leads us to define

$$I \equiv \frac{V_\phi}{p^2}. \tag{5.11}$$

While we have no proof that this Dirichlet boundary condition on the horizon is correct in the general charged case, we have determined an equivalent condition that is reminiscent of the rigidity theorem. We begin by assuming that at the event horizon

$$\left. \frac{V_\phi}{p^2} \right|_{r_h} = \Omega_\phi \Omega_\psi. \tag{5.12}$$

This implies that on the horizon

$$
\begin{aligned}
0 =& \psi_\phi - a^2 p^2 \Omega_\phi \Omega_\psi \\
=& \psi_\phi - a^2 \left(b^2 - a^2 V_\phi^2 \right) \Omega_\phi \Omega_\psi \\
=& \psi_\phi - \left(\psi^a \psi_a \phi^b \phi_b - \psi^a \phi^b \psi_b \phi_a \right) \Omega_\phi \Omega_\psi \\
0 =& \psi^a \left[\phi_a - \Omega_\phi \Omega_\psi \phi^b \left(\phi_b \psi_a - \psi_b \phi_a \right) \right],
\end{aligned} \tag{5.13}
$$

or equivalently

$$0 = \phi^a \left[\psi_a - \Omega_\phi \Omega_\psi \psi^b \left(\psi_b \phi_a - \phi_b \psi_a \right) \right], \tag{5.14}$$

where we have used the notation $\psi_\phi = \psi^a \phi_a = a^2 V_\phi$. The symmetry between these last two equivalent forms reinforces the idea that both rotational directions are on equal footing. We

also note that (5.13) and (5.14) can be written in a from even more suggestive of the rigidity theorem. This is done is section C.2. We would expect similar relationships to hold in higher dimensions and this case is considered in section C.3.

The remaining functions are for the components of the vector potential. Here we reason by analogy from the Kerr-Newman metric in 3+1 spacetime (see Appendix A). In short we assume the following boundary conditions:

$$Q^2 A_T\big|_{r_h} = \Phi_h \tag{5.15}$$

$$A_U\big|_{r_h} = \Phi_h \Omega_\phi \tag{5.16}$$

$$A_V - V_\phi A_U\big|_{r_h} = \Phi_h \Omega_\psi, \tag{5.17}$$

where the constant Φ_h is the electric potential at the event horizon and Ω_ϕ and Ω_ψ are the constants we defined earlier. The first of these equations is equivalent to

$$A_a \chi^a\big|_{r_h} = \Phi_h, \tag{5.18}$$

which is similar to the identity explained by Carter [26] in the 3+1 case. (Compare with (A.30).) We also find in section B.1 that (5.15) can be explicitly verified for charged Tangherlini black holes. We also show in section B.3 that all three of these boundary conditions can be verified explicitly for Aliev's [23] perturbative solution.

Similar to the 3+1 case (A.34) we can define the vector

$$\Lambda_a \equiv A_a - \Phi_h \Omega_\psi \psi^a - \Phi_h \Omega_\phi \phi^a \tag{5.19}$$

with properties on the horizon equivalent to the three vector potential boundary conditions. We find that the conditions (5.16), (5.17), and (5.15) are equivalent to requiring that on the event horizon

$$\Lambda_a \phi^a = 0 \tag{5.20}$$

$$\Lambda_a \psi^a = 0 \tag{5.21}$$

$$A_a \chi^a = \Lambda_a t^a = \Phi_h, \tag{5.22}$$

respectively. Similar to our choice of the rotation function W, we solve for

$$A_W \equiv A_V - V_\phi A_U \tag{5.23}$$

rather than A_V since it has a known boundary condition at the horizon. Note that the form of Λ_a is very similar to the χ^a. We make this connection more precise in Chapter 10.

Also, recall that we assume the usual boundary condition for the vector potential at spatial infinity. Specifically, we assume that each component vanishes as we approach infinity. So, to recapitulate, we have chosen to solve for the functions F, G, H, U_t, W, I, $Q^2 A_T$, A_U, and A_W. Which at the event horizon satisfy

$$\begin{aligned} F &= 0 & G &= 0 & H &= 0 \\ U_t &= \Omega_\phi & W &= \Omega_\psi & I &= \Omega_\phi \Omega_\psi \\ Q^2 A_T &= \Phi_h & A_U &= \Phi_h \Omega_\phi & A_W &= \Phi_h \Omega_\psi, \end{aligned} \tag{5.24}$$

and at spatial infinity

$$\begin{aligned} F &= 1 & G &= 1 & H &= 1 \\ U_t &= 0 & W &= 0 & I &= 0 \\ Q^2 A_T &= 0 & A_U &= 0 & A_W &= 0. \end{aligned} \tag{5.25}$$

In short we have chosen a set of scalar equations which satisfy Dirichlet boundary conditions at the horizon and at spatial infinity.

Chapter 6

Nine Scalar Equations

Now that we have found the nine scalar functions with known (or suspected) boundary conditions we can write out the Einstein-Maxwell equations for these functions in coordinate form. We will illustrate this process by one simple example, namely equation (4.41), and then quote the remaining results.

While the specifics of each equation are not tremendously enlightening there are some unifying characteristics we will exploit. For instance, we will see that in every equation we can place terms linear in the function on the left had side, and nonlinear terms on the right hand side. The left hand sides of these equations all have a similar form, specifically that of a modified Laplacian operator.

To see how these operators come about, we begin with (4.41) and using our chosen function F from (5.10) we have

$$\Delta_c \Delta^c \left(r^2 \sin\theta \cos\theta F \right) = 0. \tag{6.1}$$

We then use the following identity for arbitrary scalar functions f and g

$$\Delta_c \left(f \Delta^c g \right) = \frac{1}{\sqrt{\sigma}} \partial_c \left(f \sqrt{\sigma} \sigma^{cd} \partial_d g \right) \tag{6.2}$$

where $\sqrt{\sigma} = re^{2\alpha}$ from (2.25). We then rewrite (6.1) as

$$\partial_c \left(\sqrt{\sigma} \sigma^{cd} \partial_d \left(r^2 \sin\theta \cos\theta F \right) \right) = 0$$

$$\sin\theta \cos\theta \partial_r \left(r \left(r^2 F \right) \right) + \frac{r^2}{r} \partial_\theta \partial_\theta \left(\sin\theta \cos\theta F \right) = 0$$

$$\frac{\partial^2 F}{\partial r^2} + \frac{5}{r}\frac{\partial F}{\partial r} + \frac{1}{r^2}\frac{\partial^2 F}{\partial \theta^2} + \frac{2\cot\theta - 2\tan\theta}{r^2}\frac{\partial F}{\partial \theta} = 0. \tag{6.3}$$

This homogeneous equation can be solved by separation of variables, but we will wait until the following chapter where we will use a Green function approach.

We now define the following quantities for convenience:

$$A_V \equiv A_W + \frac{r^2 \sin^2\theta F^2}{G^2} I A_U \tag{6.4}$$

$$I_r \equiv \frac{\partial I}{\partial r} + 2I \left(\frac{1}{r} + \frac{1}{F}\frac{\partial F}{\partial r} - \frac{1}{G}\frac{\partial G}{\partial r} \right) \tag{6.5}$$

$$I_\theta \equiv \frac{\partial I}{\partial \theta} + 2I \left(\cot\theta - \frac{1}{G}\frac{\partial G}{\partial \theta} \right) \tag{6.6}$$

$$W_r \equiv \frac{\partial W}{\partial r} + \frac{r^2 \sin^2\theta F^2 I}{G^2}\frac{\partial U_t}{\partial r} \tag{6.7}$$

$$W_\theta \equiv \frac{\partial W}{\partial \theta} + \frac{r^2 \sin^2\theta F^2 I}{G^2}\frac{\partial U_t}{\partial \theta} \tag{6.8}$$

$$A_{Wr} \equiv \frac{\partial A_W}{\partial r} + 2A_W \left(\frac{1}{r} + \frac{1}{F}\frac{\partial F}{\partial r} - \frac{1}{H}\frac{\partial H}{\partial r} \right)$$
$$+ \frac{r^2 \sin^2\theta F^2}{G^2} \left[\frac{\partial I}{\partial r} A_U + \frac{\partial A_U}{\partial r} I + 2A_U I \left(\frac{2}{r} + \frac{2}{F}\frac{\partial F}{\partial r} - \frac{1}{G}\frac{\partial G}{\partial r} - \frac{1}{H}\frac{\partial H}{\partial r} \right) \right] \tag{6.9}$$

$$A_{W\theta} \equiv \frac{\partial A_W}{\partial \theta} - 2A_W \left(\tan\theta + \frac{1}{H}\frac{\partial H}{\partial \theta} \right)$$
$$+ \frac{r^2 \sin^2\theta F^2}{G^2} \left[\frac{\partial I}{\partial \theta} A_U + \frac{\partial A_U}{\partial \theta} I + 2A_U I \left(\cot\theta - \tan\theta - \frac{1}{G}\frac{\partial G}{\partial \theta} - \frac{1}{H}\frac{\partial H}{\partial \theta} \right) \right] \tag{6.10}$$

$$A_{Ur} \equiv \frac{\partial A_U}{\partial r} + 2A_U \left(\frac{1}{r} + \frac{1}{F}\frac{\partial F}{\partial r} - \frac{1}{G}\frac{\partial G}{\partial r} \right) \left(A_U + \frac{r^2 \cos^2\theta F^2 A_V I}{H^2} \right)$$
$$+ \frac{r^2 \cos^2\theta F^2 A_V}{H^2}\frac{\partial I}{\partial r} \tag{6.11}$$

$$A_{U\theta} \equiv \frac{\partial A_U}{\partial \theta} + 2A_U \left(\cot\theta - \frac{1}{G}\frac{\partial G}{\partial \theta} \right) \left(A_U + \frac{r^2 \cos^2\theta F^2 A_V I}{H^2} \right)$$
$$+ \frac{r^2 \cos^2\theta F^2 A_V}{H^2} \frac{\partial I}{\partial \theta} \tag{6.12}$$

$$A_{Tr} \equiv \frac{\partial Q^2 A_T}{\partial r} + \frac{r^2 \sin^2\theta F^2}{G^2} \frac{\partial U_t}{\partial r} \left(A_U + \frac{r^2 \cos^2\theta F^2 A_V I}{H^2} \right)$$
$$+ \frac{r^2 \cos^2\theta F^2 A_V}{H^2} \frac{\partial W}{\partial r} \tag{6.13}$$

$$A_{T\theta} \equiv \frac{\partial Q^2 A_T}{\partial \theta} + \frac{r^2 \sin^2\theta F^2}{G^2} \frac{\partial U_t}{\partial \theta} \left(A_U + \frac{r^2 \cos^2\theta F^2 A_V I}{H^2} \right)$$
$$+ \frac{r^2 \cos^2\theta F^2 A_V}{H^2} \frac{\partial W}{\partial \theta}. \tag{6.14}$$

With these definitions in place we write the differential operators and source terms for the remaining scalar equations. We begin with G and H:

$$\frac{\partial^2 G}{\partial r^2} + \frac{3}{r}\frac{\partial G}{\partial r} + \frac{1}{r^2}\frac{\partial^2 G}{\partial \theta^2} + \frac{\cot\theta - \tan\theta}{r^2}\frac{\partial G}{\partial \theta} =$$
$$\frac{1}{G}\left(\left(\frac{\partial G}{\partial r}\right)^2 + \frac{1}{r^2}\left(\frac{\partial G}{\partial \theta}\right)^2 \right) - \frac{1}{F}\frac{\partial F}{\partial r}\left(\frac{\partial G}{\partial r} + \frac{G}{r} \right)$$
$$+ \frac{r^2 \sin^2\theta F^4}{2H^2 G^3}\left(\left(\frac{\partial U_t}{\partial r}\right)^2 + \frac{1}{r^2}\left(\frac{\partial U_t}{\partial \theta}\right)^2 \right) + \frac{r^4 \cos^2\theta \sin^2\theta F^4}{2H^2 G}\left(I_r^2 + \frac{I_\theta^2}{r^2} \right)$$
$$- \frac{2r^2 \cos^2\theta F^2 G}{3H^2}\left(A_{Wr}^2 + \frac{A_{W\theta}^2}{r^2} \right) + \frac{4r^2 \sin^2\theta F^2}{3G}\left(A_{Ur}^2 + \frac{A_{U\theta}^2}{r^2} \right)$$
$$+ \frac{2F^2}{3GH^2}\left(A_{Tr}^2 + \frac{A_{T\theta}^2}{r^2} \right) \tag{6.15}$$

$$\frac{\partial^2 H}{\partial r^2} + \frac{3}{r}\frac{\partial H}{\partial r} + \frac{1}{r^2}\frac{\partial^2 H}{\partial \theta^2} + \frac{\cot\theta - \tan\theta}{r^2}\frac{\partial H}{\partial \theta} =$$
$$\frac{1}{H}\left(\left(\frac{\partial H}{\partial r}\right)^2 + \frac{1}{r^2}\left(\frac{\partial H}{\partial \theta}\right)^2 \right) - \frac{1}{F}\frac{\partial F}{\partial r}\left(\frac{\partial H}{\partial r} + \frac{H}{r} \right)$$
$$+ \frac{r^2 \cos^2\theta F^4}{2H^3 G^2}\left(W_r^2 + \frac{W_\theta^2}{r^2} \right) - \frac{r^4 \sin^2\theta \cos^2\theta F^4}{2G^2 H}\left(I_r^2 + \frac{I_\theta^2}{r^2} \right)$$
$$+ \frac{4r^2 \cos^2 F^2}{3H}\left(A_{Wr}^2 + \frac{A_{W\theta}^2}{r^2} \right) - \frac{2r^2 \sin^2\theta F^2 H}{3G^2}\left(A_{Ur}^2 + \frac{A_{U\theta}^2}{r^2} \right)$$
$$+ \frac{2F^2}{3G^2 H}\left(A_{Tr}^2 + \frac{A_{T\theta}^2}{r^2} \right). \tag{6.16}$$

Notice the symmetry between the G and H equations, where U_t is the rotational functions associated with G and W with H. In fact, for the Tangherlini black holes, where all rotational functions vanish, G and H are identical. This identity is motivated from symmetry considerations in Appendix C.

Next, equations for the functions related to rotation:

$$\frac{\partial^2 U_t}{\partial r^2} + \frac{5}{r}\frac{\partial U_t}{\partial r} + \frac{1}{r^2}\frac{\partial^2 U_t}{\partial \theta^2} + \frac{3\cot\theta - \tan\theta}{r^2}\frac{\partial U_t}{\partial \theta} =$$
$$\frac{\partial U_t}{\partial r}\left(\frac{4}{G}\frac{\partial G}{\partial r} + \frac{2}{H}\frac{\partial H}{\partial r} - \frac{5}{F}\frac{\partial F}{\partial r}\right) + \frac{1}{r^2}\frac{\partial U_t}{\partial \theta}\left(\frac{4}{G}\frac{\partial G}{\partial \theta} + \frac{2}{H}\frac{\partial H}{\partial \theta}\right)$$
$$- \frac{r^2\cos^2\theta F^2}{H^2}\left(I_r W_r + \frac{I_\theta W_\theta}{r^2}\right) - 2\left(A_{Ur}A_{Tr} + \frac{A_{U\theta}A_{T\theta}}{r^2}\right) \qquad (6.17)$$

$$\frac{\partial^2 W}{\partial r^2} + \frac{5}{r}\frac{\partial W}{\partial r} + \frac{1}{r^2}\frac{\partial^2 W}{\partial \theta^2} + \frac{\cot\theta - 3\tan\theta}{r^2}\frac{\partial W}{\partial \theta} =$$
$$\frac{\partial W}{\partial r}\left(\frac{2}{G}\frac{\partial G}{\partial r} + \frac{4}{H}\frac{\partial H}{\partial r} - \frac{5}{F}\frac{\partial F}{\partial r}\right) + \frac{1}{r^2}\frac{\partial W}{\partial \theta}\left(\frac{2}{G}\frac{\partial G}{\partial \theta} + \frac{4}{H}\frac{\partial H}{\partial \theta}\right)$$
$$- \frac{r^2\sin^2\theta F^2}{G^2}\left\{\frac{\partial U_t}{\partial r}\left[\frac{\partial I}{\partial r} + 2I\left(\frac{1}{r} + \frac{1}{F}\frac{\partial F}{\partial r} - \frac{1}{H}\frac{\partial H}{\partial r}\right)\right]\right.$$
$$\left. + \frac{1}{r^2}\frac{\partial U_t}{\partial \theta}\left[\frac{\partial I}{\partial \theta} - 2I\left(\tan\theta + \frac{1}{H}\frac{\partial H}{\partial \theta}\right)\right]\right\}$$
$$- 2\left(A_{Wr}A_{Tr} - \frac{A_{W\theta}A_{T\theta}}{r^2}\right) + \frac{r^4\cos^2\theta\sin^2\theta F^4 I}{G^2 H^2}\left(I_r W_r + \frac{I_\theta W_\theta}{r^2}\right)$$
$$+ \frac{2r^2\sin^2\theta F^2 I}{G^2}\left(A_{Ur}A_{Tr} + \frac{A_{U\theta}A_{T\theta}}{r^2}\right) \qquad (6.18)$$

$$\frac{\partial^2 I}{\partial r^2} + \frac{7}{r}\frac{\partial I}{\partial r} + \frac{1}{r^2}\frac{\partial^2 I}{\partial \theta^2} + \frac{3\cot\theta - 3\tan\theta}{r^2}\frac{\partial I}{\partial \theta} =$$

$$\frac{\partial I}{\partial r}\left(\frac{2}{G}\frac{\partial G}{\partial r} + \frac{2}{H}\frac{\partial H}{\partial r} - \frac{5}{F}\frac{\partial F}{\partial r}\right) + \frac{1}{r^2}\frac{\partial I}{\partial \theta}\left(\frac{2}{G}\frac{\partial G}{\partial \theta} + \frac{2}{H}\frac{\partial H}{\partial \theta}\right)$$

$$+ \frac{4I}{r}\left(\frac{1}{G}\frac{\partial G}{\partial r} + \frac{1}{H}\frac{\partial H}{\partial r} - \frac{2}{F}\frac{\partial F}{\partial r} + \frac{r}{GF}\frac{\partial G}{\partial r}\frac{\partial F}{\partial r} + \frac{r}{HF}\frac{\partial H}{\partial r}\frac{\partial F}{\partial r} - \frac{r}{GH}\frac{\partial G}{\partial r}\frac{\partial H}{\partial r}\right.$$

$$\left. - \frac{r}{F^2}\left(\frac{\partial F}{\partial r}\right)^2\right) + \frac{4I}{r^2}\left(\frac{\cot\theta}{H}\frac{\partial H}{\partial \theta} - \frac{\tan\theta}{G}\frac{\partial G}{\partial \theta} - \frac{1}{GH}\frac{\partial G}{\partial \theta}\frac{\partial H}{\partial \theta}\right)$$

$$- \frac{F^2}{G^2 H^2}\left(\frac{\partial U_t}{\partial r}\frac{\partial W}{\partial r} + \frac{1}{r^2}\frac{\partial U_t}{\partial \theta}\frac{\partial W}{\partial \theta}\right) - 2\left(A_{Wr}A_{Ur} + \frac{A_{W\theta}A_{U\theta}}{r^2}\right)$$

$$+ 2IF^2\left[\frac{r^4\sin^2\theta\cos^2\theta F^2}{2G^2 H^2}\left(I_r^2 + \frac{I_\theta^2}{r^2}\right) - \frac{2r^2\cos^2\theta}{3H^2}\left(A_{Wr}^2 + \frac{A_{W\theta}^2}{r^2}\right)\right.$$

$$\left. + \frac{4r^2\sin^2\theta}{3G^2}\left(A_{Ur}^2 + \frac{A_{U\theta}^2}{r^2}\right) + \frac{2}{3G^2 H^2}\left(A_{Tr}^2 + \frac{A_{T\theta}^2}{r^2}\right)\right]. \tag{6.19}$$

Last, the equations for the components of the vector potential:

$$\frac{\partial^2 Q^2 A_T}{\partial r^2} + \frac{3}{r}\frac{\partial Q^2 A_T}{\partial r} + \frac{1}{r^2}\frac{\partial^2 Q^2 A_T}{\partial \theta^2} + \frac{\cot\theta - \tan\theta}{r^2}\frac{\partial Q^2 A_T}{\partial \theta} =$$

$$\frac{\partial Q^2 A_T}{\partial r}\left(\frac{2}{G}\frac{\partial G}{\partial r} + \frac{2}{H}\frac{\partial H}{\partial r} - \frac{3}{F}\frac{\partial F}{\partial r}\right) + \frac{1}{r^2}\frac{\partial Q^2 A_T}{\partial \theta}\left(\frac{2}{G}\frac{\partial G}{\partial \theta} + \frac{2}{H}\frac{\partial H}{\partial \theta}\right)$$

$$- \frac{r^2\sin^2\theta F^2}{G^2}\left(\frac{\partial A_U}{\partial r}\frac{\partial U_t}{\partial r} + \frac{1}{r^2}\frac{\partial A_U}{\partial \theta}\frac{\partial U_t}{\partial \theta}\right) - \frac{r^2\cos^2\theta F^2}{H^2}\left(\frac{\partial A_V}{\partial r}W_r + \frac{1}{r^2}\frac{\partial A_V}{\partial \theta}W_\theta\right)$$

$$+ \frac{r^2\sin^2\theta F^2 A_U}{G^2}\left[\frac{r^2\cos^2\theta F^2}{H^2}\left(I_r W_r + \frac{I_\theta W_\theta}{r^2}\right) + 2\left(A_{Ur}A_{Tr} + \frac{A_{U\theta}A_{T\theta}}{r^2}\right)\right]$$

$$+ \frac{2r^2\cos^2\theta F^2 A_V}{H^2}\left(A_{Wr}A_{Tr} + \frac{A_{W\theta}A_{T\theta}}{r^2}\right) \tag{6.20}$$

$$\frac{\partial^2 A_U}{\partial r^2} + \frac{5}{r}\frac{\partial A_U}{\partial r} + \frac{1}{r^2}\frac{\partial^2 A_U}{\partial \theta^2} + \frac{3\cot\theta - \tan\theta}{r^2}\frac{\partial A_U}{\partial \theta} =$$

$$\frac{\partial A_U}{\partial r}\left(\frac{2}{G}\frac{\partial G}{\partial r} - \frac{3}{F}\frac{\partial F}{\partial r}\right) + \frac{2}{r^2 G}\frac{\partial A_U}{\partial \theta}\frac{\partial G}{\partial \theta} - \frac{r^2\cos^2\theta F^2}{H^2}\left(I_r\frac{\partial A_V}{\partial r} + \frac{I_\theta}{r^2}\frac{\partial A_V}{\partial \theta}\right)$$

$$- \frac{F^2}{G^2 H^2}\left(\frac{\partial U_t}{\partial r}\frac{\partial Q^2 A_T}{\partial r} + \frac{1}{r^2}\frac{\partial U_t}{\partial \theta}\frac{\partial Q^2 A_T}{\partial \theta}\right) + 2A_U F^2\left[\frac{r^4\cos^2\theta\sin^2\theta F^2}{2H^2 G^2}\left(I_r^2 + \frac{I_\theta^2}{r^2}\right)\right.$$

$$\left. - \frac{2r^2\cos^2\theta}{H^2}\left(A_{Wr}^2 + \frac{A_{W\theta}^2}{r^2}\right) + \frac{4r^2\sin^2\theta}{3G^2}\left(A_{Ur}^2 + \frac{A_{U\theta}^2}{r^2}\right)\right.$$

$$\left. + \frac{2}{3G^2 H^2}\left(A_{Tr}^2 + \frac{A_{T\theta}^2}{r^2}\right)\right] + \frac{2r^2\cos^2\theta F^2 A_V}{H^2}\left(A_{Wr}A_{Ur} + \frac{A_{W\theta}A_{T\theta}}{r^2}\right) \tag{6.21}$$

$$
\frac{\partial^2 A_W}{\partial r^2} + \frac{5}{r}\frac{\partial A_W}{\partial r} + \frac{1}{r^2}\frac{\partial^2 A_W}{\partial \theta^2} + \frac{\cot\theta - 3\tan\theta}{r^2}\frac{\partial A_W}{\partial \theta} =
$$

$$
\frac{\partial A_W}{\partial r}\left(\frac{2}{H}\frac{\partial H}{\partial r} - \frac{3}{F}\frac{\partial F}{\partial r}\right) + \frac{2}{r^2 H}\frac{\partial A_W}{\partial \theta}\frac{\partial H}{\partial \theta}
$$

$$
- \frac{r^2\sin^2\theta F^2}{G^2}\left(\frac{\partial A_U}{\partial r}\frac{\partial I}{\partial r} + \frac{1}{r^2}\frac{\partial A_U}{\partial \theta}\frac{\partial I}{\partial \theta}\right) - \frac{F^2}{G^2 H^2}\left(\frac{\partial Q^2 A_T}{\partial r}\frac{\partial W}{\partial r} + \frac{1}{r^2}\frac{\partial Q^2 A_T}{\partial \theta}\frac{\partial W}{\partial \theta}\right)
$$

$$
- 2A_W F^2\left[\frac{r^2\sin^2\theta}{3G^2}\left(A_{Ur}^2 + \frac{A_{U\theta}^2}{r^2}\right) - \frac{1}{3G^2 H^2}\left(A_{Tr}^2 + \frac{A_{T\theta}^2}{r^2}\right)\right.
$$

$$
\left. - \frac{2r^2\cos^2\theta}{3H^2}\left(A_{Wr}^2 + \frac{A_{W\theta}^2}{r^2}\right) + A_U\frac{r^2\sin^2\theta}{G^2}\left(A_{Ur}A_{Wr} + \frac{A_{U\theta}A_{W\theta}}{r^2}\right)\right]
$$

$$
- A_U I\frac{r^2\sin^2\theta F^4}{G^2}\left[\frac{r^4\cos^2\theta\sin^2\theta F^2}{G^2 H^2}\left(I_r^2 + \frac{I_\theta^2}{r^2}\right) - \frac{8r^2\cos^2\theta}{3H^2}\left(A_{Wr}^2 + \frac{A_{W\theta}^2}{r^2}\right)\right.
$$

$$
\left. + \frac{10r^2\sin^2\theta}{3G^2}\left(A_{Ur}^2 + \frac{A_{U\theta}^2}{r^2}\right) + \frac{2}{3G^2 H^2}\left(A_{Tr}^2 + \frac{A_{T\theta}^2}{r^2}\right)\right]
$$

$$
- I\frac{r^2\sin^2\theta F^2}{G^2}\left[2\frac{\partial A_U}{\partial r}\left(\frac{1}{r} + \frac{1}{F}\frac{\partial F}{\partial r} - \frac{1}{H}\frac{\partial H}{\partial r}\right) - \frac{2}{r}\frac{\partial A_U}{\partial \theta}\left(\tan\theta + \frac{1}{H}\frac{\partial H}{\partial \theta}\right)\right.
$$

$$
\left. - \frac{r^2\cos^2\theta F^2}{H^2}\left(\frac{\partial A_V}{\partial r}I_r + \frac{\partial A_V}{\partial r}\frac{I_\theta}{r^2}\right) + 2A_V\frac{r^2\cos^2\theta F^2}{H^2}\left(A_{Wr}A_{Ur} + \frac{A_{W\theta}A_{U\theta}}{r^2}\right)\right]
$$

$$
\tag{6.22}
$$

Chapter 7

Green Functions & The Numerical Method

Two of the important results given in the previous two chapters are that the scalar equations each satisfy one of a family of differential operators and each satisfies Dirichlet boundary conditions. These properties motivate the construction of Green functions for this family of operators.

In this chapter we will construct this family of Green functions and explicitly solve for the boundary terms that result from Green's identity. This analysis will give us the analytic solution for the function F immediately and motivate the lowest order radial behavior of each scalar function. We conclude the chapter with some details of our numerical method.

7.1   Construction of Green Functions

We begin with the five dimensional flat space metric in bi-azimuthal coordinates (2.24). Note that this metric has determinant

$$g = -r^6 \sin^2 \theta \cos^2 \theta. \tag{7.1}$$

We take the usual definition of the Laplacian in 5D (4 spatial dimensions) of a scalar function f as

$$
\begin{aligned}
\nabla^2 f &= \frac{1}{\sqrt{-g}} \partial_a \left(\sqrt{-g} g^{ab} \partial_b f \right) \\
&= \frac{\partial^2 f}{\partial r^2} + \frac{3}{r} \frac{\partial f}{\partial r} + \frac{1}{r^2} \frac{\partial^2 f}{\partial \theta^2} + \frac{\cot\theta - \tan\theta}{r^2} \frac{\partial f}{\partial \theta}.
\end{aligned}
\tag{7.2}
$$

By comparing with the operators that appear in the Einstein-Maxwell equations in chapter 6 we notice that each of the scalar equations satisfies (7.2) or a modification of the same. This motivates our definition of the family of differential operators

$$
\nabla^2_{(p,q)} \equiv \nabla^2 + \frac{p+q}{r} \frac{\partial}{\partial r} + \frac{p \cot\theta - q \tan\theta}{r^2} \frac{\partial}{\partial \theta},
\tag{7.3}
$$

where $p,q \in \{0, 1, 2\}$, for which we want to construct a Green function.

When constructing a Green function we typically use self-adjoint operators. These operators are of the form $w\nabla^2_{(p,q)} f$ for some scalar weight function w and must satisfy

$$
w\nabla^2_{(p,q)} f = \nabla \cdot (w\nabla f),
\tag{7.4}
$$

where ∇ is the gradient with respect to our flat space 5D metric in (2.24). In the case of the operators (7.3) w can be shown to be

$$
w = (r \sin\theta)^p (r \cos\theta)^q.
\tag{7.5}
$$

Now that we have a self-adjoint operator we can begin to determine the Green functions. As usual we want to find the Green functions $G_{(p,q)}(\vec{x}, \vec{x}')$ which satisfy

$$
w\nabla^2_{(p,q)} G_{(p,q)} = -4\pi^2 \delta(\vec{x} - \vec{x}').
\tag{7.6}
$$

Proceeding in the usual way, we begin by solving the homogeneous equation

$$
\nabla^2_{(p,q)} G_{(p,q)} = 0.
\tag{7.7}
$$

We employ separation of variables, defining $G = R(r)\Theta(\theta)$ and choosing the separation constant to be $2l(2l + p + q + 2)$. Changing coordinates to $\mu = \cos 2\theta$ we find that the angular equation becomes

$$(1 - \mu^2)\frac{d^2\Theta}{d\mu^2} - \left[\frac{p-q}{2} + \mu\left(2 + \frac{p+q}{2}\right)\right]\frac{d\Theta}{d\mu} + l\left(l + 1 + \frac{p+q}{2}\right)\Theta = 0 \qquad (7.8)$$

which is the Jacobi equation.

The solutions to (7.8) are the Jacobi polynomials $P_l^{\frac{p}{2},\frac{q}{2}}(\mu)$. These are shown (in [27] for example) to have the orthogonality relation

$$\int_{-1}^{1} P_n^{\frac{p}{2},\frac{q}{2}}(\mu)P_m^{\frac{p}{2},\frac{q}{2}}(\mu)(1 - \mu)^{\frac{p}{2}}(1 + \mu)^{\frac{q}{2}}\, d\mu = \frac{2^{1+\frac{p+q}{2}}\Gamma\left(n + 1 + \frac{p}{2}\right)\Gamma\left(n + 1 + \frac{q}{2}\right)}{n!\left(2n + 1 + \frac{p+q}{2}\right)\Gamma\left(n + 1 + \frac{p+q}{2}\right)}\delta_{nm}. \qquad (7.9)$$

Notice that the weight function (7.5) includes the angular piece needed for the orthogonality integral. The polynomials also satisfy the recursion relation

$$2(l+1)\left(l + 1 + \frac{p+q}{2}\right)\left(2l + \frac{p+q}{2}\right)P_{l+1}^{\frac{p}{2},\frac{q}{2}}(\mu) =$$
$$\left(2l + 1 + \frac{p+q}{2}\right)\left[\left(2l + \frac{p+q}{2}\right)\left(2l + 2 + \frac{p+q}{2}\right)\mu + \frac{p^2 - q^2}{4}\right]P_l^{\frac{p}{2},\frac{q}{2}}(\mu)$$
$$-2\left(l + \frac{p}{2}\right)\left(l + \frac{q}{2}\right)\left(2l + 2 + \frac{p+q}{2}\right)P_{l-1}^{\frac{p}{2},\frac{q}{2}}(\mu). \qquad (7.10)$$

Most importantly, the Jacobi polynomials form a complete set which allows us to expand the delta function in μ as a sum of Jacobi polynomials.

In order to make use of this property, we note that with respect to our four spatial dimensions

$$\delta(\vec{x} - \vec{x}') = \frac{4}{r^3}\delta(r - r')\delta(\mu - \mu')\delta(\phi - \phi')\delta(\psi - \psi'). \qquad (7.11)$$

Since we can expand $\delta(\mu - \mu')$ in terms of the Jacobi polynomials and (7.3) is independent of ϕ and ψ, it only remains to find the one dimensional Green function $g(r, r')$ satisfying

$$r^{p+q}\frac{d^2g}{dr^2} + r^{p+q-1}(p + q + 3)\frac{dg}{dr} - r^{p+q-2}4l\left(l + 1 + \frac{p+q}{2}\right) = \frac{1}{r^3}\delta(r - r'). \qquad (7.12)$$

We find the solution to be

$$g(r, r') = \begin{cases} \dfrac{r^{2l}}{r'^{2l+2+p+q}(4l+2+p+q)}\left(1 - \left(\dfrac{r_h}{r}\right)^{4l+2+p+q}\right) & r < r' \\[2ex] \dfrac{r'^{2l}}{r^{2l+2+p+q}(4l+2+p+q)}\left(1 - \left(\dfrac{r_h}{r'}\right)^{4l+2+p+q}\right) & r > r' \end{cases} \tag{7.13}$$

or more compactly

$$g(r, r') = \frac{r_<^{2l}}{r_>^{2l+2+p+q}(4l+2+p+q)}\left(1 - \left(\frac{r_h}{r_<}\right)^{4l+2+p+q}\right) \tag{7.14}$$

where r_h is the r value at the event horizon. The full Green function is found to be

$$G_{(p,q)}(r, \mu, r', \mu') = \sum_{l=0}^{\infty} \frac{l! \, \Gamma\left(l+1+\frac{p+q}{2}\right)}{\Gamma\left(l+1+\frac{p}{2}\right)\Gamma\left(l+1+\frac{q}{2}\right)} P_l^{\frac{p}{2}, \frac{q}{2}}(\mu) P_l^{\frac{p}{2}, \frac{q}{2}}(\mu')$$

$$\times \frac{r_<^{2l}}{r_>^{2l+2+p+q}(4l+2+p+q)}\left(1 - \left(\frac{r_h}{r_<}\right)^{4l+2+p+q}\right). \tag{7.15}$$

7.2   Boundary Terms

Recall that for a function f which satisfies

$$\nabla^2_{(p,q)} f = S_f, \tag{7.16}$$

Green's identity is

$$\int_V \left(f w \nabla^2_{(p,q)} G - G w \nabla^2_{(p,q)} f\right) dV = \oint_{\partial V} w \left(f \nabla G - G \nabla f\right) \cdot d\vec{a}. \tag{7.17}$$

All the functions we are solving for satisfy Dirichlet boundary conditions so we choose our Green function to satisfy homogeneous Dirichlet boundary conditions. In particular this forces

$$\oint_{\partial V} w G \nabla f = 0. \tag{7.18}$$

This relation along with (7.6) and (7.17) allows us to solve for f using

$$-4\pi^2 f - \int_V G w S_f dV = \oint_{\partial V} w f \nabla G \cdot d\vec{a} \tag{7.19}$$

or after integrating over ϕ and ψ

$$f = -\int_{r_h}^{\infty}\int_0^{\frac{\pi}{2}} GwS_f r'^3 \cos\theta' \sin\theta' dr' d\theta' - \int_0^{\frac{\pi}{2}} w f \nabla G \cdot \hat{n} r'^3 \cos\theta' \sin\theta' d\theta' \qquad (7.20)$$

where $\hat{n} = \hat{r}$ at $r' = \infty$ and $\hat{n} = -\hat{r}$ at the event horizon, denoted $r' = r_h$. Because we take f as having constant values on the boundaries, we can evaluate the boundary integral using the orthogonality of the Jacobi polynomials. At infinity the boundary term becomes

$$f\big|_{\infty}\left(1 - \left(\frac{r_h}{r}\right)^{2+p+q}\right) \qquad (7.21)$$

and at the horizon

$$f\big|_{r_h}\left(\frac{r_h}{r}\right)^{2+p+q}. \qquad (7.22)$$

We can now solve (6.3) for F immediately. We recall from (6.3) that $S_F = 0$ and $p = q = 1$. Further, from (5.24) and (5.25) we have $F\big|_{r_h} = 0$ and $F\big|_{\infty} = 1$. Direct substitution into (7.20) we find

$$F = \left(1 - \left(\frac{r_h}{r}\right)^4\right). \qquad (7.23)$$

This result is verified explicitly in Appendix B using the charged Tangherlini and MP solutions as well as Aliev's perturbative solution.

For the remaining equations it is convenient to change variables. We do this to simplify our numerical solution of the equations and to enforce boundary conditions more precisely. As before, we will set $\mu = \cos 2\theta$ with $\mu \in [-1, 1]$. In order to enforce boundary conditions at spatial infinity exactly we use a compactified coordinate, s, defined by

$$s = 1 - \frac{r_h}{r}. \qquad (7.24)$$

Note that this maps the horizon to $s = 0$ and spatial infinity to $s = 1$. Our final equation for f is then

$$f = -\int_0^1 wGS_f \frac{r_h^4}{4(1-s)^5} d\mu' ds' + f\big|_{s=0}(1-s)^{2+p+q} + f\big|_{s=1}\left(1 - (1-s)^{2+p+q}\right) \qquad (7.25)$$

where

$$w(s,\mu) = \frac{r_h^{p+q}}{2^{\frac{p+q}{2}}(1-s)^{p+q}}(1+\mu)^{\frac{p}{2}}(1-\mu)^{\frac{q}{2}} \tag{7.26}$$

and

$$G_{(p,q)}(s,\mu,s',\mu') = \sum_{l=0}^{\infty} \frac{l!\,\Gamma\left(l+1+\frac{p+q}{2}\right)}{\Gamma\left(l+1+\frac{p}{2}\right)\Gamma\left(l+1+\frac{q}{2}\right)} \frac{(1-s_>)^{2l+2+p+q}}{r_h^{2+p+q}(1-s_<)^{2l}}$$
$$\times \left(1-(1-s_<)^{4l+2+p+q}\right) P_l^{\frac{p}{2},\frac{q}{2}}(\mu) P_l^{\frac{p}{2},\frac{q}{2}}(\mu'). \tag{7.27}$$

7.3   Numerical Method

Now that we have found this family of Green functions we turn to numerical methods to solve our equation set. While (7.25) appears to be a straightforward definition for an unknown function f, recall that the term S_f in the integral conceals significant complexity.

From Chapter 6 we recall that the source terms of our partial differential equations couple each function (excluding F) to the other seven. In addition, each source is nonlinear in all nine functions. Specifically, for a given function f the source will include nonlinear terms that contain f itself. This complicated nature of the source terms encourages us to employ an iterative method to solve the equations.

Before we can begin such a process we must first be ready to evaluate the source terms. Recall from Chapter 6 that these terms can involve combinations of the functions themselves and their derivatives with respect to s and μ. In order to evaluate these combinations we specify each function at every point of an evenly spaced $(N+1) \times (M+1)$ grid. On this grid s varies from 0 to 1 in steps of $\dfrac{1}{N}$ and μ varies from -1 to 1 in steps of $\dfrac{2}{M}$. With our functions defined on this grid, we use fourth order centered difference derivatives to evaluate each function's source.

Returning to our iterative method, we begin by specifying an initial guess for each of the functions. This guess is typically motivated by the known black hole solutions in five

dimensions. We also use the boundary terms to guide our initial guess. Since these boundary terms are functions of s, they must represent at least the lowest order radial behavior of the function in the vicinity of the respective boundaries (the event horizon or spatial infinity).

Once a guess has been specified, we calculate the source terms for each of the functions. After each source has been calculated, we can use (7.25) to generate a new guess for the next iteration. In effect, we make a series of successive approximations of f. If we denote our initial guess f_0 and f_N the result of the Nth iteration, then we can rewrite (7.25) for the Nth iteration as

$$f_N = -\int_0^1 wGS_f(f_{N-1})\frac{r_h^4}{4(1-s)^5}d\mu'ds' + f\big|_{s=0}(1-s)^{2+p+q} + f\big|_{s=1}\left(1-(1-s)^{2+p+q}\right).$$
$$(7.28)$$

Notice that the integral depends on f_{N-1} from the source terms, but the boundary terms are known explicitly for the exact f. This means that the same boundary term is added after each iteration.

Before we evaluate the integral in (7.28) we must construct the Green function in the numerical code. The first obstacle is the generation of Jacobi polynomials. Clearly, we cannot generate the complete set, but using the recursion relation (7.10) we can generate the first l polynomials, where we leave l as a user defined parameter. To begin this process we take the usual definitions

$$P_0^{\frac{p}{2},\frac{q}{2}} = 1, \quad P_1^{\frac{p}{2},\frac{q}{2}} = \mu + \tfrac{p}{4}(1+\mu) - \tfrac{q}{4}(1-\mu). \tag{7.29}$$

The remainder of the integrand, such as the weight function, is straightforward to construct. We then evaluate the integral using Simpson's rule and add the appropriate boundary terms.

As stated before, the output of this process serves as the new guess for the next iteration. Of course, we do not perpetuate this process indefinitely. After each step, we calculate how much each function changed during the iteration. Once the changes in the system as a whole have become sufficiently small we say that the system has converged to a solution.

Chapter 8

Two Dimensional GR

Once the nine scalar fields have been determined we return to the remaining tensor equation; specifically, the Einstein equations on the two dimensional manifold $\mathcal{N}$. In this chapter we show that this tensorial equation can be reduced to a first order partial differential equation for one unknown function. Furthermore, we formulate this equation so that it is well suited to numerical solution.

Recall from (2.25) the line element on σ_{ab}. Then using (2.28) we find the unique components of the connection on $\mathcal{N}$:

$$
\begin{aligned}
&\Gamma^r_{rr} = \frac{\partial \alpha}{\partial r}, && \Gamma^r_{r\theta} = \frac{\partial \alpha}{\partial \theta}, && \Gamma^r_{\theta\theta} = -r - r^2 \frac{\partial \alpha}{\partial r}, \\
&\Gamma^\theta_{rr} = \frac{-1}{r^2} \frac{\partial \alpha}{\partial \theta}, && \Gamma^\theta_{r\theta} = \frac{1}{r} + \frac{\partial \alpha}{\partial r}, && \Gamma^\theta_{\theta\theta} = \frac{\partial \alpha}{\partial \theta}.
\end{aligned}
\tag{8.1}
$$

Then using (2.33) we find the Ricci tensor on $\mathcal{N}$ to be

$$
R_{ab} = - \begin{pmatrix}
\frac{1}{r^2} \frac{\partial^2 \alpha}{\partial \theta^2} + \frac{1}{r} \frac{\partial \alpha}{\partial r} + \frac{\partial^2 \alpha}{\partial r^2} & 0 \\
0 & \frac{\partial^2 \alpha}{\partial \theta^2} + r \frac{\partial \alpha}{\partial r} + r^2 \frac{\partial^2 \alpha}{\partial r^2}
\end{pmatrix}.
\tag{8.2}
$$

Using (4.34) we now write the three unique equations that must be satisfied. First, (using

the definitions from chapter 6) the r,r equation

$$
\frac{-1}{r^2}\frac{\partial^2\alpha}{\partial\theta^2} - \frac{1}{r}\frac{\partial\alpha}{\partial r} - \frac{\partial^2\alpha}{\partial r^2} = -\frac{\partial\alpha}{\partial r}\left(\frac{2}{r} + \frac{1}{F}\frac{\partial F}{\partial r}\right) + \frac{1}{r^2}\frac{\partial\alpha}{\partial\theta}\left(\cot\theta - \tan\theta\right)
$$

$$
+ \frac{1}{F}\left(\frac{\partial^2 F}{\partial\theta^2} + \frac{4}{r}\frac{\partial F}{\partial r} + \frac{2}{F}\left(\frac{\partial F}{\partial r}\right)^2\right) - \frac{2}{G}\frac{\partial G}{\partial r}\left(\frac{1}{r} + \frac{2}{F}\frac{\partial F}{\partial r} - \frac{1}{G}\frac{\partial G}{\partial r}\right)
$$

$$
- \frac{2}{H}\frac{\partial H}{\partial r}\left(\frac{1}{r} + \frac{2}{F}\frac{\partial F}{\partial r} - \frac{1}{H}\frac{\partial H}{\partial r}\right) + \frac{2}{GH}\frac{\partial G}{\partial r}\frac{\partial H}{\partial r} - \frac{r^2\sin^2\theta F^4}{2G^4H^2}\left(\frac{\partial U_t}{\partial r}\right)^2
$$

$$
+ \frac{r^4\cos^2\theta\sin^2\theta F^4}{2H^2G^2}I_r^2 - \frac{r^2\cos^2\theta F^4}{2G^2H^4}W_r^2 + \frac{2r^2\cos^2\theta F^2}{3H^2}\left(2A_{Wr}^2 - \frac{A_{W\theta}^2}{r^2}\right)
$$

$$
+ \frac{2r^2\sin^2\theta F^2}{3G^2}\left(2A_{Ur}^2 - \frac{A_{U\theta}^2}{r^2}\right) - \frac{2F^2}{G^2H^2}\left(2A_{Tr}^2 - \frac{A_{T\theta}^2}{r^2}\right). \tag{8.3}
$$

Next, the θ,θ equation:

$$
\frac{-1}{r^2}\frac{\partial^2\alpha}{\partial\theta^2} - \frac{1}{r}\frac{\partial\alpha}{\partial r} - \frac{\partial^2\alpha}{\partial r^2} = \frac{\partial\alpha}{\partial r}\left(\frac{2}{r} + \frac{1}{F}\frac{\partial F}{\partial r}\right) - \frac{1}{r^2}\frac{\partial\alpha}{\partial\theta}\left(\cot\theta - \tan\theta\right)
$$

$$
+ \frac{1}{rF}\frac{\partial F}{\partial r} + \frac{2}{r^2G}\frac{\partial G}{\partial\theta}\left(\frac{1}{G}\frac{\partial G}{\partial\theta} - \cot\theta\right) + \frac{2}{r^2H}\frac{\partial H}{\partial r}\left(\frac{1}{H}\frac{\partial H}{\partial r} + \tan\theta\right)
$$

$$
- \frac{\sin^2\theta F^4}{2G^4H^2}\frac{\partial U_t}{\partial\theta} + \frac{r^2\cos^2\theta\sin^2\theta F^4}{2H^2G^2}I_\theta^2 - \frac{\cos^2\theta F^4}{2G^2H^4}W_\theta^2
$$

$$
- \frac{2r^2\cos^2\theta F^2}{3H^2}\left(A_{Wr}^2 - \frac{2A_{W\theta}^2}{r^2}\right) - \frac{2r^2\sin^2\theta F^2}{3G^2}\left(A_{Ur}^2 - \frac{2A_{U\theta}^2}{r^2}\right)
$$

$$
+ \frac{2F^2}{3G^2H^2}\left(A_{Tr}^2 - \frac{2T_{U\theta}^2}{r^2}\right). \tag{8.4}
$$

Last, the r,θ equation

$$
\frac{\partial\alpha}{\partial r}\left(\cot\theta - \tan\theta\right) + \frac{\partial\alpha}{\partial\theta}\left(\frac{2}{r} + \frac{1}{F}\frac{\partial F}{\partial r}\right) = \frac{1}{F}\frac{\partial F}{\partial r}\left(\cot\theta - \tan\theta - \frac{2}{G}\frac{\partial G}{\partial\theta} - \frac{2}{H}\frac{\partial H}{\partial\theta}\right)
$$

$$
+ \frac{1}{H}\frac{\partial H}{\partial r}\left(\tan\theta + \frac{2}{H}\frac{\partial H}{\partial\theta}\right) - \frac{1}{G}\frac{\partial G}{\partial r}\left(\cot\theta - \frac{2}{G}\frac{\partial G}{\partial\theta}\right) + \frac{1}{H}\frac{\partial H}{\partial\theta}\left(\frac{1}{G}\frac{\partial G}{\partial r} - \frac{1}{r}\right)
$$

$$
+ \frac{1}{G}\frac{\partial G}{\partial\theta}\left(\frac{1}{H}\frac{\partial H}{\partial r} - \frac{1}{r}\right) - \frac{r^2\sin^2\theta F^4}{2G^4H^2}\frac{\partial U_t}{\partial r}\frac{\partial U_t}{\partial\theta} + \frac{r^4\cos^2\theta\sin^2\theta F^4}{2G^2H^2}I_rI_\theta
$$

$$
- \frac{r^2\cos^2\theta F^4}{2G^2H^4}W_rW_\theta + \frac{2r^2\cos^2\theta F^2}{H^2}A_{Wr}A_{W\theta} + \frac{2r^2\sin^2\theta F^2}{G^2}A_{Ur}A_{U\theta}
$$

$$
- \frac{2F^2}{G^2H^2}A_{Tr}A_{T\theta}. \tag{8.5}
$$

Recall that R_{ab} is symmetric so the θ,r equation contains no new information.

We can then subtract (8.4) from (8.3) to create one equation. We do this because the form of this new equations is very similar to (8.5) and, most importantly, the second derivatives of α cancel.

$$
\begin{aligned}
\frac{\partial \alpha}{\partial r}\left(\frac{2}{r}+\frac{1}{F}\frac{\partial F}{\partial r}\right)+\frac{\partial \alpha}{\partial \theta}\left(\cot\theta-\tan\theta\right) &= \frac{1}{F}\frac{\partial F}{\partial r}\left(\frac{1}{F}\frac{\partial F}{\partial r}-\frac{1}{r}-\frac{2}{G}\frac{\partial G}{\partial r}-\frac{2}{H}\frac{\partial H}{\partial r}\right) \\
&-\frac{1}{G}\frac{\partial G}{\partial r}\left(\frac{1}{r}-\frac{1}{G}\frac{\partial G}{\partial r}\right)+\frac{1}{r^2 G}\frac{\partial G}{\partial \theta}\left(\cot\theta-\frac{1}{G}\frac{\partial G}{\partial \theta}\right)-\frac{1}{H}\frac{\partial H}{\partial r}\left(\frac{1}{r}-\frac{1}{H}\frac{\partial H}{\partial r}\right) \\
&-\frac{1}{r^2 H}\frac{\partial H}{\partial \theta}\left(\tan\theta+\frac{1}{H}\frac{\partial H}{\partial \theta}\right)+\frac{1}{GH}\left(\frac{\partial G}{\partial r}\frac{\partial H}{\partial r}-\frac{1}{r^2}\frac{\partial G}{\partial \theta}\frac{\partial H}{\partial \theta}\right) \\
&-\frac{r^2 \sin^2\theta F^4}{4G^4 H^2}\left(\left(\frac{\partial U_t}{\partial r}\right)^2-\frac{1}{r^2}\left(\frac{\partial U_t}{\partial \theta}\right)^2\right)+\frac{r^4 \cos^2\theta \sin^2\theta F^4}{4G^2 H^2}\left(I_r^2-\frac{I_\theta^2}{r^2}\right) \\
&-\frac{r^2 \cos^2\theta F^4}{4G^2 H^4}\left(W_r^2-\frac{W_\theta^2}{r^2}\right)+\frac{r^2 \cos^2\theta F^2}{H^2}\left(A_{Wr}^2-\frac{A_{W\theta}^2}{r^2}\right) \\
&+\frac{r^2 \sin^2\theta F^2}{G^2}\left(A_{Ur}^2-\frac{A_{U\theta}^2}{r^2}\right)-\frac{F^2}{G^2 H^2}\left(A_{Tr}^2-\frac{A_{T\theta}^2}{r^2}\right).
\end{aligned}
\tag{8.6}
$$

The equations (8.5) and (8.6) form a linear system which we will invert. To make this clearer we define the right hand side of (8.5) as C and the right hand side of (8.6) as D. We also make the definitions

$$
A = \frac{2}{r}+\frac{1}{F}\frac{\partial F}{\partial r} \quad B = \cot\theta-\tan\theta.
\tag{8.7}
$$

We can then express (8.5) and (8.6) as

$$
\begin{bmatrix} B & A \\ A & \frac{-1}{r^2}B \end{bmatrix}\begin{bmatrix} \frac{\partial \alpha}{\partial r} \\ \frac{\partial \alpha}{\partial \theta} \end{bmatrix} = \begin{bmatrix} C \\ D \end{bmatrix}.
\tag{8.8}
$$

This can be easily solved for the derivatives of α

$$
\begin{aligned}
\begin{bmatrix} \frac{\partial \alpha}{\partial r} \\ \frac{\partial \alpha}{\partial \theta} \end{bmatrix} &= \frac{-r^2}{B^2+r^2 A^2}\begin{bmatrix} \frac{-1}{r^2}B & -A \\ -A & B \end{bmatrix}\begin{bmatrix} C \\ D \end{bmatrix} \\
&= \frac{1}{B^2+r^2 A^2}\begin{bmatrix} BC+r^2 AD \\ r^2\left(AC-BD\right) \end{bmatrix}.
\end{aligned}
\tag{8.9}
$$

From the theory of first order partial differential equations, either of the two equations in (8.9) determines α completely. That is, the two equations for α do not over specify the problem. Instead the two equations should be viewed as integrability conditions. We choose to solve

$$\frac{\partial \alpha}{\partial r} = \frac{BC + r^2 AD}{B^2 + r^2 A^2} \tag{8.10}$$

since the boundary condition in r is easily applied. Recall from (2.26) that at infinity α vanishes. We enforce this condition using the compactified coordinate s defined in (7.24). It is also possible to solve the θ derivative equations by enforcing local flatness as a boundary condition at either $\theta = 0$ or $\theta = \frac{\pi}{2}$.

Finally, we draw attention to the fact of α's decoupling from the elliptic equations listed in Chapter 6. While α depends on each of these functions, they do not depend on α. This allows us to first solve the elliptic equations and then use that solution to solve for α.

Chapter 9

Results

In this chapter we present and discuss our numerical results. We first demonstrate the pros and cons of our method by recovering the known solutions of the Einstein-Maxwell equations. Following this analysis, we present numerical solutions for charged MP black holes. Specifically, we consider the scalar functions satisfying the equations in Chapter 6. We do not consider the function α since it is not coupled to the other equations. Also, we note from Appendix B that for the known solutions the functional form of α is

$$\alpha = \frac{1}{2} \ln \left(\frac{\Sigma}{r^2} \right) \tag{9.1}$$

where the exact definition of Σ can be obtained from other scalar functions. It is likely that this relation also holds for charged MP black holes. If this is the case, once we have solved the coupled equation set we will also know α.

9.1   Tangherlini

We begin with the equations for a spherically symmetric black hole without electric charge. The analytic form of this black hole solution (and its charged generalization) was found by Tangherlini [12] and serves as a basic, but nontrivial, check of our equations and method.
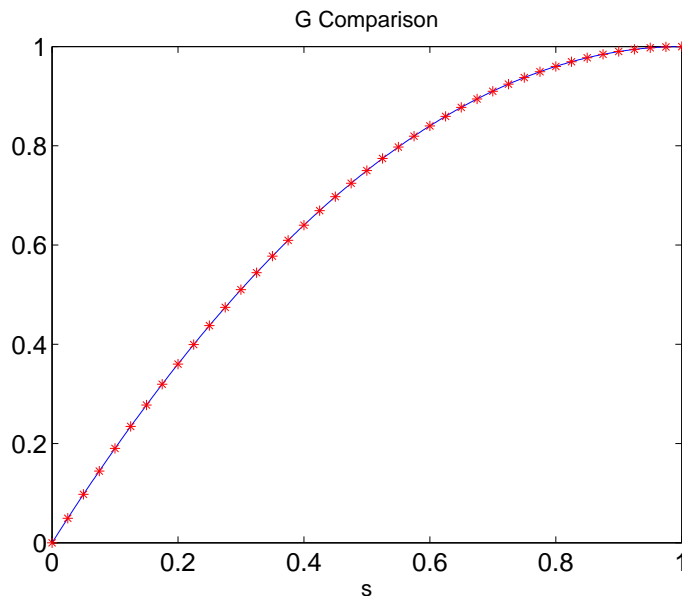
Figure 9.1 The numerical output of the function G corresponding to the Tangherlini solution denoted by a representative set of discrete points overlaid on the exact solution. For this solution we used a 401×201 grid and set $r_h = 0.5$. We see that the numerical results agree very well with the exact solution.

Since this solution does not allow rotation and is uncharged, the only nonvanishing unknown functions are G and H. Applying this to equations for G and H, (6.15) and (6.16) respectively, we find that they uncouple from one another. Furthermore, we notice that G and H satisfy identical equations. Because they also satisfy identical boundary conditions, they must be the same function. We refer to this function as G in the remainder of the section.

In addition to these simplifications, our assumption of spherical symmetry implies that G is a function of r only. In effect, our set of eight coupled partial differential equations has been reduced to one ordinary differential equation. However, we still use our Green function solver as a test of our method.

As outlined in Section 7.3 we first pick an initial guess for G and then calculate the source. We discover immediately that our initial choice for G can determine whether or not our algorithm converges. For instance, if we choose to begin with the flat space solution,
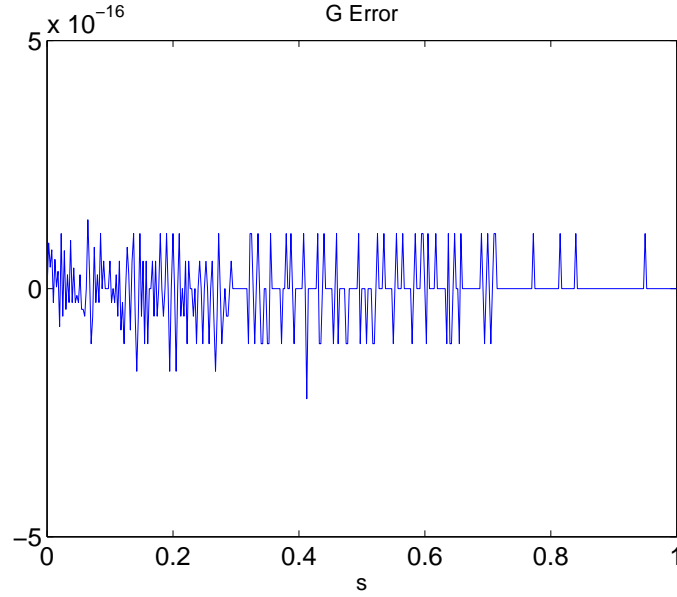
Figure 9.2 The difference between the numerical solution for Tangherlini function G and the exact solution. For this solution we used a 401×201 grid and set $r_h = 0.5$. The behavior of the error is not important, since it is at the level of machine precision. The important fact is the order of the error is 10^{-16}.

corresponding to $G = 1$, then the program begins to oscillate wildly after a few iterations. We note that this guess does not satisfy the boundary conditions for G. Apparently, a guess so far from the functional form of G is not good enough.

Recalling that the boundary term from (7.25) corresponds to at least the lowest order behavior of G, we choose this term as our initial G. From Chapter 5, G must vanish at the horizon and become 1 at spatial infinity, $s = 1$. Also, from the differential operator in (6.15) we find $p = q = 0$. Thus our initial guess G_0 is

$$G_0 = G\big|_{s=1} \left(1 - (1-s)^{2+p+q}\right)$$
$$= \left(1 - (1-s)^2\right). \tag{9.2}$$

When we use this initial guess the program converges immediately. In Fig. 9.1 we plot a representative sample of the numerical result alongside the exact solution. We can see that the two plots agree very well. We see just how well in Fig. 9.2, where we plot the difference

between the numerical and exact solutions for G. The particular behavior of the error is unimportant in this case. That the error is on the order of 10^{-16} is the important fact.

This degree of accuracy must be taken with a grain of salt. For the uncharged Tangherlini black hole it turn out that $G = G_0$. That is, the boundary integral is exactly G. We have in effect guessed the correct solution, and our program has confirmed that it is correct. Still, we gain confidence in using the boundary terms for the other functions as guides to our initial guesses.

9.2 Charged Tangherlini

The charged Tangherlini black hole shares many of the simplifications from the previous section. All functions that have to do with rotation vanish, and the remaining functions depend only on s. When we compare the source terms of G and H we see that while they might be identical, there is no immediately apparent reason why they must be. However, as we observe in Section C.2 symmetry considerations force them to be identical.

Thus, we have two independent functions to solve for: G and $Q^2 A_T$. Since we know the analytic form of G in the uncharged case we take that form as an initial guess for the charged case. Taking our lead from our experience with the uncharged case we use the boundary term $Q^2 A_T$ as our initial guess. So,

$$Q^2 A_{T0} = \Phi_h (1 - s)^2 \tag{9.3}$$

where Φ_h is the electric potential at the event horizon as defined in Chapter 5. The constant is left as a free parameter in the program with which we can increase or decrease the charge of the black hole. A similar free parameter is r_h the radial coordinate of the event horizon. This parameter can be thought of a a way to increase or decrease the mass of the black hole. We omitted it from the uncharged case because, while that black hole has mass, it turns out that G is independent of r_h in the uncharged case. When generating solutions we set

$r_h = 0.5$, which from (B.6) corresponds to setting $m = 1$ where m is the mass parameter in the Tangherlini solution.
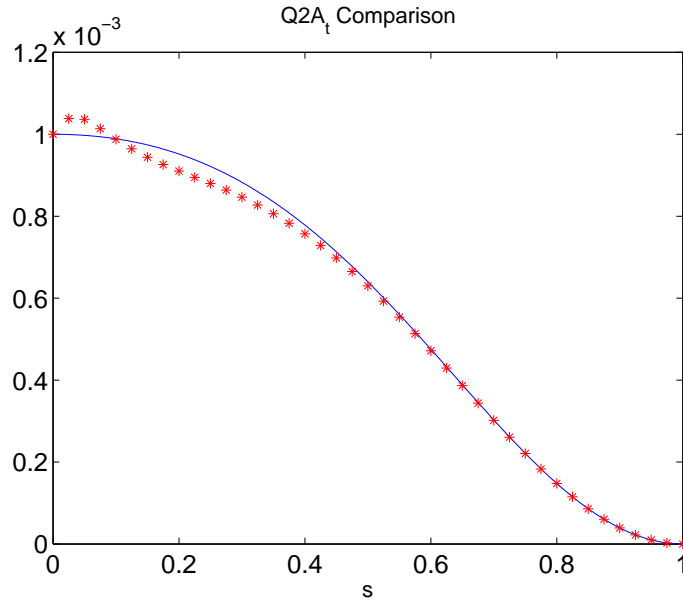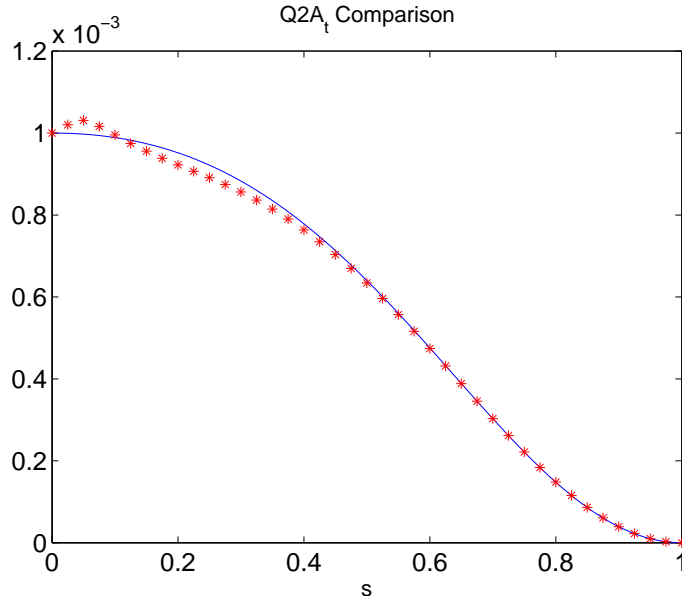

Figure 9.3 We plot $Q^2 A_T$ for a charged Tangherlini black hole. The numerical solution is compared with the exact solution. We use a 401×401 grid, $r_h = 0.5$, and $\Phi_h = 0.001$. Notice that near the event horizon, $s = 0$, the agreement is poor.

One last set of important parameters to set are the dimensions of our grid. Recall from Section 7.3 that each function is defined on an $N + 1 \times M + 1$ grid where s varies along N and μ along M. As we increase the size of N or M our numerical functions more closely approximate the continuum limit. This should increase the accuracy of our derivatives and integrations, and in short reduce the error of our method. Conversely, as the size of the grid decreases the program runs more quickly. Again, as the uncharged case had error on the order of machine precision, varying the size of the grid had little effect past a certain point. In particular we used a 401×201 grid to generate Figures 9.1 and 9.2.

Contrary to the uncharged case, charged Tangherlini black holes illustrate the effects of varying these parameters. For example, Fig. 9.3 compares the numerical and exact forms of $Q^2 A_T$. In this plot we have set $r_h = 0.5$, $\Phi_h = 0.001$ and use a 401×401 grid. It is clear from
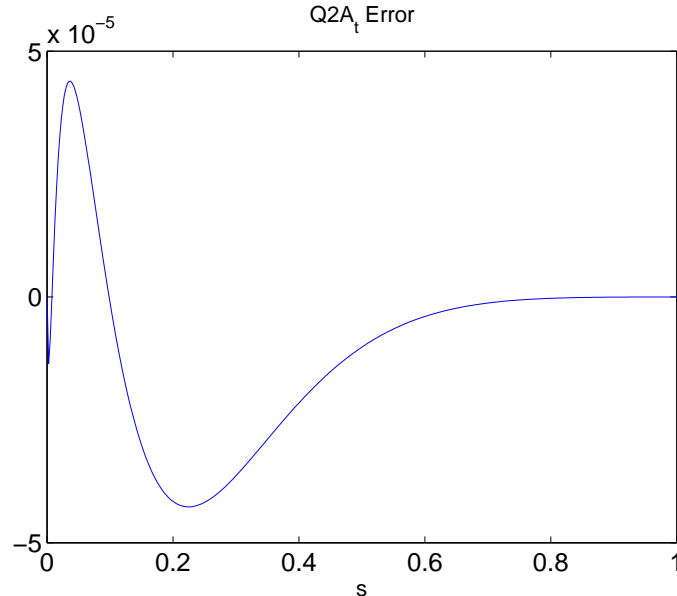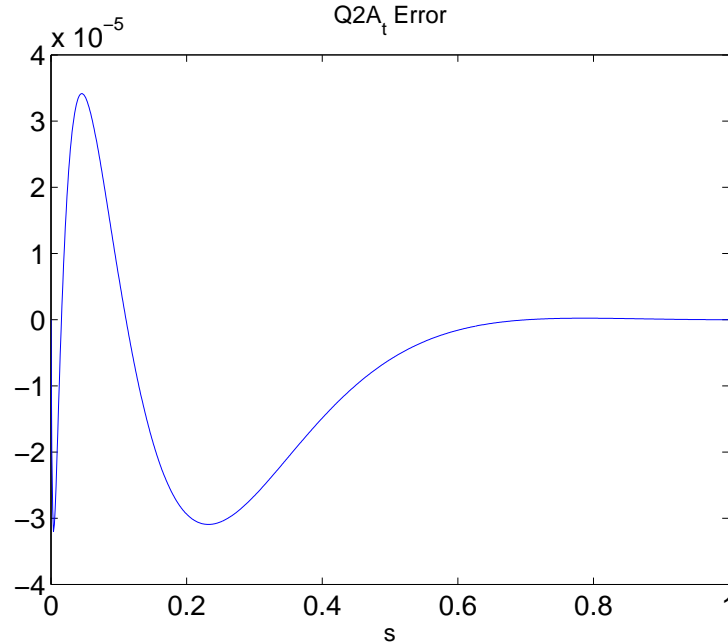
Figure 9.4 We plot the error between numerical and exact forms of $Q^2 A_T$ for a charged Tangherlini black hole. We use a 401×401 grid, $r_h = 0.5$, and $\Phi_h = 0.001$. Notice that the error has an oscillatory form. These oscillation errors seem to be sourced by the event horizon and propagate into the solution.

the figure that near the event horizon it becomes difficult to converge to the correct solution. In Fig. 9.4 we see that the numerical solution seems to have an oscillatory departure from the exact solution near the event horizon. We will see this behavior repeatedly in subsequent graphs. It appears that the event horizon acts as a source of these error oscillations, which then propagate into the full solution.

This behavior hear the horizon is unsettling, but perhaps it becomes vanishingly small as we increase the size of the grid. In Figs. 9.5 and 9.6 we compare the numerical and exact values of $Q^2 A_T$, but now we have increased the gird to 801×801. In comparing Figs. 9.3 and 9.5 we notice the discrepancy of the latter from the exact solution is slightly improved, but not as much as we might have hoped. This sentiment is confirmed as we compare Figs. 9.4 and 9.6. While the error is smaller when we use the larger grid, the change is not dramatic.

In Figs. 9.7 and 9.8 we construct plots similar to those previous, but we have increased the grid size to 1601×1601. Inspection of these plots reveals that the magnitude of the error
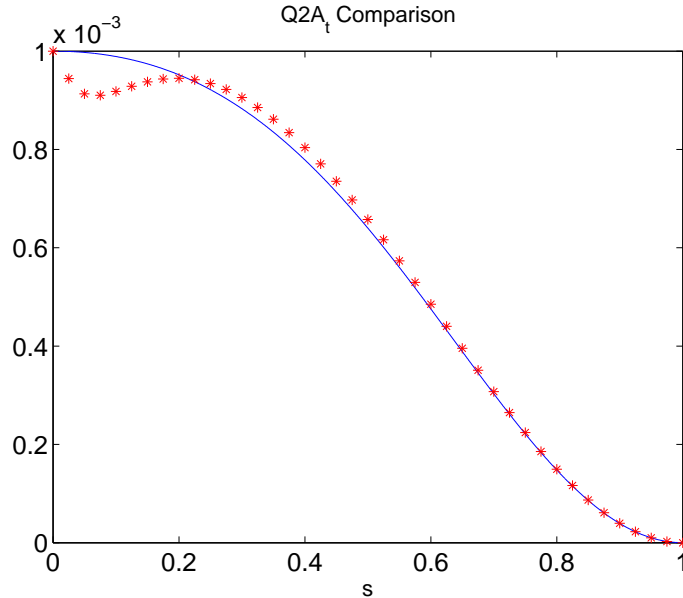
Figure 9.5 We plot $Q^2 A_T$ for a charged Tangherlini black hole. The numerical solution is compared with the exact solution. We use an 801×801 grid, $r_h = 0.5$, and $\Phi_h = 0.001$. Notice that near the event horizon, $s = 0$, the agreement is poor. However, by comparing with Fig. 9.3 we see that the discrepancy from the exact solution is slightly improved.

has not changed much, but the location and form of the error has. Specifically, the bulk of the error in Fig. 9.8 is below zero rather than the more even splits of the previous graphs.

We also consider what effect increasing the grid size has on G. In Fig. 9.9 we see that the numerical and exact solutions agree very well. In this plot we used a 1601×1601 grid, however the plot for a 401×401 grid is distinguishable. In Figs. 9.10 and 9.11 we plot the error using grid sizes 1601×1601 and 401×401 respectively. First, by comparing with Fig. 9.2 we note that the error is much larger than in the uncharged case. We also see that the decrease in the error is small, similar to what we observed with $Q^2 A_T$.

Since we have not yet shown a plot of $Q^2 A_T$ that corresponds to the exact solution, one might wonder if our equations are correct. To alleviate this fear we use the exact solution as our initial guess to check our equations. In Fig. 9.12 we compare the exact and numerical solutions when the initial guess is the exact solution. Note that the code is forced to go
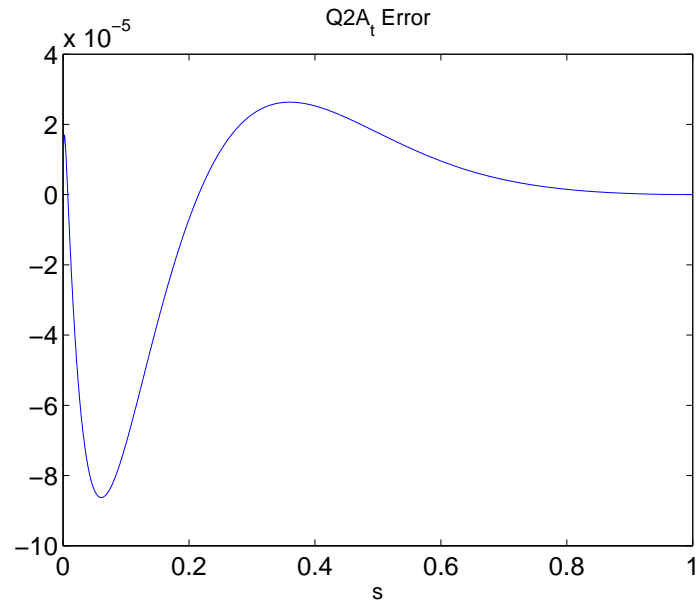
Figure 9.6 We plot the error between numerical and exact forms of $Q^2 A_T$ for a charged Tangherlini black hole. We use an 801×801 grid, $r_h = 0.5$, and $\Phi_h = 0.001$. When compared with Fig. 9.4 we see that the amplitude of the error is slightly smaller with the larger grid.

through at least two iterations, so this does check our equations.

Again, comparison of G with the exact solution appears identical to Fig. 9.9. However, the error in G and $Q^2 A_T$ as shown in Figs. 9.13 and 9.12 has gone down considerably from before. A remarkable result is that the error in G is now largest in the middle of the grid rather than at the event horizon. We also notice that while the error is much smaller than the previous charged cases, it is still much larger than the uncharged black hole. Conversely, the error $Q^2 A_T$ has the same form as in previous cases, and that while it is smaller the difference is not as dramatic as with G.

Up to this point all our results have kept Φ_h, and hence the charge of the black hole, fixed. Ideally we should be able to increase the charge of the black hole without incident until we reach some maximal amount of charge, that if passed would lead to a naked singularity[1].

[1]This is exactly what happens in the 3+1 dimensional case.

Figure 9.7 We plot $Q^2 A_T$ for a charged Tangherlini black hole. The numerical solution is compared with the exact solution. We use a 1601×1601 grid, $r_h = 0.5$, and $\Phi_h = 0.001$. Notice that near the event horizon, $s = 0$, the agreement is poor. However, by comparing with Figs. 9.3 and 9.5 we see that the discrepancy from the exact solutions takes a different form, but is not smaller in magnitude.

Unfortunately this is not the case. After increasing Φ_h to a certain point (which is not close to maximal) the program no longer converges.

In Figs. 9.16, 9.15, and 9.17 we plot the comparison of $Q^2 A_T$ with the exact solution, the error in G and the error in $Q^2 A_T$ respectively. In each of the figures $\Phi_h = 0.25$ and the grid size is 401×401. We also used the exact solution as our initial guess. With this in mind we notice immediately that the error in G is very high when compared with the $\Phi_h = 0.001$ case. Conversely, although the error in $Q^2 A_T$ appears high recall that the function itself becomes much larger. So, the error keeps about the same proportion to the value of the function. When Φ_h is increased significantly past this point the program begins to fail.

Figure 9.8 We plot the error between numerical and exact forms of $Q^2 A_T$ for a charged Tangherlini black hole. We use a 1601×1601 grid, $r_h = 0.5$, and $\Phi_h = 0.001$. When compared with Figs. 9.4 and 9.6 we see that the error has a larger negative amplitude and smaller positive amplitude.
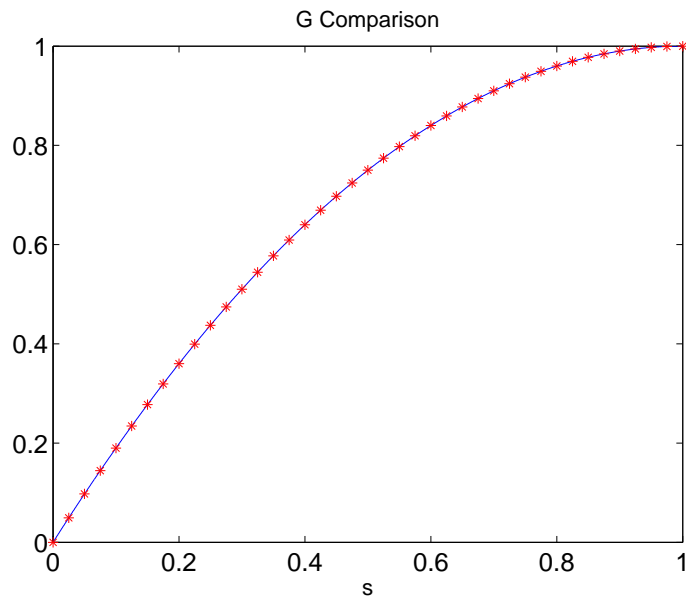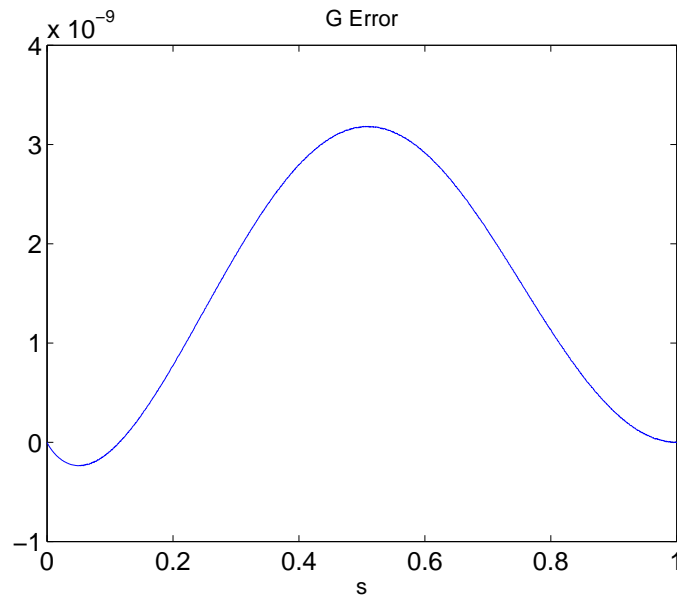

Figure 9.9 We plot G for a charged Tangherlini black hole. The numerical G is compared with the exact solution. We used a 1601×1601 grid, $r_h = 0.5$, and $\Phi_h = 0.001$. Similar to Fig. 9.1 the agreement appear to be excellent.
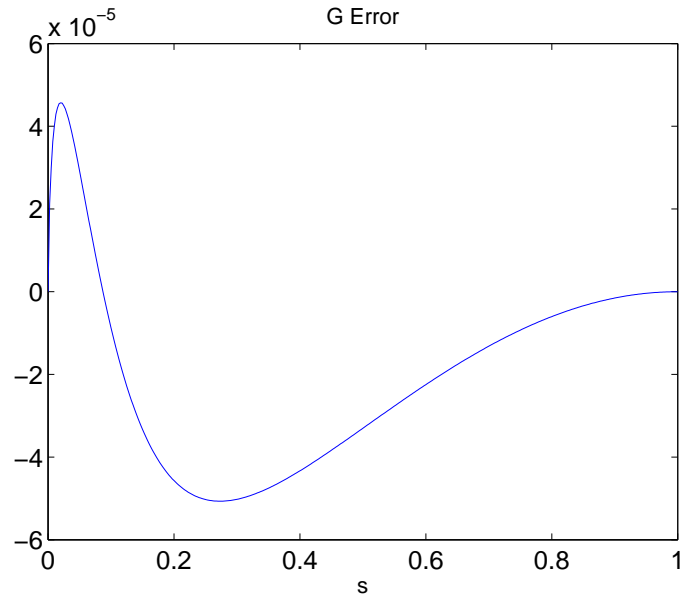
Figure 9.10 We plot G for a charged Tangherlini black hole. The numerical G is compared with the exact solution. We used a 401×401 grid, $r_h = 0.5$, and $\Phi_h = 0.001$. Notice the error has similar behavior and order as that of $Q^2 A_T$.
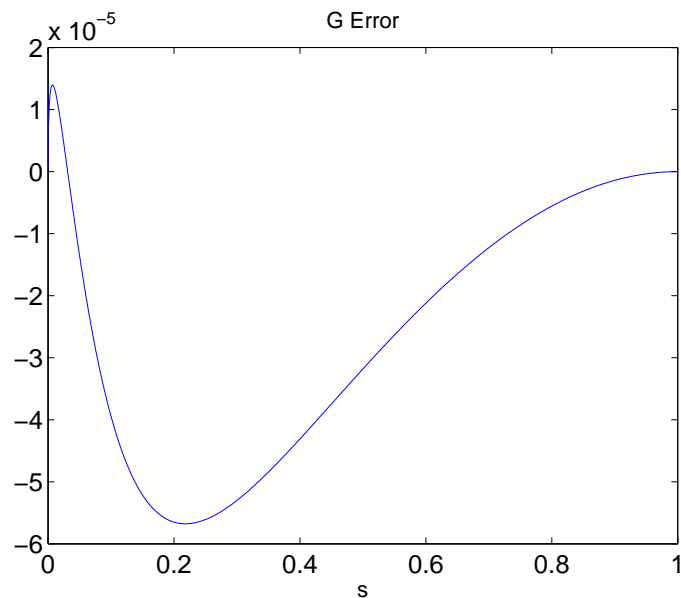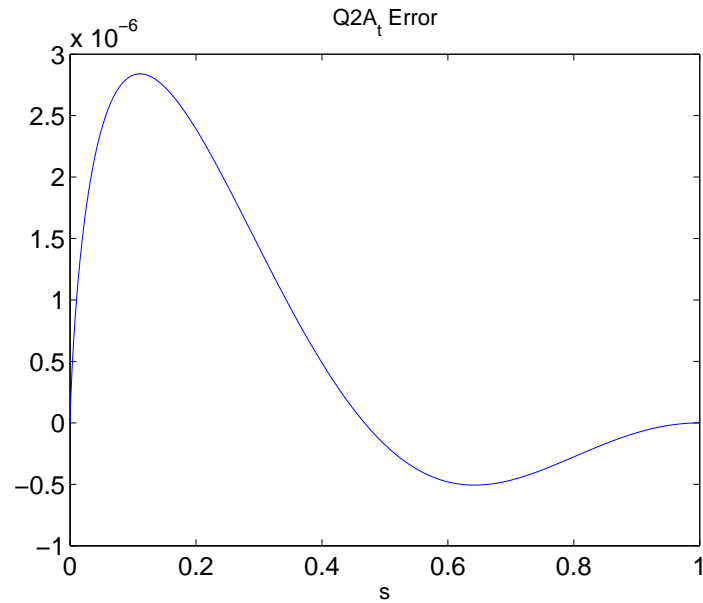

Figure 9.11 We plot the error between the numerical G for a charged Tangherlini black hole and the exact solution. We used a 1601×1601 grid, $r_h = 0.5$, and $\Phi_h = 0.001$. Compare with Fig. 9.10 and note that the total error is slightly reduced.
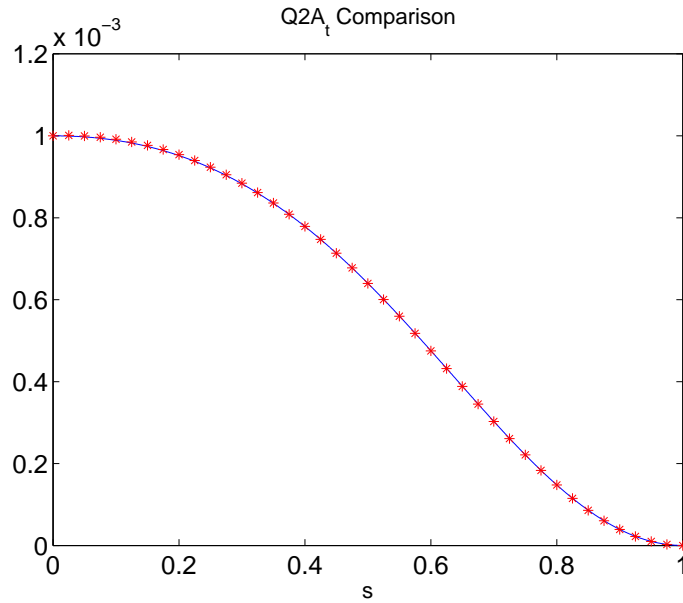
Figure 9.12 We plot the error between the numerical $Q^2 A_T$ for a charged Tangherlini black hole and the exact solution. We used a 1601×1601 grid, $r_h = 0.5$, and $\Phi_h = 0.001$. In this case we take the exact solution as our initial guess. Note that the numerical solution agrees with the exact solution.

Figure 9.13 We plot G for a charged Tangherlini black hole. The numerical G is compared with the exact solution. We used a 1601×1601 grid, $r_h = 0.5$, and $\Phi_h = 0.001$. In this case we use the exact solution as our initial guess. Notice that the error is still greater than the uncharged case, Fig. 9.2 but smaller than all other charged cases.
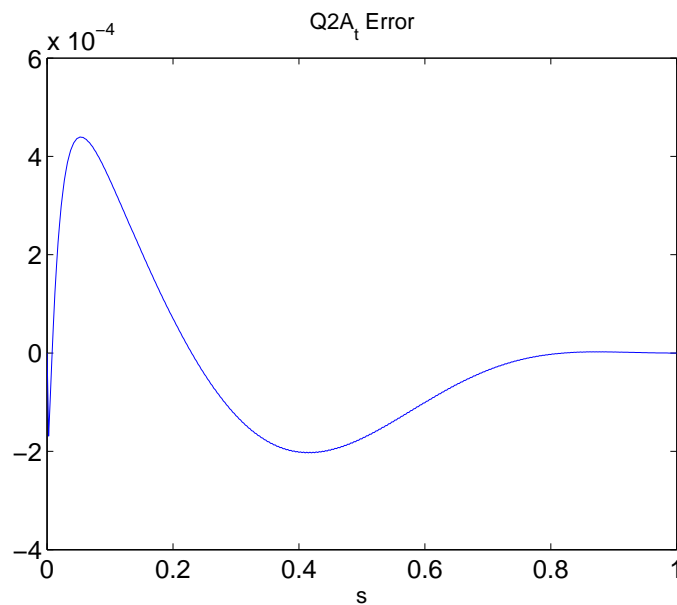
Figure 9.14 We plot the error between the numerical $Q^2 A_T$ for a charged Tangherlini black hole and the exact solution. We used a 1601×1601 grid, $r_h = 0.5$, and $\Phi_h = 0.001$. Notice that the error is significantly smaller than previous cases.
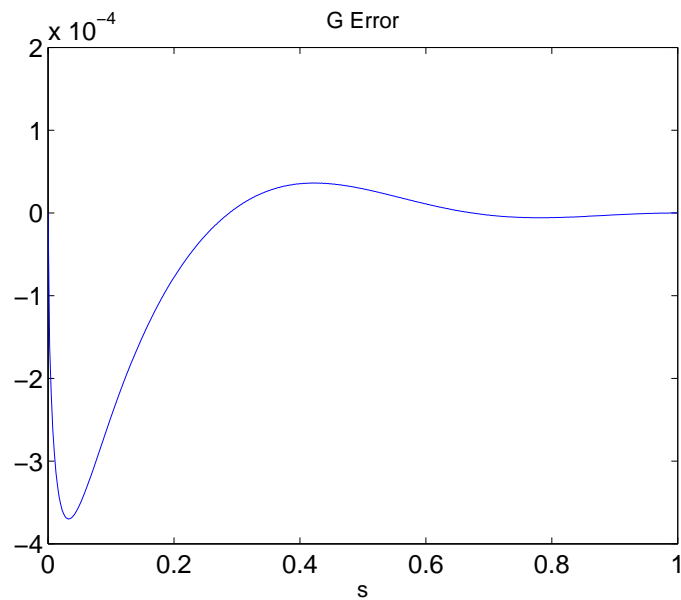
Figure 9.15 We plot the error between the numerical and exact G for a charged Tangherlini black hole. We used a 401×401 grid, $r_h = 0.5$, and $\Phi_h = 0.25$. In this case we use the exact solution as our initial guess. Notice the order of the error is larger than before.
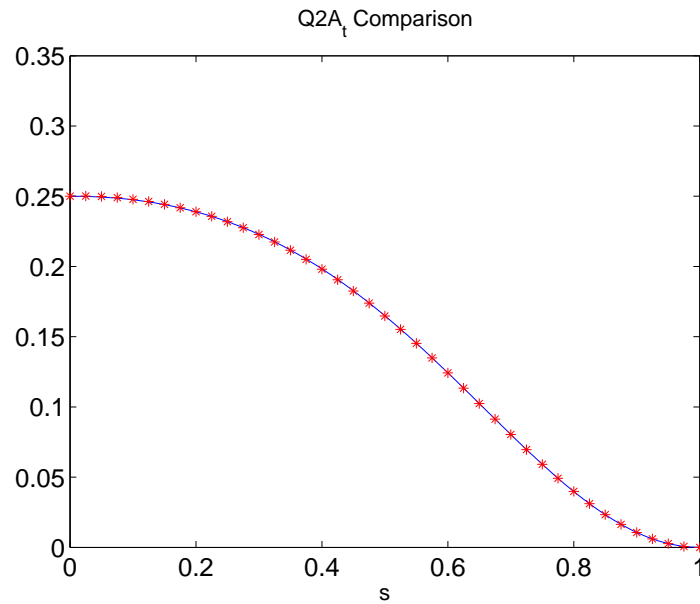
Figure 9.16 We compare the numerical $Q^2 A_T$ for a charged Tangherlini black hole and the exact solution. We used a 401×401 grid, $r_h = 0.5$, and $\Phi_h = 0.25$. Our initial guess was the exact solution. Notice that the agreement is excellent.

Figure 9.17 We plot the error between the numerical $Q^2 A_T$ for a charged Tangherlini black hole and the exact solution. We used a 401×401 grid, $r_h = 0.5$, and $\Phi_h = 0.25$. We see that the error is similar in behavior and order to the error in G.

9.3 Myers-Perry

The rotating black hole solution found by Myers and Perry [14] is considerably more compli-cated than the Tangherlini black holes. This family of black holes solutions is not spherically symmetric, so each function we solve for will in general depend on both s and μ. We must also account for the three rotation functions U_t, W, and I, and recognize that G and H are no longer identical.

We will also find the same type of instability in the MP code that we found in charged Tangherlini. When our initial guess is not very close to the exact solution we have oscillatory error propagating from the horizon. In addition we will find oscillating error in μ along the horizon. Also, similar to the behavior we found when varying Φ_h, the parameters Ω_ψ and Ω_ϕ can only be increased so much before the code fails to converge.

9.3.1 One Rotation

We begin by considering a MP black hole with only one nonzero angular momentum. This limited case is useful place to begin. The single rotation code is more stable in both the charged and uncharged cases. A solid background in the uncharged case will prepare us for the charged case which we consider later.

As we have shown in Appendix C the functions U_t and W are conjugate under a symmetry transformation. This is a consequence of the arbitrariness of the labels ϕ and ψ that we have assigned to the two spacelike Killing vectors. This is why there is no need to discuss the two possibilities of single rotation. In this section we will assume that U_t and I are identically zero, but choosing W and I to be zero would give equivalent results.

When we consider equation (6.15) with I, U_t and the vector potential set to zero we notice that G decouples from the other equations. In particular it reduces to the same source terms for the uncharged Tangherlini black hole. In Fig. 9.18 we plot the numerical result for G

on an 801×801 grid with $r_h = 0.5$ and $\Omega_\psi = 0.1$. However, G becomes independent of these parameters as it decouples from the other equations. It is also independent of μ since it reduces to the Tangherlini case. The error, as seen in Fig. 9.19, is of order 10^{-16}. This agreement appears in the same way as it did in the uncharged Tangherlini case.
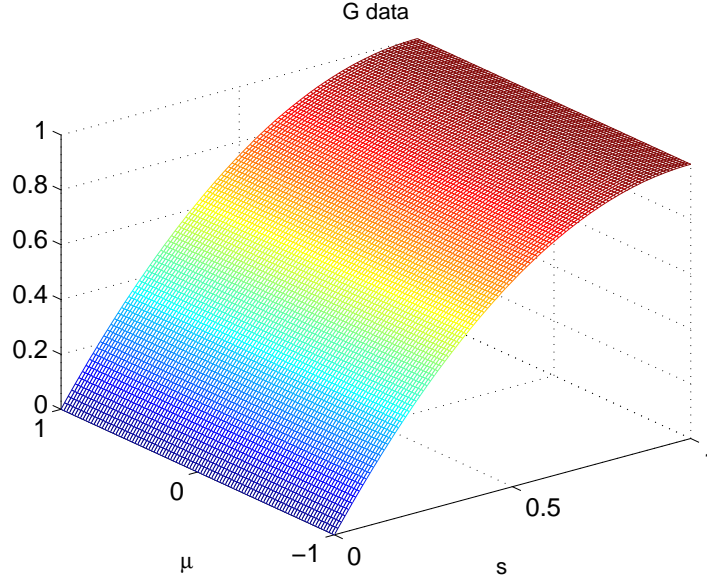

Figure 9.18 The numerical results for G from a single rotation MP black hole. These results were calculated on an 801×801 grid with $r_h = 0.5$ and $\Omega_\phi = 0.1$. However, since G uncouples from the other equations in this case the result is independent of these parameters.

The function H does not reduce to a previous case. However, as shown in Fig. 9.20 H appears to be identical to G. Closer inspection of H reveals it is μ dependent, but on a smaller scale.

We now take the Tangherlini solution as our initial guess supplemented by the boundary term for W. Specifically,

$$W_0 = \Omega_\psi \left(\frac{r_h}{r} \right)^4, \tag{9.4}$$

where we set $\Omega_\psi = 0.001$. In this case H appears exactly as in Fig. 9.20. In Fig. 9.21 we plot the error in H between the numerical and exact solution. While the error in H is much larger than in G, the order of the error is significantly smaller than the order of H. We also
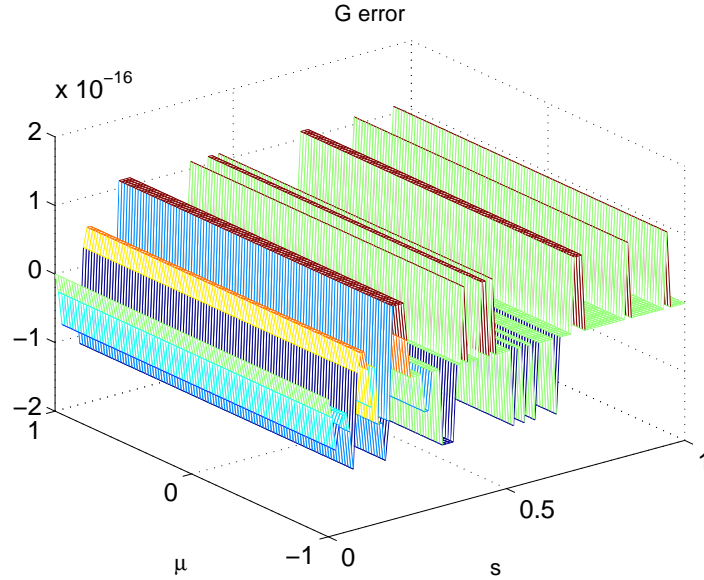
Figure 9.19 Error between the numerical and exact G for single rotation MP black hole. These results were calculated on an 801×801 grid with $r_h = 0.5$ and $\Omega_\phi = 0.1$. Similar to Fig. 9.2 only the order of the error is important.

notice that the error is largest near the event horizon, and propagates out from the horizon. This behavior is similar to what we saw with $Q^2 A_T$ in section 9.2. In addition we notice error oscillations in μ along the event horizon.

The appearance of error at the event horizon will be a common theme for the remainder of our results. For instance, in Fig. 9.22 we see that W exhibits this error plainly. We can see why this error is so apparent in W as opposed to H by looking at Fig. 9.23. The error is order 10^{-4}, which is the same as the error in H. But W itself is order 10^{-3} while H is order 1. This is why the error is more visible in W than H.

It is important to recognize that these oscillations in μ at the horizon are numerical artifacts. Consider Figs. 9.24 and 9.25. In the former we see many oscillations, which correspond to the error in W. The latter plot gives a more regular dependence. This is the real μ dependence of W which appears to be approximately odd about $\mu = 0$. In short, not only do we have error propagating in s from the event horizon we also see error oscillating
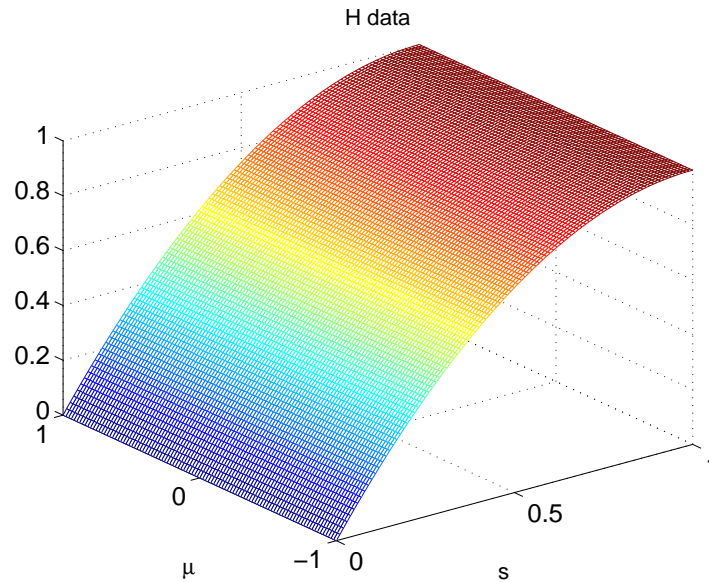
Figure 9.20 The numerical results for H from a single rotation MP black hole. These results were calculated on an 801×801 grid with $r_h = 0.5$ and $\Omega_\phi = 0.1$. While this functions appears very similar to G (see Fig. 9.18) it is μ dependent on a smaller scale.

in μ close to the horizon.

As we did in section 9.2 we can reduce this error some by guessing the correct solution at the outset. This also serves as a check on the validity of our equations. We also illustrate some of the range of Ω_ψ for which the code still converges. For the following plots we use the exact solution as our initial guess and take $\Omega_\psi = 0.1$.

First, recall that these changes have no effect on G. The function H also appears the same, but as seen in Fig. 9.26 its error does change. Because we have started with the exact solution the error oscillations have been decreased, however the larger magnitude of Ω_ψ keeps something of them present.

In Figs. 9.27 and 9.28 we plot W and its error respectively. When examining W alone we cannot see the error oscillations close to the event horizon. This is because the error in W, though larger than before, is smaller relative to the order of W itself. When we look at the μ dependence of W (see Fig. 9.29) we find the that these oscillations are still present.
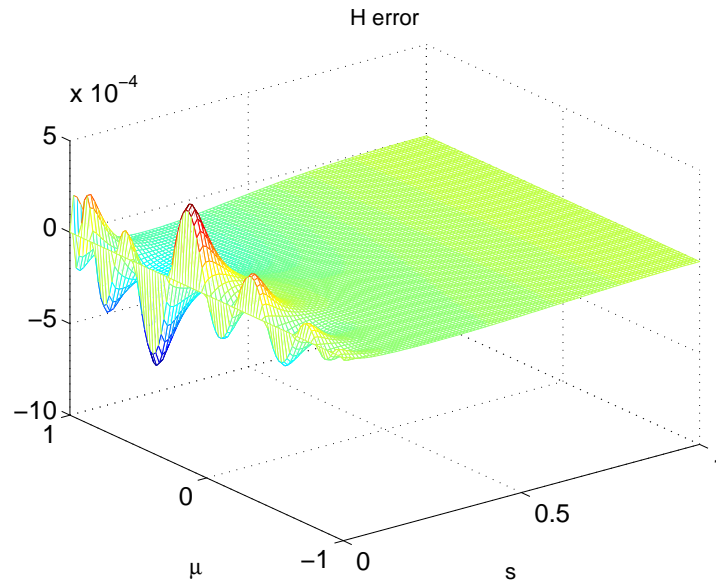
Figure 9.21 Error in H between the numerical and exact solution single rotation MP black hole. We used an 801×801 grid with $r_h = 0.5$ and $\Omega_\psi = 0.001$. Notice that the error is order 10^{-4} while H is order 1. The bulk of the error appears at the event horizon. Notice the appearance of error oscillations in μ along the horizon.

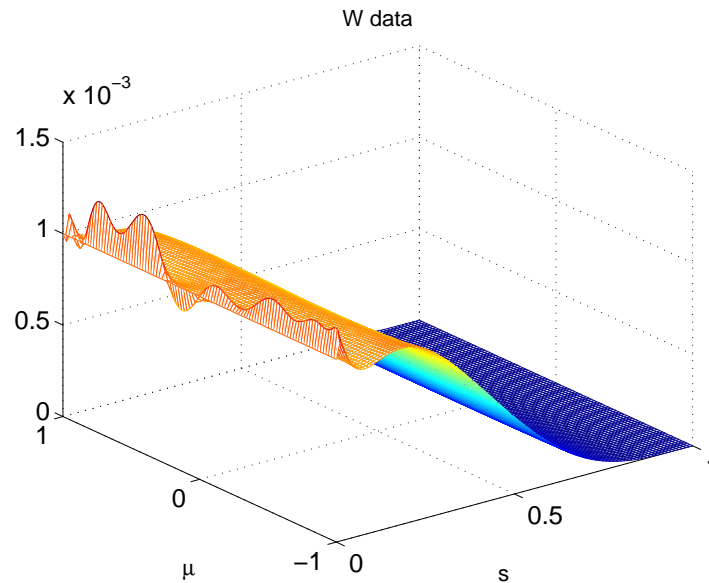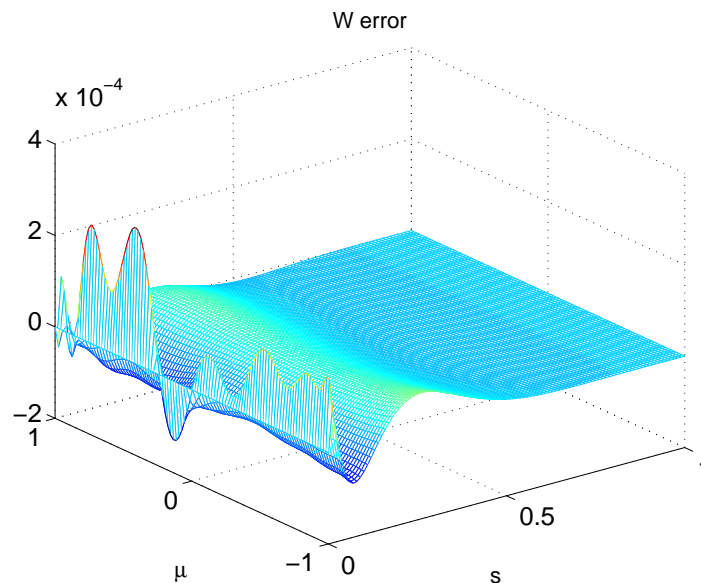However, they disappear as we move away from the horizon and leave W with the same μ dependence we saw in Fig. 9.25.

Figure 9.22 The numerical results for W from a single rotation MP black hole. We used an 801×801 grid with $r_h = 0.5$ and $\Omega_\psi = 0.001$. Notice the erroneous oscillations near the event horizon.

Figure 9.23 Error in W between the numerical and exact solutions for a single rotation black hole. We used an 801×801 grid with $r_h = 0.5$ and $\Omega_\psi = 0.001$. We clearly see oscillatory error propagating from the horizon and along the horizon. Notice that the error is only one order of magnitude smaller that the order of the function.
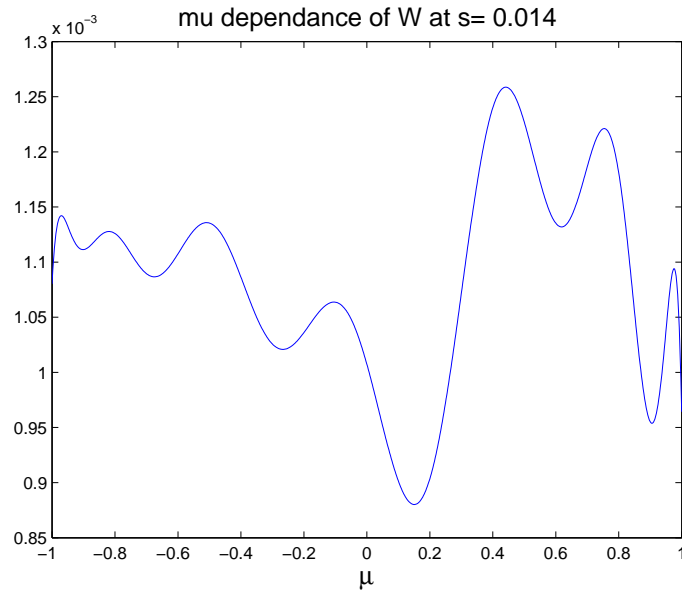
Figure 9.24 We plot the μ dependence of numerical W close to the horizon of a single rotation MP black hole. We used an 801×801 grid with $r_h = 0.5$ and $\Omega_\psi = 0.001$. Compare with Fig. 9.25.
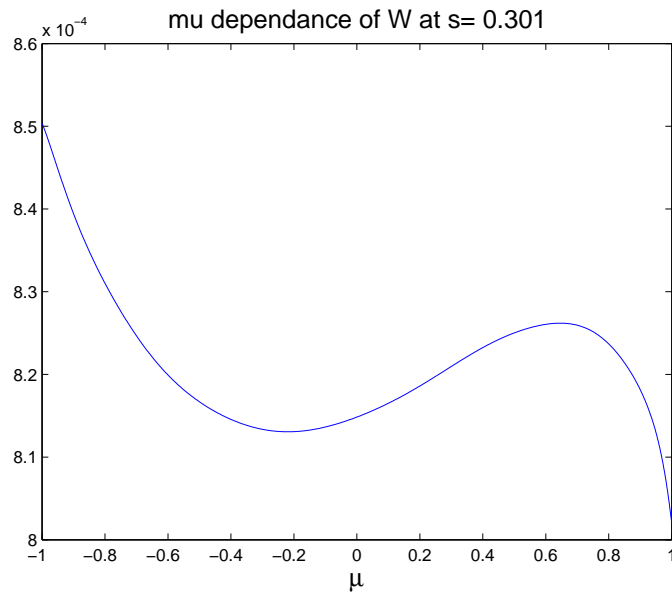

Figure 9.25 We plot the μ dependence of numerical W close to the horizon of a single rotation MP black hole. We used an 801×801 grid with $r_h = 0.5$ and $\Omega_\psi = 0.001$. Notice that away from the horizon the μ dependence is very regular. Compare with Fig. 9.24.
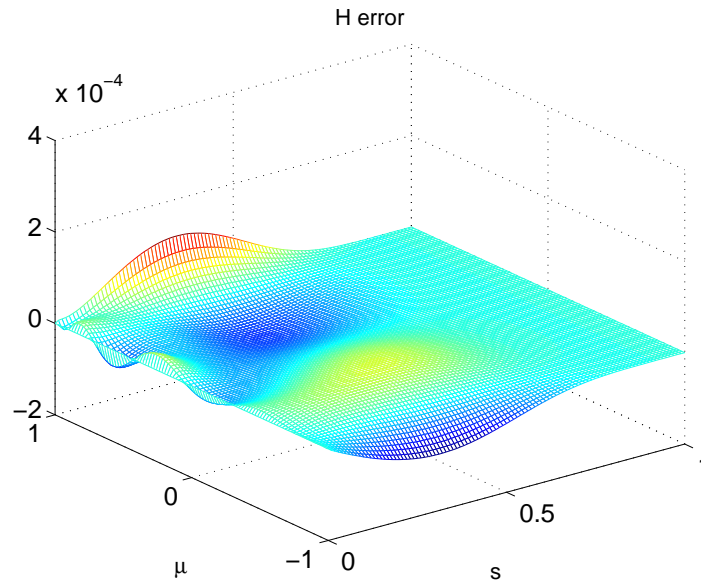
Figure 9.26 Error in H between numerical and exact forms of a single rotation MP black hole with $\Omega_\psi = 0.1$. In this case we have used the exact solution as our initial guess. Notice that the error oscillations in μ have been reduced.
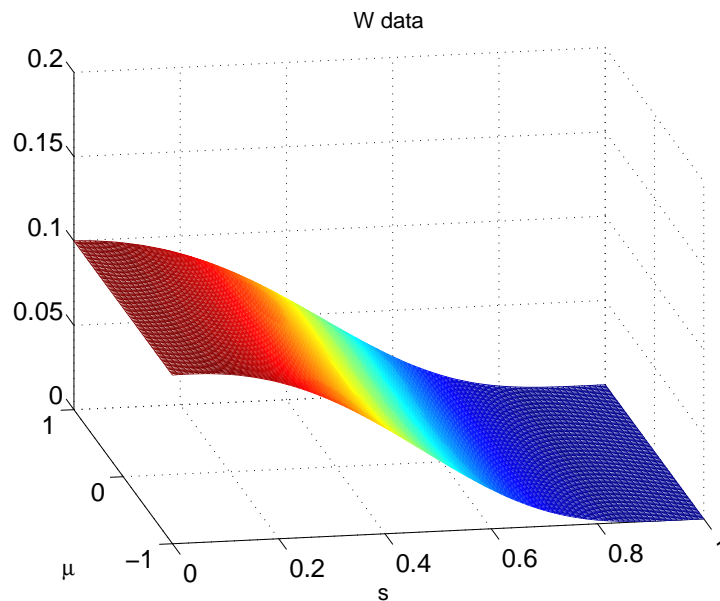

Figure 9.27 Numerical W for a single rotation MP black hole with $\Omega_\psi = 0.1$. Notice that error oscillations near the horizon are not visible due to the increased magnitude of W itself.
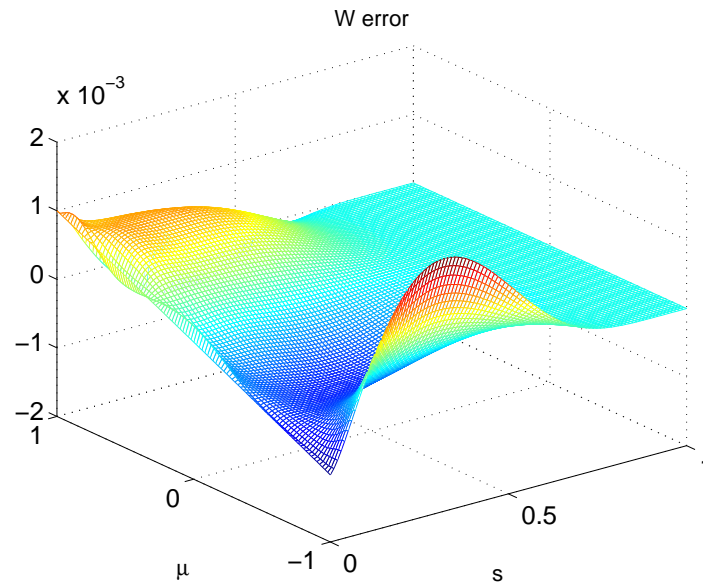
Figure 9.28 Error in W for a single rotation MP black hole with $\Omega_\psi = 0.1$. Notice that the order of the error is larger than Fig. 9.23, but is smaller relative to the order of W.
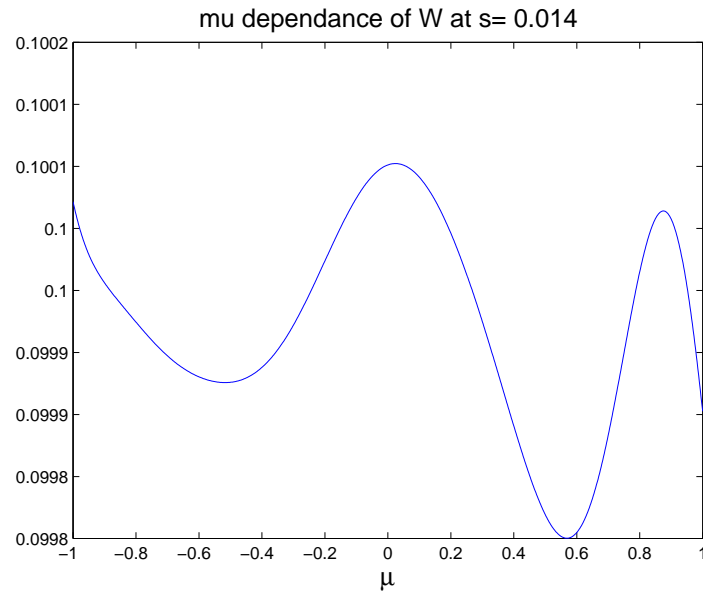

Figure 9.29 We plot the μ dependence of W for single rotation MP black hole with $\Omega_\psi = 0.1$. Notice the error oscillations are still present close to the horizon.

9.3.2 Two Rotations

The main difference introduced by having two nonzero angular momenta is the connection between the two rotational planes. This connection is encoded in the function I. Unfortunately, we find that I can be very unstable and can make the code diverge whenever it is nonzero. Unsurprisingly, this instability begins at the event horizon in a manner similar to the numerical error exposed in the previous section.

A natural first thought upon seeing this divergence is that the code is incorrect. However, by using the exact solution as our initial guess we can check that the source terms are accurate. The integrater is identical to the previous cases which led to reasonable accuracy and convergence. We are left then to speculate that the system is unstable, specifically in the function I.

We will illustrate some of the symptoms of this instability. We assume the exact solution for a MP black hole with $\Omega_\psi = \Omega_\phi = 0.001$ and define the functions on an 801×801 grid. The functions G and H look identical to Figs. 9.18 and 9.20 respectively at the large scale. However, in Figs. 9.30 and 9.31 we see that they each have a different dependence on μ.

Their respective dependences appear to be reflections of one another across $\mu = 0$. A similar occurrence shows up in the plots of their errors. In Figs. 9.32 and 9.33 we plot the error in G and H respectively. We clearly see that their respective error plots are mirror images about $\mu = 0$.

This reflection symmetry is also present in U_t and W. In Figs. 9.34 and 9.35 we plot the μ dependence of U_t and W respectively. The symmetry in their dependence is unsurprising in the light of our analysis in Appendix C. In that appendix we show that letting μ become $-\mu$ and exchanging Ω_ψ and Ω_ϕ we take U_t into W and vice versa. Since we have set $\Omega_\phi = \Omega_\psi$ U_t and W should differ exactly by mirror μ dependence about $\mu = 0$.

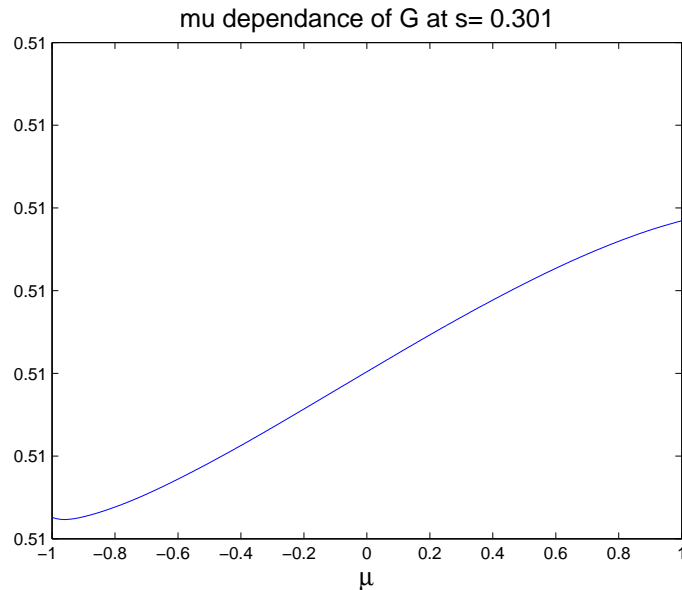Along with this expected symmetry, we find symmetry in their error plots as well. In

Figure 9.30 We plot the μ dependence of G for a MP black hole with $\Omega_\psi = \Omega_\phi = 0.001$. Note the mirror symmetry with Fig. 9.31.

Figs. 9.36 and 9.37 we plot the error in U_t and W respectively. Notice that similar to the case with G and H their error is symmetric about $\mu = 0$.

Finally, we consider the function I. In Fig. 9.38 we plot I. Recall that at the horizon I should have the value $\Omega_\phi \Omega_\psi = 10^{-6}$. This also serves as the maximum value for I. Thus we see that the entire plot is dominated by error. In fact, plotting the error in I gives back the same plot. So, while the other functions were not rendered useless, I becomes all error. The cause likely corresponds to the spike at $\mu = -1$ close to the horizon. However, we have not yet discovered how to prevent this numerical divergence.
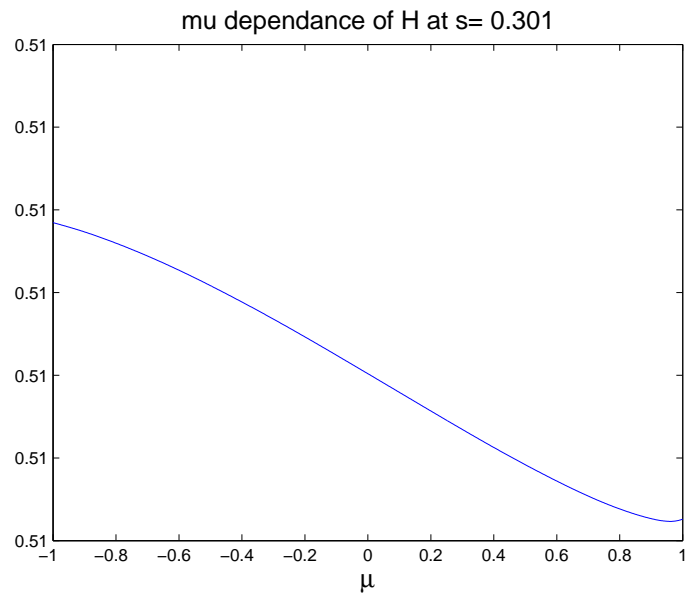
Figure 9.31 We plot the μ dependence of H for a MP black hole with $\Omega_\psi = \Omega_\phi = 0.001$. Note the mirror symmetry with Fig. 9.30.
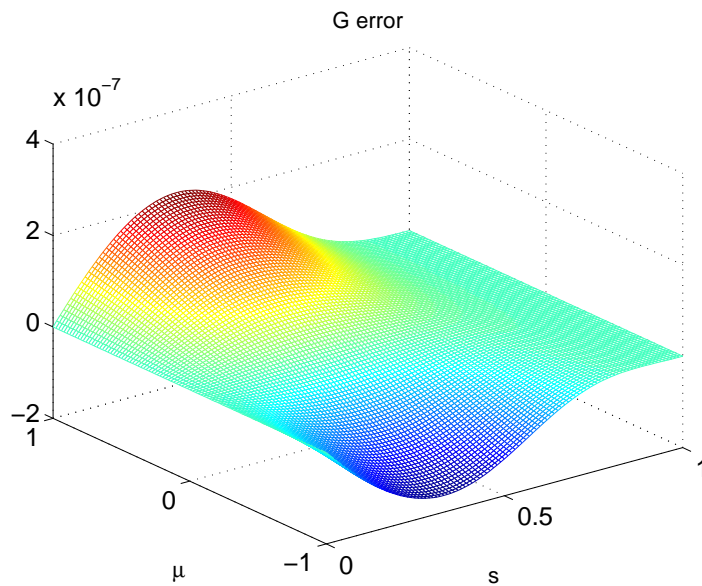

Figure 9.32 We plot the error in G for a MP black hole with $\Omega_\psi = \Omega_\phi = 0.001$. Notice the mirror symmetry in μ with Fig. 9.33.
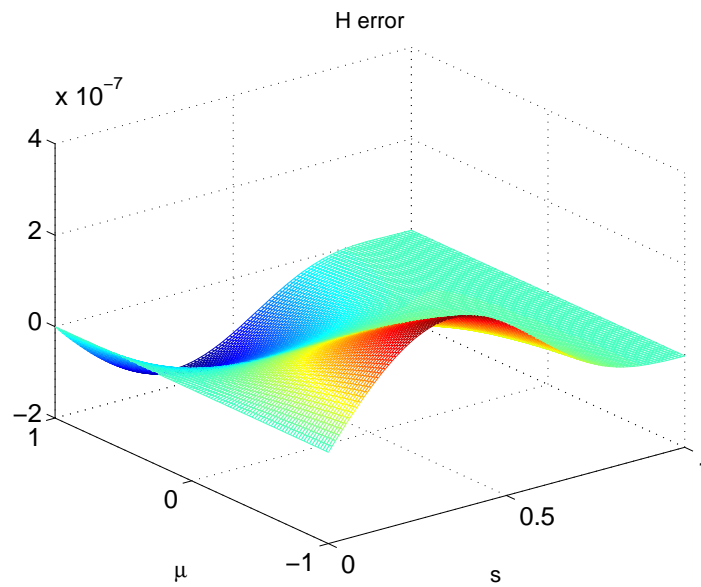
Figure 9.33 We plot the error in H for a MP black hole with $\Omega_\psi = \Omega_\phi = 0.001$. Notice the mirror symmetry in μ with Fig. 9.32.
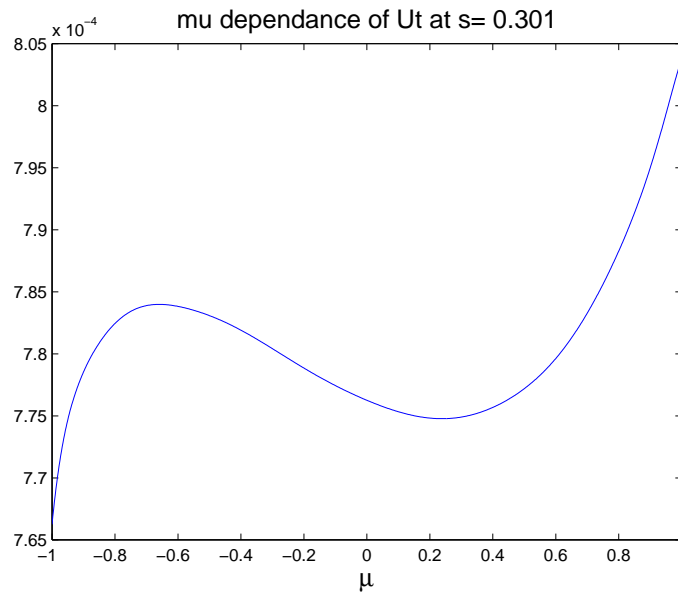

Figure 9.34 We plot the μ dependence of U_t for a MP black hole with $\Omega_\psi = \Omega_\phi = 0.001$. Note the mirror symmetry with Fig. 9.35.
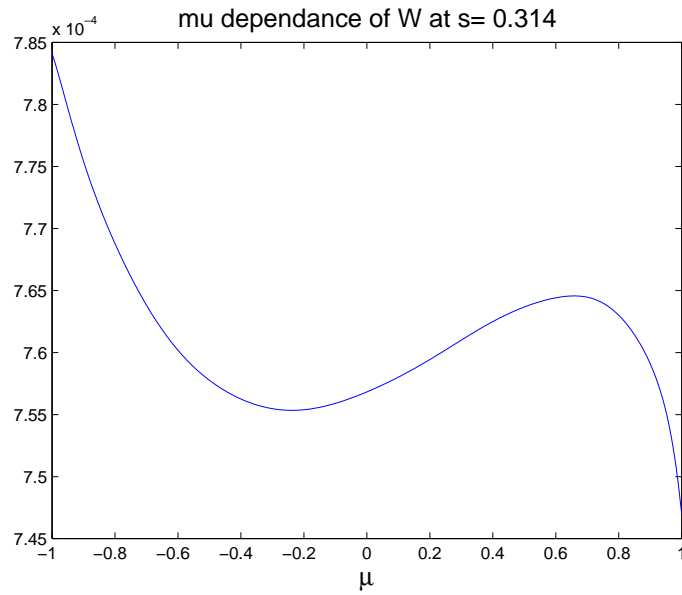
Figure 9.35 We plot the μ dependence of W for a MP black hole with $\Omega_\psi = \Omega_\phi = 0.001$. Note the mirror symmetry with Fig. 9.34.

Figure 9.36 We plot the error in U_t for a MP black hole with $\Omega_\psi = \Omega_\phi = 0.001$. Notice the mirror symmetry in μ with Fig. 9.37.
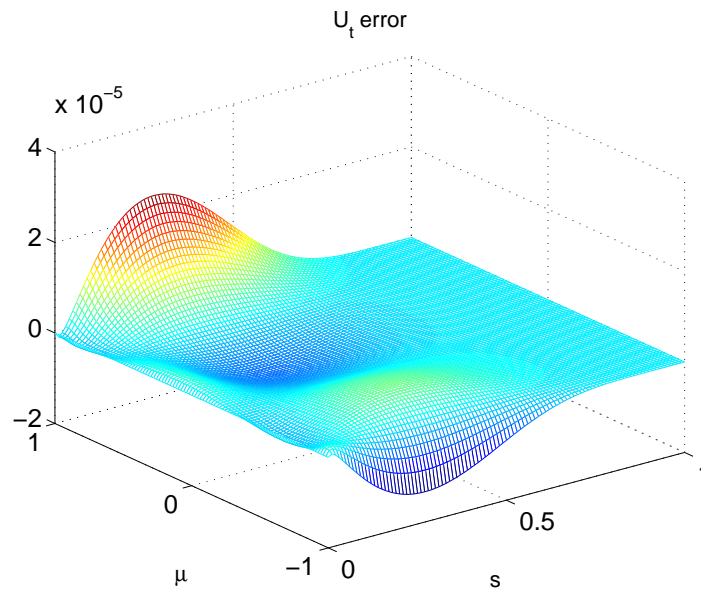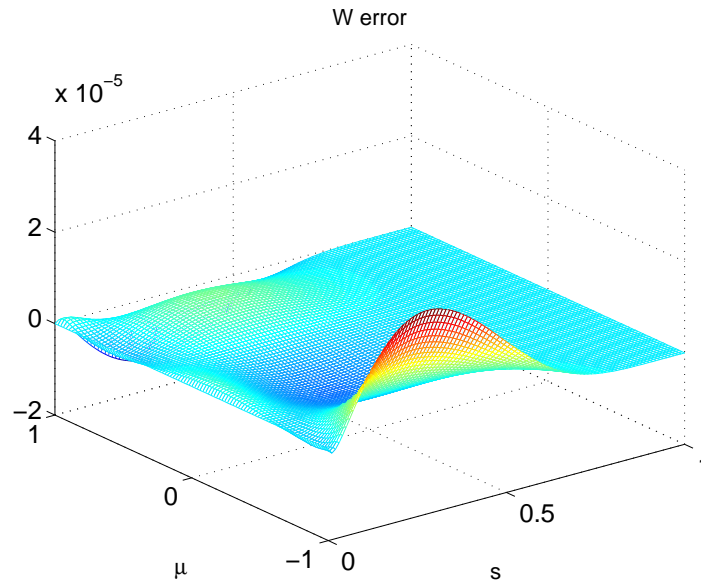
Figure 9.37 We plot the error in W for a MP black hole with $\Omega_\psi = \Omega_\phi = 0.001$. Notice the mirror symmetry in μ with Fig. 9.36.
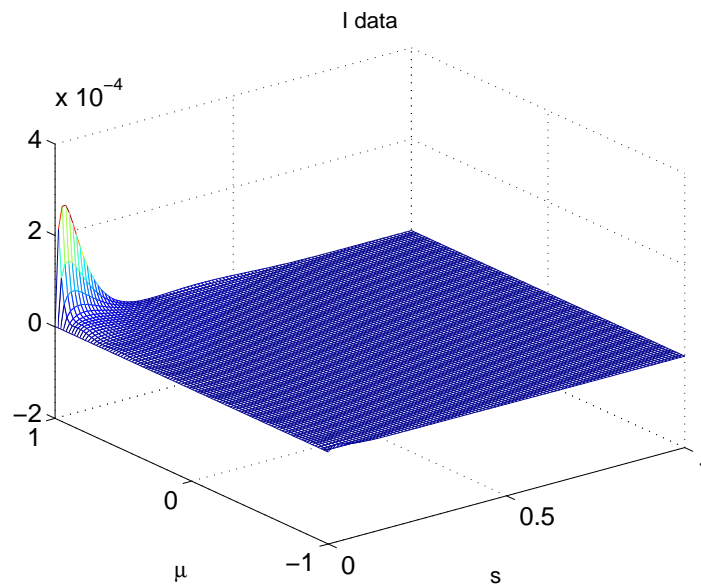

Figure 9.38 We plot I for a MP black hole with $\Omega_\psi = \Omega_\phi = 0.001$. This plot is completely dominated by the error in I. The order of I is only 10^{-6}.

9.4 Charged Myers-Perry

Now that we have verified, at least as far as possible, the validity of our method we turn our attention to charged MP black holes. We find that many of the behaviors we have noted in the previous sections carry over into the rotating, charged case. This is true both in the true behavior of the functions and the error inherent in our method.

As an analytic solution for these black holes has yet to be found, we extract information about the form of the unknown functions to guide further work. In particular we find some numerical evidence for the boundary conditions we have assumed for the projections of the vector potential. We also find an identical divergent behavior in the numerical solution for I as in the uncharged case.

9.4.1 One Rotation

As with the MP black holes we first consider single rotation solutions. As in the uncharged case, these solutions are numerically more stable and contain much of the important functional behavior. For ease of comparison to the uncharged case we choose nonzero rotation in the ψ direction. This means the functions I, U_t, and A_U are set to zero. The plots in this section we generated on an 801×801 grid with $r_h = 0.5$.

We have seen in the previous sections that the closer our initial guess is to the exact solution the smaller the error. With this in mind we do not simply take the MP solution supplemented by boundary terms as our initial guess. Instead we begin with the pertubative solution discovered by Aliev [23]. The exact form of the initial guess can be found in section B.3.

Initially, we set $\Omega_\psi = 0.001$ and $\Phi_h = 0.001$ to attempt to keep the error at the horizon small. We first notice that unlike the uncharged case G does not reduce to a μ independent form. While Fig. 9.39 does not appear μ dependent, we see in Fig. 9.40 that G does have

nontrivial variation in μ. In particular, G appears to be even about $\mu = 0$.
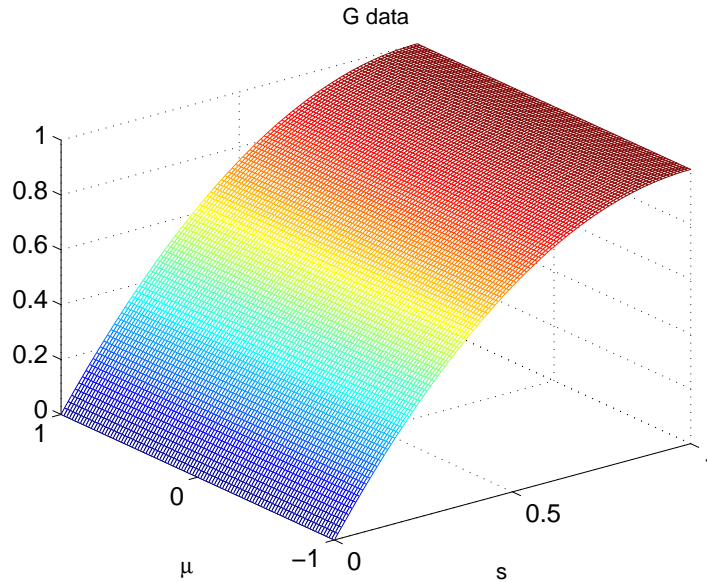

Figure 9.39 Numerical result for G for a charged rotating black hole with $\Phi_h = 0.001$ and $\Omega_\psi = 0.001$. While G appears unchanged from the uncharged case, it now has μ dependence, see Fig. 9.40.

Similar to previous solutions H appears identical to G on large scales. However, as we see in Fig. 9.41 it has a different μ dependence. It is also important to notice that very close to the horizon both H and G have error oscillations which disappear as we move away from the horizon. We claim that these oscillations are not part of the true solution because they also appeared in the uncharged case in which we could confirm that they are erroneous. These oscillations near the horizon appear in every subsequent graph, but we will forgo pointing them out unless they are of particular interest.

Next, we consider $Q^2 A_T$. In Fig. 9.42 we see that the form of $Q^2 A_T$ seems identical to the charged Tangherlini case. However, as is the case with H and G there is a small scale μ dependence. We see in Fig. 9.43 that this dependence seems to be approximately even about $\mu = 0$.

In Figs. 9.44 and 9.45 we plot the W and its μ dependence respectively. Notice that
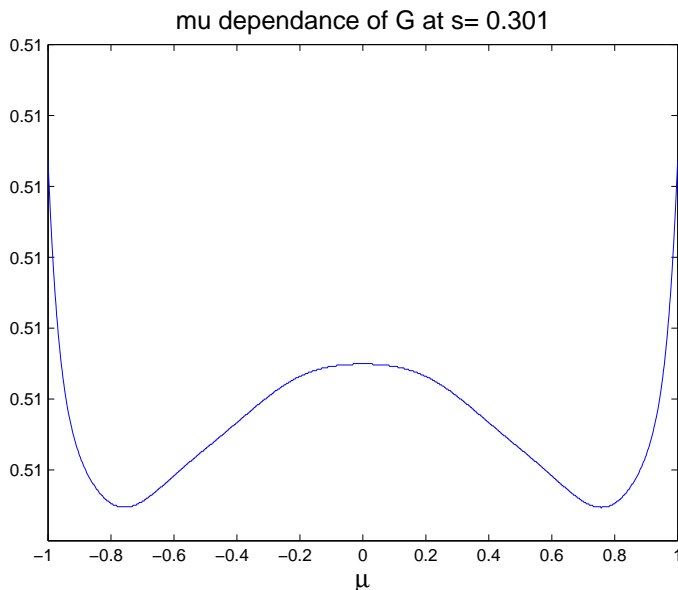
Figure 9.40 We plot the μ dependence of G for a charged, singly rotating black hole with $\Phi_h = 0.001$ and $\Omega_\psi = 0.001$. Note that unlike the uncharged case G has nontrivial μ dependence.

unlike the uncharged case, there are no visible error oscillations near the horizon even though the values of Ω_ψ are identical. These oscillations are present on a smaller scale, but disappear quickly as we move away from the horizon.

In contrast to the improved behavior at the horizon exhibited by W, we see in Fig. 9.46 that A_W has very large oscillations at the horizon. We presume that these oscillations are error because they are of the same form as error in other functions. Recall that the function I also seems to be unstable close to the horizon. It may be the case that functions which connect physical properties, for instance I connects the two spins and A_W connects spin and charge, are more unstable than the other functions. After these initial oscillations at the horizon, we see in Fig. 9.47 the μ dependence of A_W takes a form very similar to W.
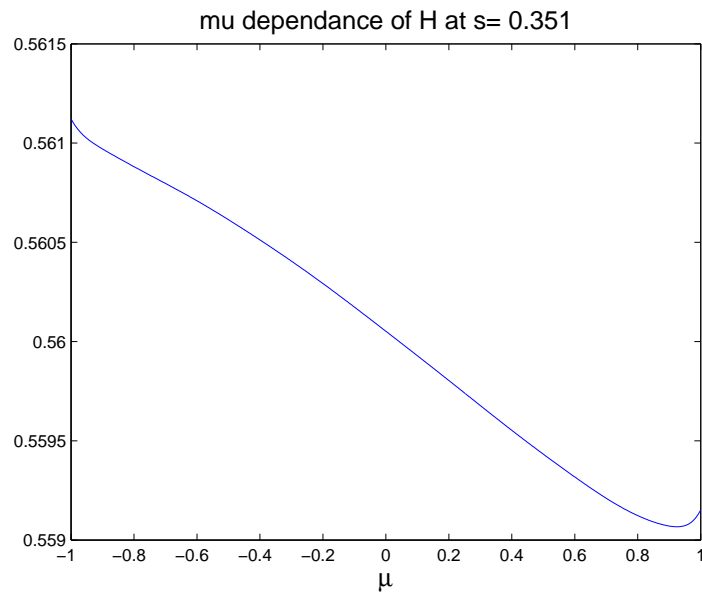
Figure 9.41 We plot the μ dependence of H for a charged, singly rotating black hole with $\Phi_h = 0.2$ and $\Omega_\psi = 0.1$. This general form of this dependence is not dependent on Φ_h and Ω_ψ. Compare with Fig. 9.40.
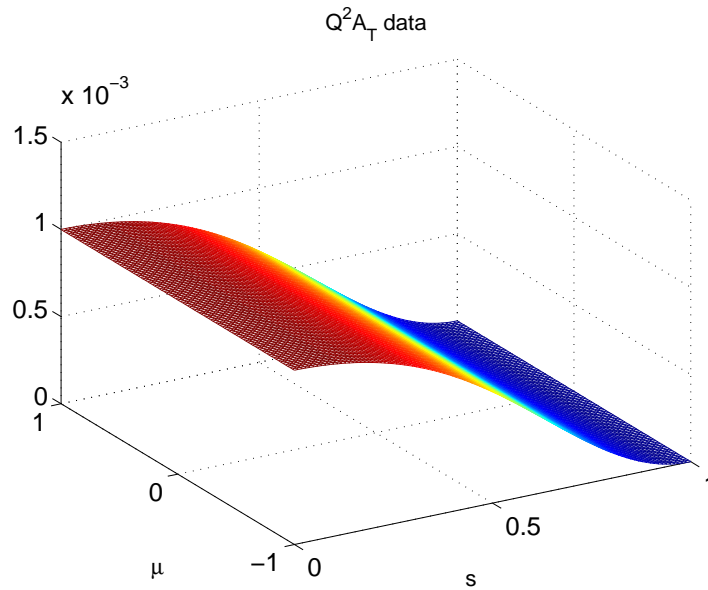
Figure 9.42 Numerical result for $Q^2 A_T$ in a singly rotating, charged black hole with $\Phi_h = 0.001$ and $\Omega_\psi = 0.001$.

Figure 9.43 We plot the μ dependence of $Q^2 A_T$ in a singly rotating, charged black hole with $\Phi_h = 0.001$ and $\Omega_\psi = 0.001$.

Figure 9.44 Numerical result for W in a singly rotating, charged black hole with $\Phi_h = 0.001$ and $\Omega_\psi = 0.001$.

Figure 9.45 We plot the μ dependence of W in a singly rotating, charged black hole with $\Phi_h = 0.001$ and $\Omega_\psi = 0.001$.

Figure 9.46 Numerical result for A_W in a singly rotating, charged black hole with $\Phi_h = 0.001$ and $\Omega_\psi = 0.001$. We take the large oscillations in μ at the even horizon to be error.
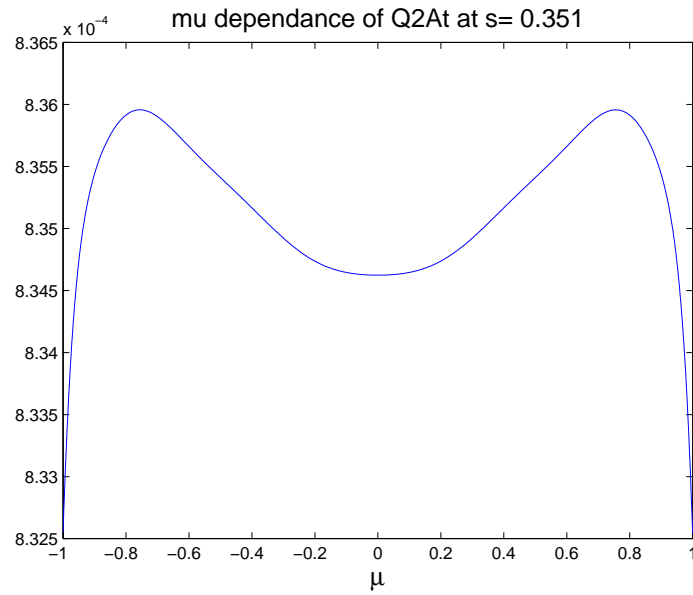
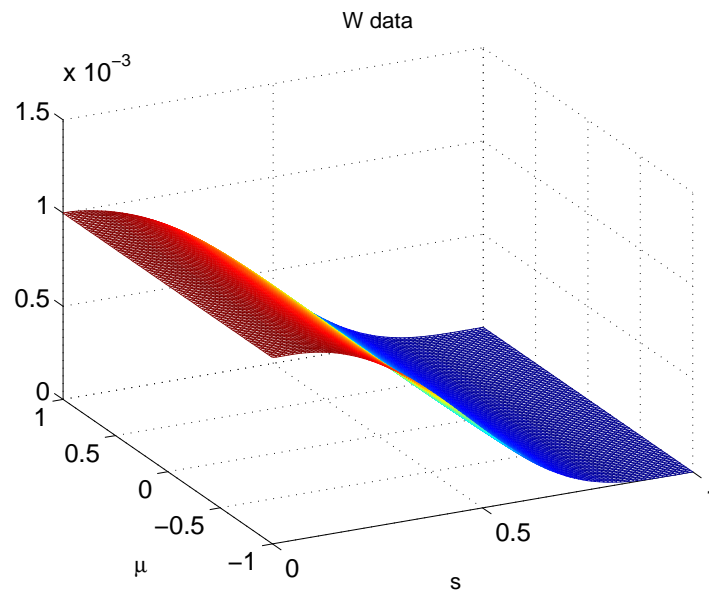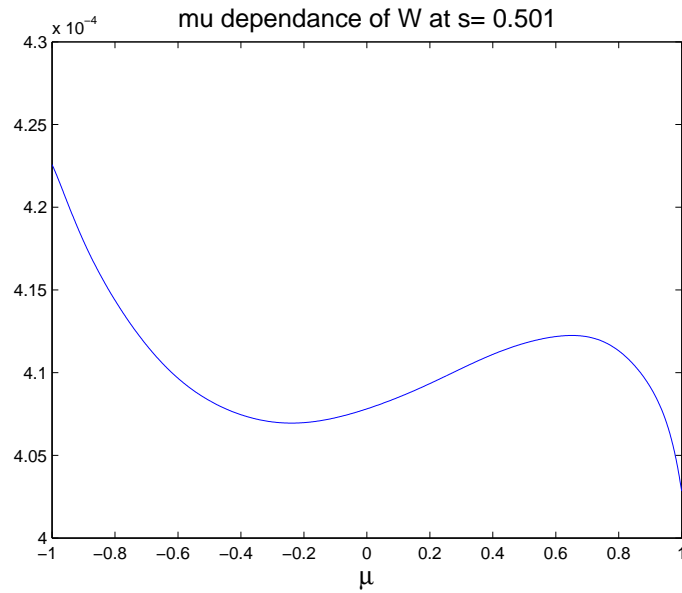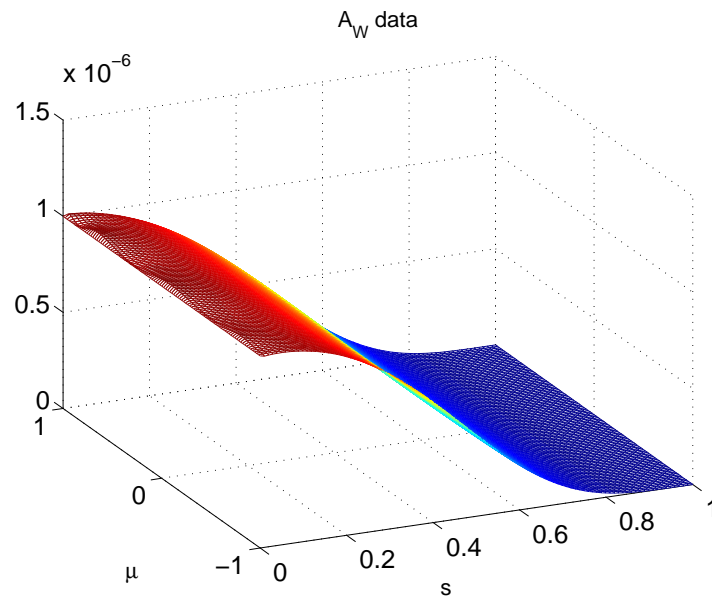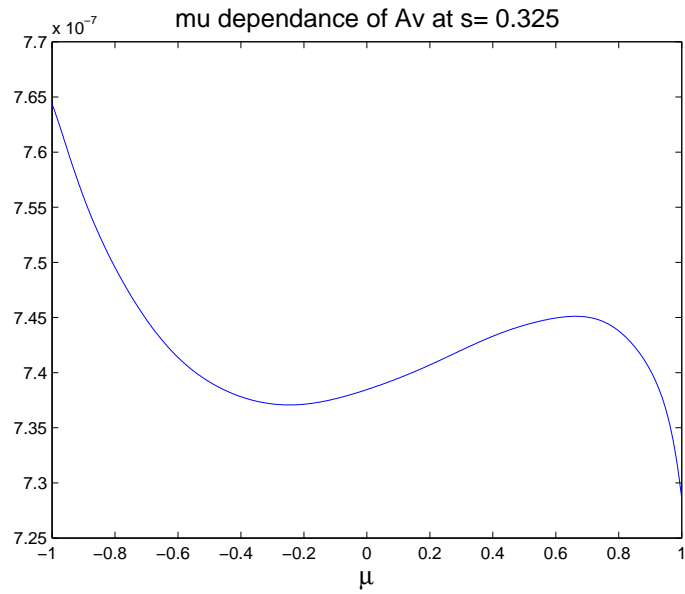**Figure 9.47** We plot the μ dependence of A_W in a singly rotating, charged black hole with $\Phi_h = 0.001$ and $\Omega_\psi = 0.001$. Close to the event horizon there is a more complicated dependence which we take to be erroneous.

9.4.2   Two Rotations

Finally, we consider the most general case. That of a charged black hole with two nonzero angular momenta. Like the uncharged case we find that our method is unstable in the function I. Knowing this, there is not much new information that we can extract beyond what was found in the singly rotating case. One conclusion we do confirm is the symmetry relations between the functions.

From the uncharged case we saw that even when the exact solution was the initial guess, the program did not converge. Knowing this it is unlikely that any initial guess would allow the charged case to converge. However, we expect better results with a better guess. We take as our initial guess the ansatz used by Aliev [23] that lead to the perturbative solution.

For convenience in defining this ansatz we define the following:

$$r_h^2 = \frac{\sqrt{(m - a^2 - b^2)^2 - 4(q^2 - ab)}}{4} \tag{9.5}$$

$$R = r^2 + \frac{m - a^2 - b^2}{2} + \frac{r_h^4}{r^4} \tag{9.6}$$

$$A = R + a^2 \tag{9.7}$$

$$B = R + b^2 \tag{9.8}$$

$$\Sigma = r^2 + \frac{m + \cos 2\theta (a^2 - b^2)}{2} + \frac{r_h^4}{r^4} \tag{9.9}$$

$$D = \Sigma AB + \left(m - \frac{q^2}{R}\right)\left(Ab^2 \cos^2\theta + Ba^2 \sin^2\theta\right) \tag{9.10}$$

where q is a charge parameter and a and b are rotation parameters relating to ϕ and ψ respectively. The ansatz is as follows:

$$G = rF\sqrt{\frac{\Sigma B + \left(m - \frac{q^2}{R}\right)b^2 \cos^2\theta}{D}} \tag{9.11}$$

$$H = rF\sqrt{\frac{\Sigma}{\Sigma B + \left(m - \frac{q^2}{R}\right)b^2 \cos^2\theta}} \tag{9.12}$$

$$U_t = -\frac{aB\left(m - \frac{q^2}{R}\right)}{D} \tag{9.13}$$

$$W = -\frac{bA\left(m - \frac{q^2}{R}\right)}{D} \tag{9.14}$$

$$I = \frac{ab\left(m - \frac{q^2}{R}\right)}{D} \tag{9.15}$$

$$Q^2 A_T = -\frac{q\sqrt{3}AB}{2D} \tag{9.16}$$

$$A_U = \frac{aq\sqrt{3}B}{2D} \tag{9.17}$$

$$A_W = \frac{bq\sqrt{3}A}{2D} \tag{9.18}$$

where F is defined by equation (7.23). We choose this guess because, unlike the perturbative solution, it incorporates the complexity of the MP solution. In addition is includes a coupling to electric charge very much like the Kerr-Newman solution in four dimensions. It also reduces to the MP and charged Tangherlini solutions in the appropriate limits.

This guess also satisfies as the boundary conditions of all our functions and the leading order radial behavior of each function corresponds to the boundary terms associated to each function by Green's identity. In addition, while it is not an exact solution, Aliev has shown that it does satisfy the Einstein-Maxwell equations when the values of a and b are very small.

With this initial guess we employ our method on an 801×801 grid with $\Omega_\phi = \Omega_\psi = \Phi_h = 0.001$. Many of the plots appear very similar to previous cases, but we include them for completeness. For most we do not include a plot of μ dependence. This is because the form of the μ dependence is similar to previous cases.

We do briefly focus on the μ dependence of A_U and A_W. Notice in Figs. 9.56 and 9.57 the mirror symmetry between A_U and A_W. This case is similar to that of U_t and W and occurs for the same reason. In the language of Appendix C A_U and A_W are conjugate to each other under the exchange of Ω_ϕ and Ω_ψ with μ becoming $-\mu$.

While we do not have sufficient accuracy to make specific analysis of these results, we
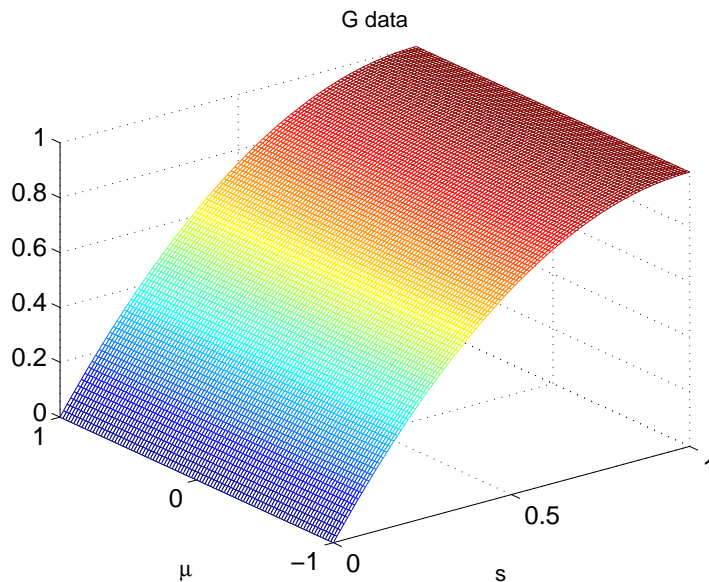
Figure 9.48 Plot of G for charged MP black hole using an 801×801 grid with $\Omega_\phi = \Omega_\psi = \Phi_h = 0.001$.

have confirmed the symmetry properties of these functions. The conjugate behavior of W and U_t as well as A_U and A_W show this most clearly. However, the self conjugate behavior of $Q^2 A_T$ also verifies our analysis. Recall from Fig. 9.43 that the μ dependence of $Q^2 A_T$ is symmetric about $\mu = 0$. A graph similar to this occurs in the two rotation case. This follows from self-conjugacy since the symmetry transformation exchanges Ω_ϕ and Ω_ψ while taking μ to $-\mu$. Since we have set the two horizon velocities to be equal, invariance under this transformation amounts to symmetry about $\mu = 0$.
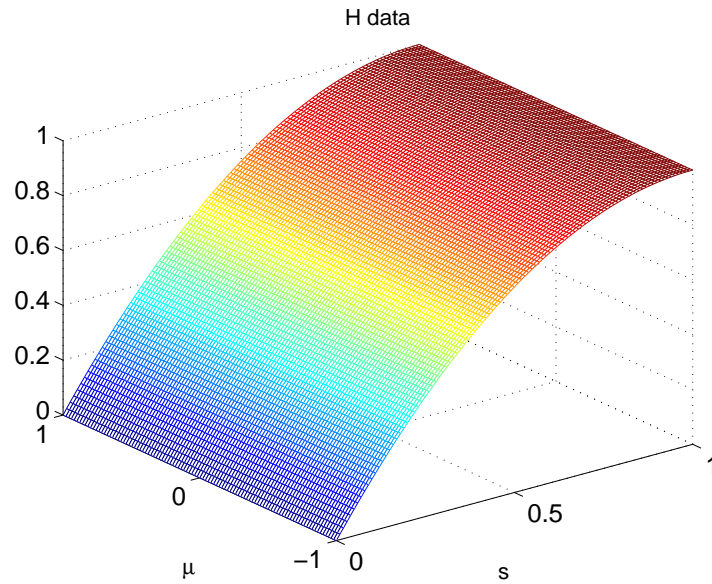
Figure 9.49 Plot of H for charged MP black hole using an 801×801 grid with $\Omega_\phi = \Omega_\psi = \Phi_h = 0.001$.
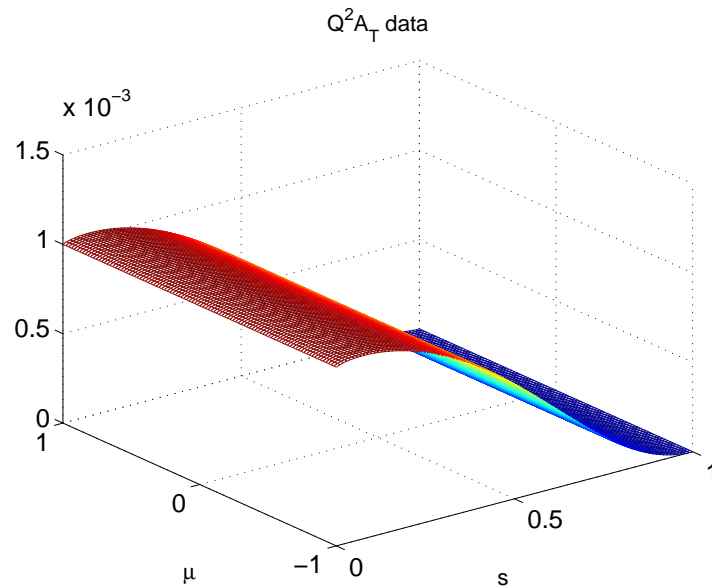
Figure 9.50 Plot of $Q^2 A_T$ for charged MP black hole using an 801×801 grid with $\Omega_\phi = \Omega_\psi = \Phi_h = 0.001$.
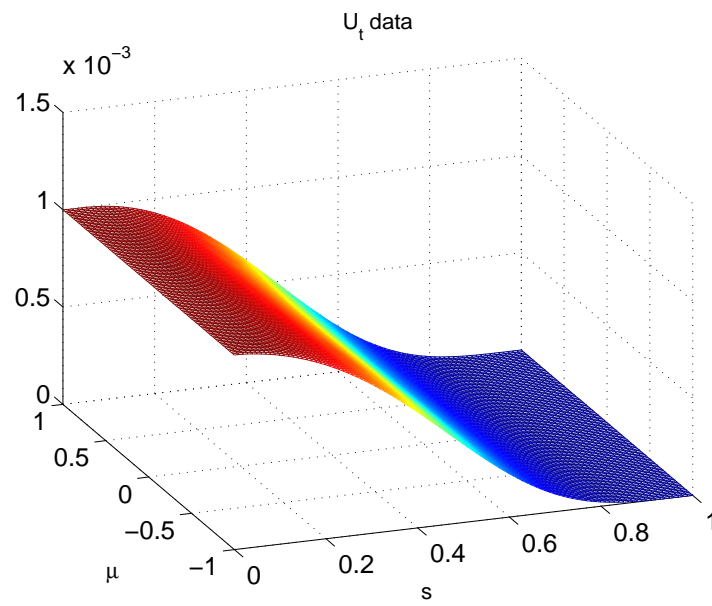
Figure 9.51 Plot of U_t for charged MP black hole using an 801×801 grid with $\Omega_\phi = \Omega_\psi = \Phi_h = 0.001$.
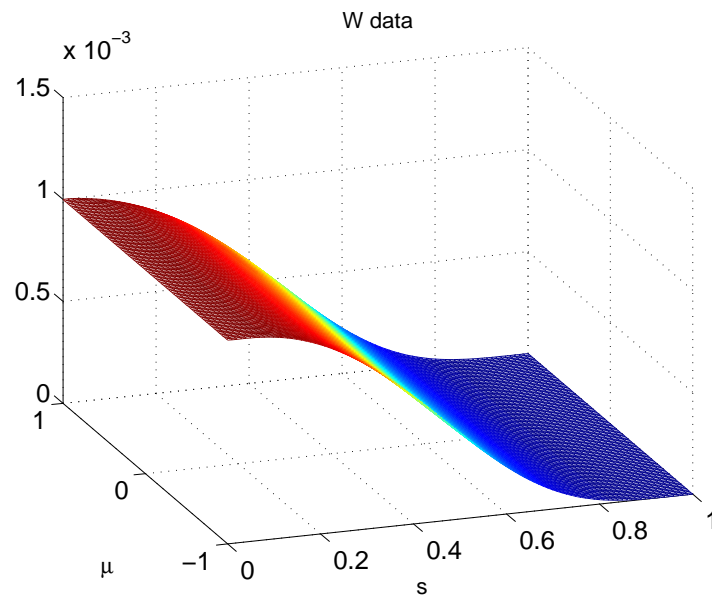
Figure 9.52 Plot of W for charged MP black hole using an 801×801 grid with $\Omega_\phi = \Omega_\psi = \Phi_h = 0.001$.
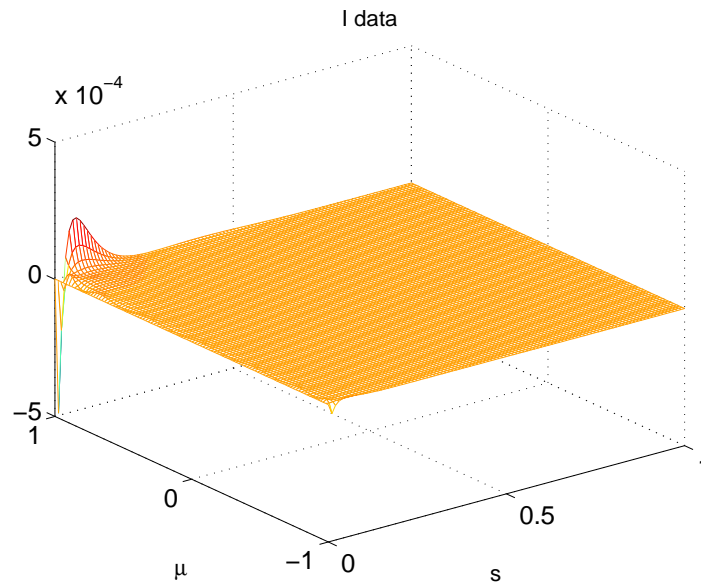
Figure 9.53 Plot of I for charged MP black hole using an 801×801 grid with $\Omega_\phi = \Omega_\psi = \Phi_h = 0.001$. This bulk of this plot is likely error.
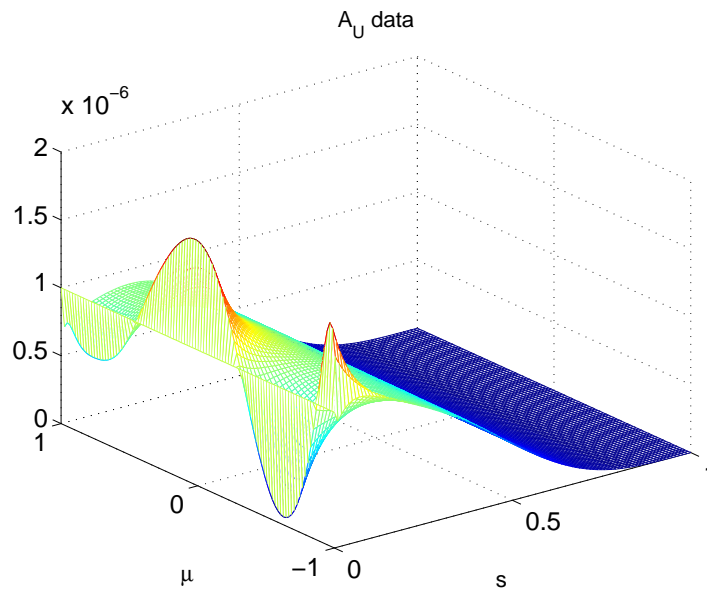
Figure 9.54 Plot of A_U for charged MP black hole using an 801×801 grid with $\Omega_\phi = \Omega_\psi = \Phi_h = 0.001$. Note the large oscillations. These are assumed to be erroneous.
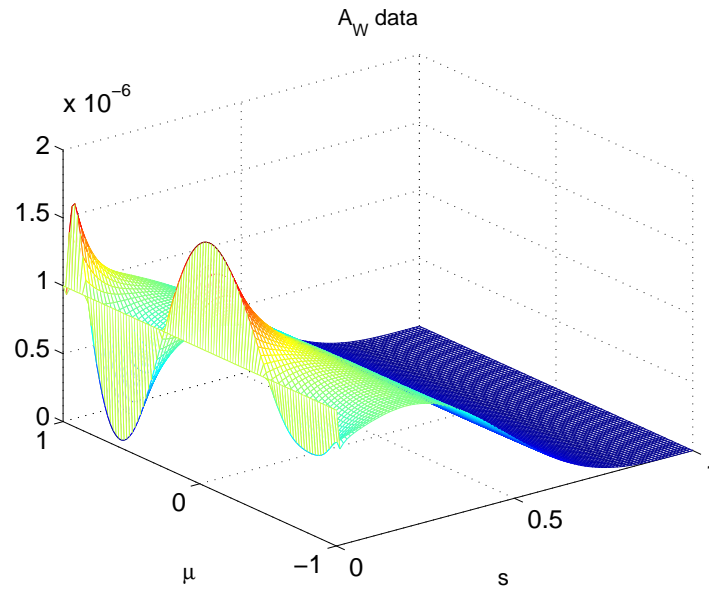
Figure 9.55 Plot of A_W for charged MP black hole using an 801×801 grid with $\Omega_\phi = \Omega_\psi = \Phi_h = 0.001$. Note the large oscillations. These are assumed to be erroneous.
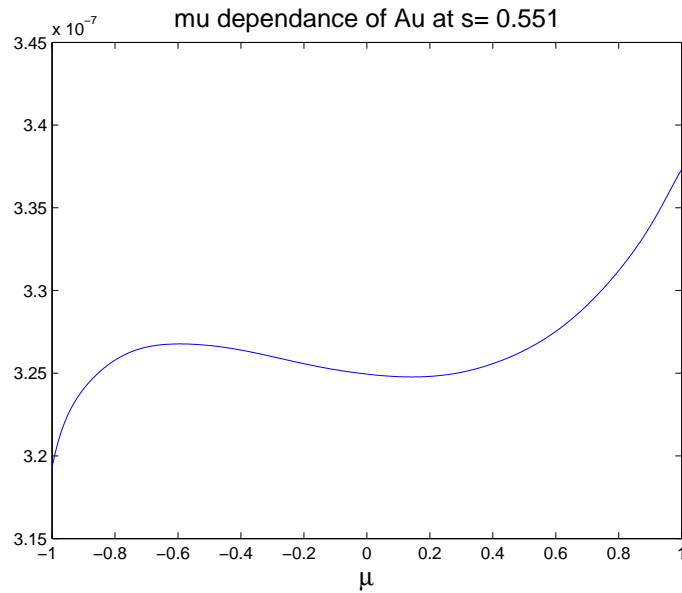
Figure 9.56 We plot the μ dependence of A_U for charged MP black hole using an 801×801 grid with $\Omega_\phi = \Omega_\psi = \Phi_h = 0.001$. Note the symmetry with Fig. 9.57.
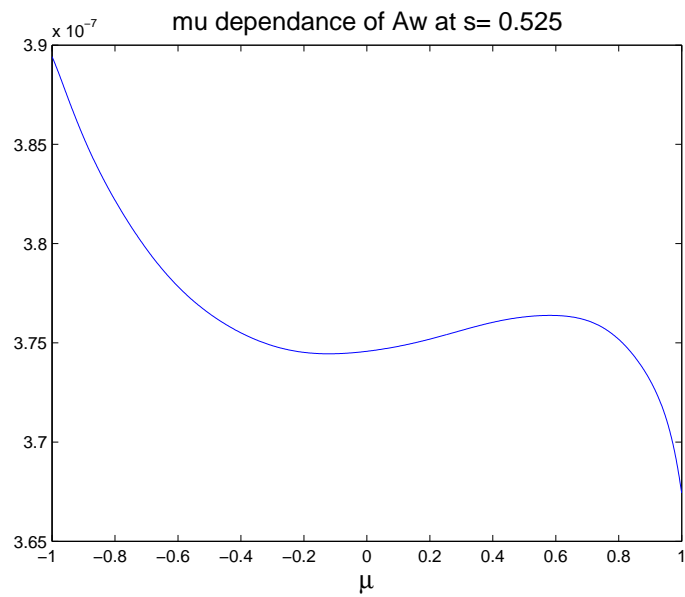
Figure 9.57 We plot the μ dependence of A_W for charged MP black hole using an 801×801 grid with $\Omega_\phi = \Omega_\psi = \Phi_h = 0.001$. Note the symmetry with Fig. 9.56.

Chapter 10

Conclusion

While an analytic charged MP solution remains elusive we have made significant progress toward that result. Our approach to the Einstein-Maxwell equations have led to numerical solutions corresponding to charged MP black holes. At present the instability of the function I prevents serious analysis of the most general case, however even these cases can be plumbed for information.

While these numerical solutions are limited by the ranges of charge and rotation for which the code converges, they are completely general in a different sense. Previous numerical solutions [20, 21] focused on single rotations or equal rotations, but our method can take any combinations of spins smaller than a certain magnitude. It is also worth noting that these rotation values are not so small as to simply reconstruct Aliev's pertubative solution [23]. Our solutions give structure to functions quadratic in rotation, and appear more similar to the MP solution than the perturbation.

Along the way to creating these solutions we have found an analytic solution for the function F. Surprisingly, F seems to take on the same form for all 4+1 black holes whose event horizon is a topological sphere. This new result appeared naturally from our dimensional reduction of the Einstein-Maxwell equations.

Our alternative dimensional reduction as outlined in Appendix C gives us additional information about the functions which come out of the decomposition. We have shown explicitly the form of a symmetry operation derived from the symmetric nature of the Killing vector fields ϕ^a and ψ^a. In addition, each of the nine scalar functions behaves simply under this symmetry operation. That is to say, the three functions U_t, A_U, and H can be transformed into W, A_W, and H_W respectively by exchanging Ω_ϕ and Ω_ψ and letting θ become $\frac{\pi}{2} - \theta$. Thus, in a sense only three of these six functions are unique. We have also shown that F, I, and $Q^2 A_T$ are self conjugate under this transformation. This means that they must exhibit certain symmetries in their functional form. We have verified these symmetries numerically for all functions other than I.

We have also motivated, but have not proved, the existence of a vector Λ_a which is a modification of the vector potential A_a. We conjecture that this Λ_a plays a role similar to χ^a of the rigidity theorem. Recall that for an $N + 1$ spacetime such that $\lfloor \frac{N}{2} \rfloor = M$ with a timelike Killing vector field t^a and spacelike Killing vector fields $\phi_{(i)}^a$ $i \in \{1 \dots M\}$ with closed orbits, there exists a vector

$$\chi^a \equiv t^a - \sum_{i=1}^{M} \Omega_i \phi_{(i)}^a \tag{10.1}$$

where the Ω_is are constants corresponding to angular velocities of the horizon. This vector is null on the horizon and orthogonal to each of the Killing vector fields of the spacetime on the horizon. We conjecture that

$$\Lambda_a \equiv A_a - \Phi_h \sum_{i=1}^{M} \Omega_i \phi_{(i)}^a \tag{10.2}$$

where Φ_h is the electric potential at the horizon has the properties that at the horizon it is orthogonal to each of the $\phi_{(i)}^a$s and furthermore satisfies

$$A_a \chi^a \big|_{r_h} = \Lambda_a t^a \big|_{r_h} = \Phi_h. \tag{10.3}$$

In concert with this rigidity-theorem-like vector Λ_a we have postulated for the connections between rotation and electric charge we also posit the existence of rigidity-theorem-like

vectors related to the connection between different rotational planes. We define the vectors

$$\zeta_{(i)}^a \equiv \phi_{(i)}^a - \Omega_i \sum_{\substack{j=1 \\ i \neq j}}^{M} \Omega_j V_{(j)}^a \tag{10.4}$$

where the $V_{(j)}^a$s are defined by equation C.47. We claim that for $i \neq j$ these vectors satisfy

$$\zeta_{(i)}^a \phi_{a(j)}\big|_{r_h} = 0. \tag{10.5}$$

As we explicitly show in section C.3, using these two rigidity-like theorems along with the original rigidity vector χ^a allows one to dimensionally reduce the above specified $N + 1$ dimensional spacetime in a Kaluza-Klein like manner while ensuring that each scalar function generated by the decomposition satisfies Dirichlet boundary conditions in electrovac spacetimes.

While we have not yet found an analytic form for the charged MP solution we have made definite progress. We plan to continue to refine our code to reduce the error in our algorithm and begin extracting what we can about the analytic form of our solutions. We hope then to use our numerical solutions and analytical knowledge of the functional forms generated by our method to obtain an analytic solution of the Einstein-Maxwell equations corresponding to a charged MP black hole.

Appendix A

3+1 Formalism and E&M Boundary Conditions

In this appendix we apply the formalism we employed in chapter 2 to a 3+1 spacetime. We then use this formalism to examine the KN solution. We pay particular attention to the functional forms and boundary conditions of functions similar to those chosen in chapter 5.

Similar to chapter 2 we assume a differentiable manifold $\mathcal{M}$ with metric g_{ab} which is both stationary and axisymmetric. These properties correspond to Killing vector fields ϕ^a and t^a with norms

$$\phi^a \phi_a = s^2 \quad t^a t_a = -c^2. \tag{A.1}$$

We choose coordinates adapted to the Killing vectors and define the scaled vectors

$$Y^a \equiv \frac{1}{s^2}(\partial_\phi)^a \quad M^a \equiv \frac{-1}{Q^2}\left((\partial_t)^a - \phi_t Y^a\right), \tag{A.2}$$

where $Q^2 = c^2 + \dfrac{\phi_t^2}{s^2}$. Similar to chapter 2, we can express the metric as

$$g_{ab} = \sigma_{ab} + s^2 Y_a Y_b - Q^2 M_a M_b, \tag{A.3}$$

where σ_{ab} is the metric on the two dimensional submanifold which is orthogonal to both Y^a and M^a. Note also that by construction Y^a and M^a are orthogonal to each other. We also

define the function

$$\omega = \frac{\phi_t}{s^2},$$ (A.4)

which at the event horizon can be shown to be the constant Ω_h, thought of as the angular velocity of the event horizon.

This last statement is a result of the rigidity theorem [7]. This theorem proves that there is a vector χ^a defined as

$$\chi^a = t^a - \Omega_h \phi^a,$$ (A.5)

which on the event horizon satisfies

$$\chi^a \chi_a = 0 \quad \chi^a t_a = 0 \quad \chi^a \phi_a = 0.$$ (A.6)

(Compare with (5.1) and (5.2) in the 4+1 case.) It is straightforward to show that the properties of χ^a on the horizon result in

$$Q^2\big|_{r_h} = 0$$ (A.7)

$$w\big|_{r_h} = \Omega_h.$$ (A.8)

We also have a vector potential A_a. As in chapter 4 the portion of A_a which is on the two manifold vanishes. The remaining scalar functions are $A_M \equiv A_a M^a$ and $A_Y \equiv A_a Y^a$. From the uniqueness theorems in 3+1 dimensions we know the KN solution is the unique stationary axisymmetric solution of the Einstein-Maxwell equations. We can then use the KN metric and vector potential to calculate the boundary values of the functions generated by the above formalism.

Beginning with Wald [9] we can write the KN solution in Boyer-Lindquist coordinates as

$$ds^2 = -\frac{\Delta \Sigma}{\rho} dt^2 + \Sigma \left(\frac{dr^2}{\Delta} + d\theta^2 \right) + \frac{\rho \sin^2 \theta}{\Sigma} \left(d\phi^2 - \frac{a(2mr - q^2)}{\rho} dt \right)^2$$ (A.9)

$$A_a = -\frac{qr}{\Sigma} \left[(dt)_a - a \sin^2 \theta (d\phi)_a \right],$$ (A.10)

where m, a, and q are mass, rotation, and charge parameters respectively. We also define

$$\Sigma \equiv r^2 + \cos^2\theta \quad \Delta \equiv r^2 - 2mr + a^2 + q^2 \quad \rho \equiv \left(r^2 + a^2\right)^2 - \Delta a^2 \sin^2\theta, \tag{A.11}$$

with the outer event horizon given by the largest root of $\Delta = 0$ namely,

$$r_h = m + \sqrt{m^2 - a^2 - q^2}. \tag{A.12}$$

We want to use an isotropic radial coordinate $\bar{r}$ since we have assumed that σ_{ab} is conformally flat. This coordinate transformation must satisfy

$$\frac{dr}{\sqrt{\Delta}} = \frac{d\bar{r}}{\bar{r}}. \tag{A.13}$$

We pick the solution

$$r = \bar{r} + m + \frac{\bar{r}_h^2}{\bar{r}}, \tag{A.14}$$

where

$$\bar{r}_h^2 = \frac{\sqrt{m^2 - a^2 - q^2}}{2}, \tag{A.15}$$

because this gives r and $\bar{r}$ the same asymptotic behavior. We can then rewrite (A.9) and (A.10) as

$$ds^2 = -\frac{\overline{\Delta\Sigma}}{\overline{\rho}}dt^2 + \frac{\overline{\Sigma}}{\bar{r}^2}\left(d\bar{r}^2 + \bar{r}^2 d\theta^2\right) + \frac{\overline{\rho}\sin^2\theta}{\overline{\Sigma}}\left(d\phi^2 - \frac{a(2mr - q^2)}{\overline{\rho}}dt\right)^2 \tag{A.16}$$

$$A_a = -\frac{qr}{\overline{\Sigma}}\left[(dt)_a - a\sin^2\theta(d\phi)_a\right], \tag{A.17}$$

where r and barred quantities are taken as functions of $\bar{r}$. We can then compare with the line element from (A.3)

$$ds^2 = -Q^2 dt^2 + e^{2\alpha}\left(d\bar{r}^2 + \bar{r}^2 d\theta^2\right) + s^2\left(d\phi + \omega dt\right)^2. \tag{A.18}$$

We immediately find

$$Q = \sqrt{\frac{\overline{\Delta\Sigma}}{\overline{\rho}}} \tag{A.19}$$

$$sQ = \overline{r}\sin\theta\left(1 - \frac{\overline{r}_h^2}{\overline{r}^2}\right) \equiv \overline{r}\sin\theta F \tag{A.20}$$

$$\omega = -\frac{a}{\overline{\rho}}\left(2mr - q^2\right) \tag{A.21}$$

$$\alpha = \frac{1}{2}\ln\left(\frac{\overline{\Sigma}}{\overline{r}^2}\right) \tag{A.22}$$

$$Q^2 A_M = -\frac{qr(r^2 + a^2)}{\overline{\rho}} \tag{A.23}$$

$$A_Y = \frac{aqr}{\overline{\rho}}. \tag{A.24}$$

As expected from asymptotic flatness, at spatial infinity

$$Q \to 1 \qquad F \to 1 \qquad \omega \to 0$$
$$\alpha \to 0 \quad Q^2 A_M \to 0 \quad A_Y \to 0. \tag{A.25}$$

At the event horizon the results are more interesting. As expected from the rigidity theorem, at the horizon

$$Q = 0 \quad F = 0. \tag{A.26}$$

We also find the explicit form of Ω_h:

$$\Omega_h \equiv \omega\big|_{\overline{r}_h} = -\frac{a}{2m(m + 2\overline{r}_h) - q^2}. \tag{A.27}$$

The behavior of the E&M fields are particularly interesting. At the event horizon

$$Q^2 A_M\big|_{\overline{r}_h} = -\frac{q(m + 2\overline{r}_h)}{2m(m + 2\overline{r}_h) - q^2} \equiv \Phi_h \tag{A.28}$$

$$A_Y\big|_{\overline{r}_h} = \frac{aq(m + 2\overline{r}_h)}{[2m(m + 2\overline{r}_h) - q^2]^2} = \Phi_h\Omega_h, \tag{A.29}$$

where Φ_h is a constant electric potential at the horizon. This first result is equivalent at the horizon to the identity denoted by Carter in [26]

$$\chi^a A_a = \Phi_h. \tag{A.30}$$

The second has (as far as we are aware) not been previously recognized. Note the following equivalence at the horizon

$$A_Y = \Phi_h \Omega_h$$

$$A_\phi = s^2 \Phi_h \Omega_h$$

$$A_\phi - \Phi_h \Omega_h \phi^a \phi_a = 0$$

$$(A_a - \Phi_h \Omega_h \phi_a) \, \phi^a = 0. \tag{A.31}$$

Now, consider this orthogonality at the horizon as well as the following

$$Q^2 A_M = A_t - w A_\phi$$

$$= At - \frac{A_\phi}{s^2} \phi_t$$

$$= \left(A_a - \frac{A_\phi}{s^2} \phi_a \right) t^a, \tag{A.32}$$

If we then take (A.28) and (A.29) as given at the horizon (A.32) becomes

$$(A_a - \Phi_h \Omega_h \phi_a) \, t^a = \Phi_h. \tag{A.33}$$

It is suggestive that the vector

$$\Lambda_a \equiv A_a - \Phi_h \Omega_h \phi_a, \tag{A.34}$$

(which is somewhat reminiscent of χ^a) should have the particular behavior of (A.33) and (A.31) at the horizon. We conjecture that there is some electromagnetism rigidity-like theorem for Einstein-Maxwell spacetimes that motivates these results from a general framework. The full conjecture is stated in Chapter 10.

Appendix B

4+1 Formalism Applied to Known Solutions

In this appendix we consider the form and asymptotic behavior of the scalar functions, as chosen in chapter 5, of the charged Tangherlini and MP solutions. We also analyze the perturbative charged rotating solution found by Aliev. In fact the behavior of the functions in these known solutions, as well as the KN solution in Appendix A, are the motivations for the function choices in chapter 5.

B.1   Charged Tangherlini

We begin with the charged Tangherlini line element and vector potential in Boyer-Lindquist type coordinates [12]

$$ds^2 = -\left(1 - \frac{m}{r^2} + \frac{q^2}{r^4}\right)dt^2 + \left(1 - \frac{m}{r^2} + \frac{q^2}{r^4}\right)^{-1}dr^2$$
$$+ r^2\left(d\theta^2 + \sin^2\theta d\phi^2 + \cos^2\theta d\psi^2\right) \tag{B.1}$$

$$A_a = -\frac{q\sqrt{3}}{2r^2}(dt)_a, \tag{B.2}$$

where m and q are mass and charge parameters respectively. The vanishing of the g_{tt} component defines the location of the outer event horizon as

$$r_h^2 = \frac{m + \sqrt{m^2 - 4q^2}}{2}. \tag{B.3}$$

We need to express the metric in an isotropic radial coordinate $\bar{r}$ since σ_{ab} is explicitly conformally flat. This transformation must satisfy

$$\frac{r\,dr}{\sqrt{r^4 - mr^2 + q^2}} = \frac{d\bar{r}}{\bar{r}}. \tag{B.4}$$

We pick the solution

$$r^2 = \bar{r}^2 + \frac{m}{2} + \frac{\bar{r}_h^4}{\bar{r}^2}, \tag{B.5}$$

where

$$\bar{r}_h^2 = \frac{\sqrt{m^2 - 4q^2}}{4}, \tag{B.6}$$

to give r and $\bar{r}$ the same asymptotic behavior. This allows us to rewrite (B.1) as

$$ds^2 = -\frac{\bar{r}^4}{r^4}\left(1 - \frac{\bar{r}_h^4}{\bar{r}^4}\right)^2 dt^2 + \frac{r^2}{\bar{r}^2}\left(d\bar{r}^2 + \bar{r}^2 d\theta^2\right) + r^2\left(\sin^2\theta\, d\phi^2 + \cos^2\theta\, d\psi^2\right), \tag{B.7}$$

where r is taken to be the function of $\bar{r}$ defined in (B.5).

We can now compare with the simplified form of (2.21):

$$ds^2 = -Q^2 dt^2 + e^{2\alpha}\left(d\bar{r}^2 + \bar{r}^2 d\theta^2\right) + p^2\left(d\phi + U_t dt\right)^2 + a^2\left(d\psi + V_t dt\right)^2$$

$$+ a^2\left(d\psi + V_\phi d\phi\right)^2 - a^2 d\psi^2 + 2a^2 V_t V_\phi dt d\phi. \tag{B.8}$$

Then, using the functions defined in chapter 5 we find

$$apQ = \bar{r}^2 \sin\theta \cos\theta \left(1 - \frac{\bar{r}_h^4}{\bar{r}^4}\right) = \bar{r}^2 \sin\theta \cos\theta F \tag{B.9}$$

$$G = H = \frac{F}{\sqrt{1 + \frac{m}{2\bar{r}^2} + \frac{\bar{r}_h^4}{\bar{r}^4}}} \tag{B.10}$$

$$\alpha = \frac{1}{2}\ln\left(1 + \frac{m}{2\bar{r}^2} + \frac{\bar{r}_h^4}{\bar{r}^4}\right) \tag{B.11}$$

$$Q^2 A_T = -\frac{q\sqrt{3}}{2r^2} \tag{B.12}$$

$$U_t = W = I = A_V = A_U = 0. \tag{B.13}$$

Notice that as claimed in Chapter 6 $H = G$ for black holes without rotation. Also, we have explicitly verified the form of F which was derived in section 7.2.

In agreement with asymptotic flatness and our E&M convention, at spatial infinity

$$F \to 1 \quad G = H \to 1 \quad \alpha \to 0 \quad Q^2 A_T \to 0. \tag{B.14}$$

At the event horizon F, G, and H vanish, but

$$Q^2 A_T\big|_{\bar{r}_h} = -\frac{q\sqrt{3}}{4\bar{r}_h^2 + m} \equiv \Phi_h, \tag{B.15}$$

is a constant we define as the electric potential at the horizon Φ_h.

B.2 Myers-Perry

We begin with the MP line element in bi-azimuthal Boyer-Lindquist like coordinates [14]

$$\begin{aligned}
ds^2 =& -\left(1 - \frac{m}{\Sigma}\right)dt^2 + \Sigma\left(\frac{r^2}{\Pi}dr^2 + d\theta^2\right) - \frac{2ma\sin^2\theta}{\Sigma}dtd\phi - \frac{2mb\cos^2\theta}{\Sigma}dtd\psi \\
&+ \sin^2\theta\left(r^2 + a^2 + \frac{ma^2\sin^2\theta}{\Sigma}\right)d\phi^2 + \cos^2\theta\left(r^2 + b^2 + \frac{mb^2\cos^2\theta}{\Sigma}\right)d\psi^2 \\
&+ \frac{2mab\sin^2\theta\cos^2\theta}{\Sigma}d\phi d\psi,
\end{aligned} \tag{B.16}$$

where m is a mass parameter and a and b are independent rotation parameters. Also,

$$\Sigma = r^2 + a^2 \cos^2 \theta + b^2 \sin^2 \theta \tag{B.17}$$

$$\Pi = \left(r^2 + a^2\right)\left(r^2 + b^2\right) - mr^2, \tag{B.18}$$

and the location of the outer event horizon is determined by the largest positive root of $\Pi = 0$ or

$$r_h^2 = \frac{m - a^2 - b^2 + \sqrt{(m - a^2 - b^2)^2 - 4a^2 b^2}}{2}. \tag{B.19}$$

To transform into an isotropic radial coordinate $\bar{r}$ we must satisfy

$$\frac{r\,dr}{\sqrt{\Pi}} = \frac{d\bar{r}}{\bar{r}}. \tag{B.20}$$

We pick the solution

$$r^2 = \bar{r}^2 + \frac{m - a^2 - b^2}{2} + \frac{\bar{r}_h^4}{\bar{r}^2}, \tag{B.21}$$

where

$$\bar{r}_h^2 = \frac{\sqrt{(m - a^2 - b^2)^2 - 4a^2 b^2}}{4}. \tag{B.22}$$

For convenience we define the following quantities

$$A \equiv \bar{r}^2 + \frac{m + a^2 - b^2}{2} + \frac{\bar{r}_h^4}{\bar{r}^2} \tag{B.23}$$

$$B \equiv \bar{r}^2 + \frac{m - a^2 + b^2}{2} + \frac{\bar{r}_h^4}{\bar{r}^2}. \tag{B.24}$$

We then rewrite (B.16) as

$$\begin{aligned}
ds^2 = &-\left(1 - \frac{m}{\overline{\Sigma}}\right) dt^2 + \frac{\overline{\Sigma}}{\bar{r}^2}\left(d\bar{r}^2 + \bar{r}^2 d\theta^2\right) - \frac{2ma \sin^2 \theta}{\overline{\Sigma}} dt d\phi - \frac{2mb \cos^2 \theta}{\overline{\Sigma}} dt d\psi \\
&+ \sin^2 \theta \left(A + \frac{ma^2 \sin^2 \theta}{\overline{\Sigma}}\right) d\phi^2 + \cos^2 \theta \left(B + \frac{mb^2 \cos^2 \theta}{\overline{\Sigma}}\right) d\psi^2 \\
&+ \frac{2mab \sin^2 \theta \cos^2 \theta}{\overline{\Sigma}} d\phi d\psi,
\end{aligned} \tag{B.25}$$

where

$$\overline{\Sigma} = \bar{r}^2 + \frac{m + (a^2 - b^2) \cos 2\theta}{2} + \frac{\bar{r}_h^4}{\bar{r}^2}. \tag{B.26}$$

We now compare (B.8) and (B.25). So, using the functions defined in chapter 5 we obtain

$$apQ = \bar{r}^2 \sin\theta \cos\theta \left(1 - \frac{\bar{r}_h^4}{\bar{r}^4}\right) = \bar{r}^2 \sin\theta \cos\theta F \tag{B.27}$$

$$G = \bar{r}F\sqrt{\frac{\overline{\Sigma}}{\overline{\Sigma}B + mb^2\cos^2\theta}} \tag{B.28}$$

$$H = \bar{r}F\sqrt{\frac{\overline{\Sigma}B + +mb^2\cos^2\theta}{\overline{\Sigma}AB + m\left(Ab^2\cos^2\theta + Ba^2\sin^2\theta\right)}} \tag{B.29}$$

$$\alpha = \frac{1}{2}\ln\left(\frac{\overline{\Sigma}}{\bar{r}^2}\right) \tag{B.30}$$

$$U_t = -\frac{maB}{\overline{\Sigma}AB + m\left(Ab^2\cos^2\theta + Ba^2\sin^2\theta\right)} \tag{B.31}$$

$$W = -\frac{mbA}{\overline{\Sigma}AB + m\left(Ab^2\cos^2\theta + Ba^2\sin^2\theta\right)} \tag{B.32}$$

$$I = \frac{mab}{\overline{\Sigma}AB + m\left(Ab^2\cos^2\theta + Ba^2\sin^2\theta\right)}. \tag{B.33}$$

Notice that as with the charged Tangherlini solution we have verified the form of F.

In agreement with asymptotic flatness, at spatial infinity we have

$$F \to 1 \quad G \to 1 \quad H \to 1 \quad \alpha \to 0$$

$$U_t \to 0 \quad W \to 0 \quad I \to 0. \tag{B.34}$$

At the horizon

$$F \to 0 \quad G \to 0 \quad H \to 0. \tag{B.35}$$

In agreement with the rigidity theorem [19], at the horizon we make the definitions

$$U_t\big|_{\bar{r}_h} \equiv \Omega_\phi = -\frac{a(a^2 - b^2 - m - 4\bar{r}_h^2)}{m(a^2 + b^2 - m - 4\bar{r}_h^2)} \tag{B.36}$$

$$W\big|_{\bar{r}_h} \equiv \Omega_\psi = -\frac{b(b^2 - a^2 - m - 4\bar{r}_h^2)}{m(a^2 + b^2 - m - 4\bar{r}_h^2)}. \tag{B.37}$$

A more surprising result is

$$I\big|_{\bar{r}_h} = -\frac{2ab}{m(a^2 + b^2 - m - 4\bar{r}_h^2)} = \Omega_\phi\Omega_\psi, \tag{B.38}$$

which we discuss further in Chapters 5 and 10 as well as in Appendix C.

B.3 Aliev Perturbation

We begin with the line element and vector potential found by Aliev [23] in bi-azimuthal Boyer-Lindquist type coordinates with mass and charge parameters m and q respectively

$$ds^2 = - \left(1 - \frac{m}{r^2} + \frac{q^2}{r^4}\right) dt^2 + \left(1 - \frac{m}{r^2} + \frac{q^2}{r^4}\right)^{-1} dr^2$$

$$+ r^2 \left(d\theta^2 + \sin^2\theta d\phi^2 + \cos^2\theta d\psi^2\right)$$

$$- \frac{2}{r^2}\left(m - \frac{q^2}{r^2}\right)\left(a\sin^2\theta dt d\phi + b\cos^2\theta dt d\psi\right) \tag{B.39}$$

$$A_a = -\frac{q\sqrt{3}}{2r^2}\left[(dt)_a - a\sin^2\theta(d\phi)_a - b\cos^2\theta(d\psi)_a\right], \tag{B.40}$$

with the perturbative condition that terms quadratic or higher in the rotation parameters a and b vanish.

Notice the similarities between (B.39) and the charged Tangherlini metric (B.1). In fact, the transformation to an isotropic radial coordinate $\bar{r}$, the radial location of the event horizon, and the functional forms of α, F, G, and H are all identical to the results from section B.1. So, using (B.5) and (B.6) we can rewrite the metric as

$$ds^2 = -\left(1 - \frac{m}{r^2} + \frac{q^2}{r^4}\right) dt^2 + \frac{r^2}{\bar{r}^2}\left(d\bar{r}^2 + \bar{r}^2 d\theta^2\right) + r^2\sin^2\theta\left[d\phi - \frac{a}{r^4}\left(m - \frac{q^2}{r^2}\right) dt\right]^2$$

$$+ r^2\cos^2\theta\left[d\psi - \frac{b}{r^4}\left(m - \frac{q^2}{r^2}\right) dt\right]^2, \tag{B.41}$$

where r is a function of $\bar{r}$. Another immediate result is that the function I must be identically zero. This is consistent with the MP solution. Recall from (B.33) that I of order ab and hence must vanish in our perturbative limit.

The remaining functions can be identified through comparison with (B.8) as

$$U_t = -\frac{a}{r^4}\left(m - \frac{q^2}{r^2}\right) \tag{B.42}$$

$$W = V_t = -\frac{b}{r^4}\left(m - \frac{q^2}{r^2}\right) \tag{B.43}$$

$$Q^2 A_T = -\frac{q\sqrt{3}}{2r^2} \tag{B.44}$$

$$A_U = \frac{aq\sqrt{3}}{2r^4} \tag{B.45}$$

$$A_W = \frac{bq\sqrt{3}}{2r^4}. \tag{B.46}$$

In agreement with asymptotic flatness and our convention for E&M each of these five functions vanish at spatial infinity. In accordance with the higher dimensional rigidity theorem [19] we make the identifications

$$U_t\big|_{\bar{r}_h} \equiv \Omega_\phi = -\frac{a}{2\bar{r}_h^2 + \frac{m}{2}} \tag{B.47}$$

$$V_t\big|_{\bar{r}_h} \equiv \Omega_\psi = -\frac{b}{2\bar{r}_h^2 + \frac{m}{2}}. \tag{B.48}$$

Then, making the extension from Carter [26]

$$Q^2 A_T\big|_{\bar{r}_h} \equiv \Phi_h = -\frac{q\sqrt{3}}{2\left(2\bar{r}_h^2 + \frac{m}{2}\right)}. \tag{B.49}$$

Similar to the result in (A.29) we also find

$$A_U\big|_{\bar{r}_h} = \frac{bq\sqrt{3}}{2\left(2\bar{r}_h^2 + \frac{m}{2}\right)^2} = \Phi_h\Omega_\phi \tag{B.50}$$

$$A_W\big|_{\bar{r}_h} = \frac{aq\sqrt{3}}{2\left(2\bar{r}_h^2 + \frac{m}{2}\right)^2} = \Phi_h\Omega_\psi. \tag{B.51}$$

This serves as partial validation of our choice of functions and boundary conditions in chapter 5, wherein we also discuss the behavior of a special vector (5.19) which is equivalent to these boundary conditions, similar to the 3+1 case as explained at the end of Appendix A.

Appendix C

Symmetric Formalism

In this appendix we show how to decompose the Einstein-Maxwell equations using the assumed symmetries of the spacetime while retaining the inherent symmetry between the two spacelike Killing vector fields. While we do not use this formalism to generate a new set of partial differential equations, we do find aspects of our problem which become more clear in a symmetric formalism. We also present a method for carrying out such a decomposition in an $N + 1$ spacetime with $M = \lfloor \frac{N}{2} \rfloor$ commuting spacelike Killing vector fields.

C.1   Basic Structures

As in Chapter 2 we assume a five dimensional differentiable manifold $\mathcal{M}$ with metric g_{ab}. We also assume the existence of three mutually commuting Killing vector fields. One of these is assumed to be timelike, and is denoted t^a. The remaining two are both spacelike Killing vector fields with closed orbits. We denote them as ϕ^a and ψ^a. We label their norms as

$$t^a t_a = -c^2, \quad \phi^a \phi_a = b^2, \quad \psi^a \psi_a = a^2, \tag{C.1}$$

and choose coordinates on the manifold adapted to these vectors fields:

$$t^a = (\partial_t)^a, \quad \phi^a = (\partial_\phi)^a, \quad \psi^a = (\partial_\psi)^a. \tag{C.2}$$

We also define the following quantities for convenience:

$$t^a \psi_a = \psi_t, \quad t^a \phi_a = \phi_t, \quad \psi^a \phi_a = \psi_\phi. \tag{C.3}$$

We now wish to project out the subspace spanned by ψ^a and ϕ^a without removing the symmetry between the two vector fields. So, in contrast to (2.9) we define

$$^{(3)}g_{ab} = g_{ab} - K_{ab}, \tag{C.4}$$

where $^{(3)}g_{ab}$ is the three dimensional metric on the submanifold orthogonal to both ψ^a and ϕ^a. We first note that K_{ab} must be symmetric. Next, by enforcing orthogonality we find

$$^{(3)}g_{ab}\psi^a = 0 = \psi_b - K_{\psi b} \Rightarrow K_{\psi b} = \psi_b \tag{C.5}$$

$$^{(3)}g_{ab}\phi^a = 0 = \phi_b - K_{\phi b} \Rightarrow K_{\phi b} = \phi_b. \tag{C.6}$$

It follows that

$$K_{\psi\psi} = a^2, \quad K_{\phi\phi} = b^2, \quad K_{\psi\phi} = \psi_\phi. \tag{C.7}$$

At this point we do not actually know if such a K_{ab} exists. However, we will show that it not only exists, but has a very convenient decomposition.

Knowing that K_{ab} must be symmetric and supposing it's tensorial form comes from products of ψ^a and ϕ^a we takes ansatz

$$K_{ab} = c_1 \left(\psi_a \phi_b + \psi_b \phi_a \right) + c_2 \psi_a \psi_b + c_3 \phi_a \phi_b, \tag{C.8}$$

where the c_is are as yet undetermined coefficients. By enforcing the orthogonality conditions (C.7) we find

$$K_{ab} = \frac{b^2}{D} \psi_a \psi_b + \frac{a^2}{D} \phi_a \phi_b - \frac{\psi_\phi}{D} \left(\psi_a \phi_b + \psi_b \phi_a \right), \tag{C.9}$$

where

$$D \equiv a^2 b^2 - \psi_\phi^2. \tag{C.10}$$

Now that we know that $^{(3)}g_{ab}$ is a well defined quantity, we can project the timelike Killing vector into the three dimensional manifold. In exact agreement with Chapter 2 we find

$$^{(3)}t^a = t^a - W\psi^a - U_t\phi^a, \tag{C.11}$$

which has the same norm $-Q^2$ as defined by (2.12). Then we define the two dimensional metric σ_{ab} on the submanifold $\mathcal{N}$ orthogonal to all the Killing vectors as

$$\sigma_{ab} = g_{ab} - K_{ab} + Q^2 T_a T_b. \tag{C.12}$$

C.2   Properties of Symmetric Projection

We now compare some of the naturally occurring functions in the symmetric formalism to the functions chosen in Chapter 5. We will see that many of the functions with Dirichlet boundary conditions on the horizon are directly related to K_{ab}. To see this we write our definition of K_{ab} in a more suggestive way

$$K_{ab} = \psi_a \widetilde{V}_b + \phi_a \widetilde{U}_b, \tag{C.13}$$

where we have made the definitions

$$\widetilde{V}_b \equiv \frac{b^2}{D}\psi_b - \frac{\psi_\phi}{D}\phi_b \tag{C.14}$$

$$\widetilde{U}_b \equiv \frac{a^2}{D}\phi_b - \frac{\psi_\phi}{D}\psi_b. \tag{C.15}$$

Notice that $\widetilde{V}_b$ and $\widetilde{U}_b$ satisfy

$$\begin{aligned}\psi^a \widetilde{V}_a = 1 \quad & \psi^a \widetilde{U}_a = 0 \\ \phi^a \widetilde{V}_a = 0 \quad & \phi^a \widetilde{U}_a = 1,\end{aligned} \tag{C.16}$$

and

$$\widetilde{V}^a \widetilde{V}_a = \frac{b^2}{D} \quad \widetilde{U}^a \widetilde{U}_a = \frac{a^2}{D} \quad \widetilde{V}^a \widetilde{U}_a = -\frac{\psi_\phi}{D}. \tag{C.17}$$

Comparing with the vectors and functions defined in Chapters 2 and 5 we find that $\widetilde{U}_a = U_a$. We then immediately associate

$$p^2 = \frac{D}{a^2}, \quad U_t = t^a \widetilde{U}_a, \quad A_U = A^a \widetilde{U}_a. \tag{C.18}$$

These associations alone are unsurprising. The more interesting results are

$$W = t^a \widetilde{V}_a, \quad A_W = A^a \widetilde{V}_a, \quad I = \widetilde{V}^a \widetilde{U}_a. \tag{C.19}$$

Note that many of the functions with Dirichlet boundary conditions on the horizon appear as contractions with $\widetilde{V}_a$ and $\widetilde{U}_a$. We also find

$$DQ^2 = r^4 \sin^2 \theta \cos^2 \theta F^2. \tag{C.20}$$

This relation shows a drawback of this formalism. We showed in Chapter 7 that F can be solved for analytically by combining the equations for three naturally occurring functions. In the symmetric formalism however, equations for D are quite unwieldy making the equation for F less plain.

An important aspect of the relations above is that $\widetilde{V}_a$ and $\widetilde{U}_a$ are conjugate to each other under the transformation

$$\psi^a \to \phi^a \quad \phi^a \to \psi^a. \tag{C.21}$$

We will refer to this symmetry transformation as τ and denote its action

$$\tau(\psi^a) = \phi^a, \tag{C.22}$$

and similar. With this in mind we notice that

$$\tau(U_t) = W, \quad \tau(W) = U_t, \quad \tau(A_U) = A_W, \quad \tau(A_W) = A_U. \tag{C.23}$$

We then say that U_t and W are a conjugate pair, and similar for A_U and A_W. It is also easy to see that $Q^2 A_T$, F, and I are invariant (or self-conjugate) under τ.

After these observations it is natural to wonder about the properties of G and H. Recall from (5.10) that G is related to aQ and H to pQ. Of a, p, and Q only a does not naturally appear in the symmetric formalism. However, p^2 has naturally occurring symmetry conjugate function we denote p_W^2. From the definition of p^2 we can easily find

$$\widetilde{V}^a \widetilde{V}_a = \frac{D}{b^2} \equiv p_W^2.$$ (C.24)

We can then define

$$p_W Q = r \cos \theta H_W,$$ (C.25)

where H_W is the conjugate function to H. It is worthwhile to note that when ψ_ϕ vanishes, that is when one of the rotations vanishes, p_W^2 reduces to a^2. This, and the lack of θ dependence, explains why $G = H$ for Tangherlini black holes.

In the definition of H_W and F we have tacitly introduced the bi-azimuthal coordinates discussed in Chapter 2. We need to find the effect of τ on these coordinates. It is sufficient to find what transformation takes $\phi \to \psi$ and vice versa while leaving the line element (2.24) invariant. It is straightforward to check that this condition is satisfied by

$$\tau(\phi) = \psi, \quad \tau(\psi) = \phi, \quad \tau(\theta) = \frac{\pi}{2} - \theta.$$ (C.26)

We note one last property of τ. As W and U_t and conjugate and $Q^2 A_T$ is self conjugate it must follow that

$$\tau(\Omega_\phi) = \Omega_\psi, \quad \tau(\Omega_\psi) = \Omega_\phi, \quad \tau(\Phi_h) = \Phi_h.$$ (C.27)

We are now in the position to make the following claim about the functional form of the nine scalar functions expressed in bi-azimuthal coordinates. We claim that the three functions F, I, and $Q^2 A_T$ must be invariant under τ. Further, the remaining six functions belong to conjugate pairs. For example, if we were to discover the functional form of U_t then by exchanging Ω_ϕ with Ω_ψ and $\sin \theta$ with $\cos \theta$ we would then have the functional form of W.

We also make a few final observations about the equations (5.13) and (5.14) in the context of the symmetric formalism. Specifically, we can rewrite (5.13) as

$$\psi^a \left[\phi_a - \Omega_\psi \Omega_\phi D\widetilde{V}_a \right] \Big|_{r_h} = 0, \tag{C.28}$$

and (5.14) as

$$\phi^a \left[\psi_a - \Omega_\psi \Omega_\phi D\widetilde{U}_a \right] \Big|_{r_h} = 0. \tag{C.29}$$

This rewriting makes these relations appear even more similar to the rigidity theorem vector χ^a. In particular we can define the vectors

$$\zeta^a_{(\psi)} \equiv \psi^a - \Omega_\psi \Omega_\phi D\widetilde{U}^a \tag{C.30}$$

$$\zeta^a_{(\phi)} \equiv \phi^a - \Omega_\psi \Omega_\phi D\widetilde{V}^a, \tag{C.31}$$

which satisfy

$$\zeta^a_{(\psi)} \phi_a \big|_{r_h} = \zeta^a_{(\phi)} \psi_a \big|_{r_h} = 0. \tag{C.32}$$

C.3   An N+1 Symmetric Formalism

In this section we construct the symmetric projector K_{ab} for spacetimes of $N+1$ dimension. In so doing we also create the quantities we need to extend the rigidity-theorem-like vectors discussed at the end of the previous section to arbitrary dimension.

We begin with a simpler case. Let $\mathcal{M}$ have dimension $N+1$ such that $\lfloor \frac{N}{2} \rfloor = 3$. Suppose further that there exist three spacelike Killing vector fields with closed orbits. We denote them

$$\phi^a_{(1)}, \quad \phi^a_{(2)}, \quad \phi^a_{(3)}, \tag{C.33}$$

where the notation (i) labels a vector rather than indicating the index of a vector.

By proceeding in an analogous manner to section C.1 we define

$$^{(3)}g_{ab} = g_{ab} - K_{ab}. \tag{C.34}$$

Enforcing orthogonality between the Killing vector fields and $^{(3)}g_{ab}$ we find K_{ab} has the form

$$K_{ab} = \frac{1}{D} \left[\phi_{a(1)} V_{b(1)} + \phi_{a(2)} V_{b(2)} + \phi_{a(3)} V_{b(3)} \right], \tag{C.35}$$

where using the shorthand $\phi_{(i,j)} \equiv \phi_{(i)}^a \phi_{a(j)}$ we have defined

$$D \equiv \phi_{(1,1)}\phi_{(2,2)}\phi_{(3,3)} - \phi_{(1,1)}\phi_{(2,3)}^2 - \phi_{(2,2)}\phi_{(3,1)}^2 - \phi_{(3,3)}\phi_{(1,2)}^2 + 2\phi_{(1,2)}\phi_{(2,3)}\phi_{(1,3)}, \tag{C.36}$$

and

$$V_{(1)}^a = \phi_{(1)}^a \left(\phi_{(2,2)}\phi_{(3,3)} - \phi_{(2,3)}^2 \right) + \phi_{(2)}^a \left(\phi_{(1,3)}\phi_{(2,3)} - \phi_{(1,2)}\phi_{(3,3)} \right)$$

$$+ \phi_{(3)}^a \left(\phi_{(1,2)}\phi_{(2,3)} - \phi_{(2,2)}\phi_{(1,3)} \right) \tag{C.37}$$

$$V_{(2)}^a = \phi_{(2)}^a \left(\phi_{(1,1)}\phi_{(3,3)} - \phi_{(1,3)}^2 \right) + \phi_{(1)}^a \left(\phi_{(1,3)}\phi_{(2,3)} - \phi_{(1,2)}\phi_{(3,3)} \right)$$

$$+ \phi_{(3)}^a \left(\phi_{(1,2)}\phi_{(1,3)} - \phi_{(1,1)}\phi_{(1,3)} \right) \tag{C.38}$$

$$V_{(3)}^a = \phi_{(3)}^a \left(\phi_{(1,1)}\phi_{(2,2)} - \phi_{(1,2)}^2 \right) + \phi_{(1)}^a \left(\phi_{(1,2)}\phi_{(2,3)} - \phi_{(1,3)}\phi_{(2,2)} \right)$$

$$+ \phi_{(2)}^a \left(\phi_{(1,2)}\phi_{(1,3)} - \phi_{(1,1)}\phi_{(2,3)} \right). \tag{C.39}$$

Notice that we can write these in a more compact fashion using antisymmetrization

$$D = 3! \phi_{(1)}^{[a} \phi_{(2)}^{b} \phi_{(3)}^{c]} \phi_{a(1)} \phi_{b(2)} \phi_{c(3)} \tag{C.40}$$

$$V_{(1)}^a = 3! \phi_{(1)}^{[a} \phi_{(2)}^{b} \phi_{(3)}^{c]} \phi_{b(2)} \phi_{c(3)} \tag{C.41}$$

$$V_{(2)}^a = 3! \phi_{(2)}^{[a} \phi_{(3)}^{b} \phi_{(1)}^{c]} \phi_{b(3)} \phi_{c(1)} \tag{C.42}$$

$$V_{(3)}^a = 3! \phi_{(3)}^{[a} \phi_{(1)}^{b} \phi_{(2)}^{c]} \phi_{b(1)} \phi_{c(2)}. \tag{C.43}$$

We are now ready for the general case. Let $\mathcal{M}$ be $N + 1$ dimensional with $\lfloor \frac{N}{2} \rfloor = M$ allowing a timelike Killing vector field t^a. Suppose further that there exist M spacelike Killing vector fields with closed orbits labeled $\phi_{(i)}^a$ with $i \in \{1 \ldots M\}$. We can then define

$$^{(N-M+1)}g_{ab} = g_{ab} - K_{ab}, \tag{C.44}$$

where

$$K_{ab} = \frac{1}{D} \sum_{i=1}^{M} \phi_{a(i)} V_{b(i)}. \tag{C.45}$$

In this last equation we use the following definitions

$$D \equiv M! \phi_{(1)}^{[a_1} \cdots \phi_{(M)}^{a_M]} \phi_{a_1(1)} \cdots \phi_{a_M(M)} \tag{C.46}$$

$$V_{(i)}^a \equiv M! \phi_{(i)}^{[a} \phi_{(i+1)}^{b_1} \cdots \phi_{(i-1)}^{b_{M-1}]} \phi_{b_1(i+1)} \cdots \phi_{b_{M-1}(i-1)}, \tag{C.47}$$

where lists from $(i+1)$ to $(i-1)$ the label (1) follows (M) in the cyclic manner. These structures define the symmetric projector for the spacetime with properties specified above. We can also use these structures to construct rigidity theorem like vectors that give rise to boundary conditions like (5.11).

While the definition for $V_{(i)}^a$ is motivated, we can make the definition more rigorous. Recall from the rigidity theorem that the vector

$$\chi^a = t^a - \sum_{i=i}^{M} \Omega_i \phi_{(i)}^a \tag{C.48}$$

satisfies the relations

$$\phi_{(i)}^a \chi_a \big|_{r_h} = 0 \tag{C.49}$$

at the horizon. We can think of these M equations as determining the M constants Ω_i. Using induction it can be shown that

$$\Omega_i = \frac{1}{D} M! \phi_{(i)}^{[a} \phi_{(i+1)}^{b_1} \cdots \phi_{(i-1)}^{b_{M-1}]} t_a \phi_{b_1(i+1)} \cdots \phi_{b_{M-1}(i-1)} \bigg|_{r_h}. \tag{C.50}$$

Using the $M = 1$ and $M = 2$ cases as a guide we assume

$$V_{(i)}^a t_a \big|_{r_h} = \Omega_i \tag{C.51}$$

from which we recover (C.47).

Notice that by using (C.47) we can determine many of the properties of K_{ab}. Notice first

$$V_{(i)}^a \phi_{a(j)} = \begin{cases} D & i = j \\ 0 & i \neq j \end{cases}. \tag{C.52}$$

It immediately follows that $K_a{}^a = M$ and

$$K_{ab}\phi^b_{(i)} = \phi_{a(i)}. \qquad (C.53)$$

In short K_{ab} behaves as the metric of the submanifold $\mathcal{P}$ of $\mathcal{M}$ spanned by the $\phi^a_{(i)}$s. Equivalently, it is a projector from $\mathcal{M}$ into $\mathcal{P}$.

We now use K_{ab} to connect the various rigidity theorem like vectors we have introduced in Chapter 10. Notice that we can easily define the scalar functions ω_i by

$$\omega_i \equiv V^a_{(i)}t_a, \qquad (C.54)$$

so that $\omega_i\big|_{r_h} = \Omega_i$. We now use (C.44) to understand χ^a. Specifically,

$$^{(N-M+1)}g^a{}_b t^b\big|_{r_h} = \chi^a. \qquad (C.55)$$

Thus, χ^a is the projection of the timelike Killing vector field into the submanifold orthogonal to all $\phi^a_{(i)}$s. In light of this definition the orthogonality between χ^a and the $\phi^a_{(i)}$s becomes obvious. From (C.55) we can also make the definition

$$^{(N-M+1)}g_{ab}t^a t^b = Q^2. \qquad (C.56)$$

It also seems likely that the combination DQ^2 satisfies

$$DQ^2 = AF(r,\theta_i)F^2 \qquad (C.57)$$

where $AF(r,\theta_i)$ are terms defined by asymptotic flatness and

$$F = 1 - \left(\frac{r_h}{r}\right)^{2M}, \qquad (C.58)$$

for the isotropic radial coordinate r.

Similar to above analysis we can define the scalar functions

$$A_{\omega_i} \equiv \frac{1}{D}V^a_{(i)}A_a, \qquad (C.59)$$

where A_a is the electromagnetic vector potential. We take these functions as satisfying

$$A_{\omega_i}\big|_{r_h} = \Phi_h \Omega_i \tag{C.60}$$

at the event horizon. Then the vector Λ_a defined in (10.2) can be expressed as

$$\Lambda_a \equiv A_a - \Phi_h \sum_{i=1}^{M} \Omega_i \phi_{(i)}^a = {}^{(N-M+1)}g_a{}^b A_b\big|_{r_h}. \tag{C.61}$$

Once again, the orthogonality of Λ_a and the $\phi_{(i)}^a$s immediately follows. We can also define the function

$$Q^2 A_T \equiv {}^{(N-M+1)}g_a{}^b A_b t^a. \tag{C.62}$$

Then at the horizon we have

$$Q^2 A_T\big|_{r_h} = \chi^a A_a\big|_{r_h} = \Lambda_a t^a\big|_{r_h} \equiv \Phi_h. \tag{C.63}$$

Last, we define the functions

$$W_{(i,j)} \equiv \frac{\phi_{(i,j)}}{D} \tag{C.64}$$

which are associated with the overlap between the ith and jth Killing vectors. These functions are assumed to have the boundary condition

$$W_{(i,j)}\big|_{r_h} = \Omega_i \Omega_j \tag{C.65}$$

at the horizon. Now, we construct the projectors $K_{(i)ab}$ by

$$K_{(i)ab} \equiv \frac{1}{D} \sum_{\substack{j=1 \\ i \neq j}}^{M} V_{(j)a} \phi_{(j)b}. \tag{C.66}$$

These projectors act as a metric on the submanifold spanned by $\{\phi_{(1)}^a \cdots \phi_{(M)}^a\} \backslash \{\phi_{(i)}^a\}$, or all the spacelike Killing vectors other than $\phi_{(i)}^a$. In addition this subspace is orthogonal to $\phi_{(i)}^a$. Using these projectors we can rewrite equation (10.4) as

$$\zeta_{(i)}^a \equiv \left(K^a{}_b - K_{(i)b}^a\right) \phi_i^b\big|_{r_h}. \tag{C.67}$$

We note the similarity of this relation to equations (C.55) and (C.61) with $\left(K^a_{\ b} - K^a_{(i)b}\right)$ playing a role similar to $^{(N-M+1)}g_a^{\ b}$.

Let us consider the implications of these special vectors, assuming we have correctly guessed their behavior. By reducing the dimension of the $N+1$ Einstein-Maxwell equations, using K_{ab} and t^a to project out the $M+1$[1] dimensions associated with the Killing vector fields, we are left with the $N-M$ dimensional Einstein-Maxwell equations and a set of scalar fields. These fields correspond to the unique metric coefficients in the $M+1 \times M+1$ block of the metric spanned by the Killing vectors and the $M+1$ nonzero components of the vector potential. More specifically, the scalar equations must determine $\frac{(M+1)(M+2)}{2}$ metric coefficients and $M+1$ components of the vector potential for a total of $\frac{(M+4)(M+1)}{2}$ scalar functions.

Now, using the properties of χ^a we can find Dirichlet boundary conditions at the horizon for $M+1$ functions. Namely,

$$Q^2\big|_{r_h} = 0 \quad \omega_i\big|_{r_h} = \Omega_i. \tag{C.68}$$

Next, using Λ_a we find

$$Q^2 A_T\big|_{r_h} = \Phi_h, \quad A_{\omega_i}\big|_{r_h} = \Phi_h \Omega_i, \tag{C.69}$$

determining a further $M+1$ Dirichlet boundary conditions. The properties of the $\zeta^a_{(i)}$s yield

$$W_{(i,j)}\big|_{r_h} = \Omega_i \Omega_j. \tag{C.70}$$

This accounts for another $\frac{M(M-1)}{2}$ boundary conditions, bringing our total to $\frac{M^2+3M+4}{2}$. Comparing this with our $\frac{(M+4)(M+1)}{2}$ unknown functions we seem to be M boundary conditions short. At this point we again take the $4+1$ case as our guide. We define the norms

$$V^a_{(i)} V_{(i)a} \equiv p^2_{(i)}, \tag{C.71}$$

---

[1] Again, we take $\lfloor \frac{N}{2} \rfloor = M$.

and then define the functions

$$H_{(i)} AF_{(i)} \equiv Qp_i, \tag{C.72}$$

where again the functions $AF_{(i)}$ will be determined by asymptotic flatness. Since Q vanishes at the horizon, we find the same result for each $H_{(i)}$. This gives us the boundary conditions for the last M functions.

Each of these functions has simple behavior at spatial infinity. That is they either vanish or become 1. Thus, we have chosen a set of functions with Dirichlet boundary conditions that completely determines the unique unknown components of the metric and the vector potential.

Bibliography

[1] M. Heusler, *Black Hole Uniqueness Theorems* (Cambridge University Press, 1996).

[2] E. T. Newman, E. Couch, K. Chinnapared, A. Exton, A. Prakash, and R. Torrence, "Metric of a Rotating Charged Mass," J. Math. Phys. **6,** 918–919 (1965).

[3] K. Schwarzschild, "Über das Gravitationsfeld eines Massenpunktes nach der Einsteinschen Theorie," Sitzber. Deut. Akad. Wiss. Berlin (Math. Phys.) pp. 189–196 (1916).

[4] H. Reissner, "Über die Eigengravitation des elektrischen Felds nach der Einsteinshen Theorie," Ann. Physik **50,** 106–120 (1916).

[5] G. Nordstrom, "On the Energy of the Gravitational Field in Einstein's Theory," Proc. Kon. Ned. Akad. Wet. **20,** 1238–1245 (1918).

[6] R. P. Kerr, "Gravitational Field of a Spinning Mass as an Example of Algebraically Special Metrics," Phys. Rev. Lett. **11,** 237–238 (1963).

[7] S. W. Hawking and G. F. R. Ellis, *The Large Scale Structure of Space-Time* (Cambridge University Press, 1973).

[8] G. D. Birkhoff, *Relativity and Modern Physics* (Harvard University Press, 1923).

[9] R. M. Wald, *General Relativity* (University of Chicago Press, 1984).

[10] T. Kaluza, "On the Problem of Unity In Physics," Sitzunger. Preuss. Akad. Wiss. Berlin (Math. Phys.) p. 966 (1921).

[11] O. Klein, "Quantum Theory and Five-Dimensional Theory of Relativity," Zeit. Phys. **37,** 895 (1926).

[12] R. R. Tangherlini, "Schwarzschild field in n dimensions and the dimensionality of space problem," Nuovo Cim. **37,** 636 (1963).

[13] G. W. Gibbons, D. Ida, and T. Shiromizu, "Uninqueness and non-uniqueness of static black holes in higher dimensions," Phys. Rev. Lett. **89,** 041101 (2002).

[14] R. C. Myers and M. J. Perry, "Black Holes in Higher Dimensional Space-Times," Ann. Phys. **172,** 304–347 (1986).

[15] R. Emparan and H. S. Reall, "A rotating black ring in five dimensions," Phys. Rev. Lett. **88,** 101101 (2002).

[16] R. Emparan, T. Harmark, V. Niarchos, N. A. Obers, and M. J. Rodriguez, "The phase structure of higher-dimensional black rings and black holes," JHEP **10,** 110 (2007).

[17] S. Hollands and S. Yazadjiev, "Uniqueness Theorem for 5-Dimensional Black Holes with Two Axial Killings Fields," Commun. Math. Phys. **283,** 749–768 (2008).

[18] S. Hollands and S. Yazadjiev, "A uniqueness theorem for five-Dimensional Einstein-Maxwell black holes," Class. Quantum Grav. 25 (2008).

[19] S. Hollands, A. Ishibashi, and R. M. Wald, "A Higher Dimensional Stationary Rotating Black Hole Must be Axisymmetric," Commun. Math. Phys. 271 (2007).

[20] J. Kunz, F. Navarro-Lérida, and A. K. Petersen, "Five-Dimensional Charged Rotating Black Holes," Phys. Lett. B **614,** 104–112 (2006).

[21] J. Kunz, F. Navarro-Lérida, and J. Viebahn, "Charged Rotating Black Holes in Odd Dimensions," Phys. Lett. B **639,** 362–367 (2006).

[22] A. N. Aliev and V. P. Frolov, "Five-dimensional rotating black hole in a uniform magnetic field: The gyromagnetic ratio," Phys. Rev. D 69 (2004).

[23] A. N. Aliev, "Rotating black holes in higher dimensional Einstein-Maxwell gravity," Phys. Rev. D 74 (2006).

[24] R. Geroch, "A Method for Generating Solutions of Einstein's Equations," J. Math. Phys. **12,** 918–923 (1971).

[25] *Black Holes, Les Houches 1972*, C. DeWitt and B. S. DeWitt, eds., (Gordon and Breach Science Publishers, 1973).

[26] *General Relativity: An Einstein Centenary Survey*, S. W. Hawking and W. Israel, eds., (Cambridge University Press, 1979).

[27] P. Dennery and A. Krzywicki, *Mathematics For Physicists* (Dover Publications, Inc., 1996).